Spring 5-7-2016

Regulation of cid-mediated cell death in Staphylococcus aureus

Ian H. Windham
University of Nebraska Medical Center

Regulation of *cid*-mediated cell death in *Staphylococcus aureus*

By

Ian Holt Windham

A Dissertation

Presented to the Faculty of

The Graduate College of the University of Nebraska

In Partial Fulfillment of the requirements

For the Degree of Doctor of Philosophy

Pathology and Microbiology

Under the supervision of Kenneth W. Bayles, Ph.D

University of Nebraska Medical Center

Omaha, Ne

April, 2016

Regulation of *cid*-mediated cell death in *Staphylococcus aureus*

Ian H. Windham, Ph.D

University of Nebraska Medical Center, 2016

Advisor: Kenneth W. Bayles, Ph.D

The death and lysis of a subpopulation of cells in *Staphylococcus aureus* biofilms is thought to benefit the surviving population by releasing extracellular DNA, a critical component of the biofilm extracellular matrix. Although the means by which *S. aureus* controls cell death and lysis is not completely understood, studies implicate the role of the *cidABC, alsSD* and *lrgAB* operons in this process. This dissertation has focused on the regulation of *cidABC* and *alsSD* expression, which is mediated, primarily, by the LysR-Type Transcriptional Regulator (LTTR) known as CidR. To better define the role of CidR in regulating *cidABC* and *alsSD* transcription we produced a series of mutations in the *cidABC* and *alsSD* promoter regions to identify a putative CidR-binding site, TAGTA-N-TACAAA. Although CidR was found to directly interact with this site, these studies also revealed that the induction of *cidABC* and *alsSD* transcription is modulated by two other transcriptional regulators, CcpA and SrrAB, linking *cidABC* and *alsSD* to carbon catabolite repression and respiration. Perhaps most interestingly, a phenotype associated with the *cidB* was also identified; disrupting *cidB* in the *srrAB* mutant background resulted in a decrease in the levels of ROS and sensitivity to ROS, rescuing stationary phase survival. The results of this study further expand upon the *cidABC* and *alsSD* regulatory network of as well as the role this regulon plays in cell death.

Table of Contents

Acknowledgements

This dissertation is the end product of years of research, which would have not been possible without the aid of others. I first need to thank Ken, for guidance, support and most of all patience. I would like to thank the rest of the Bayles lab for their aid in my development as a scientist; Jeff Bose, for his mentorship and teaching me everything I know about genetics; Vinai, for his encouragement in writing; Marat, who just to keep up with him in conversation forced me to learn more metabolism in six month than I had learned in the previous six years; Jennifer, who is probably now tired of finding things for me; Todd, Vijay, Sujata and Sam, for technical assistance; and my fellow graduate students Casey, McKenzie and Derek, for their discussions, ideas and generally keeping me on track.

Lastly, I would like to thank my family for their support. I would first like to thank my parents, who, when faced with a two-year old toddler that declared their intention to pursue a career in science, met this pronouncement with humor and encouragement. I would like to thank my brother Isaac, who despite not pursuing a career in science nonetheless kept me on my toes with questions.

This document is dedicated in loving memory of Isaiah Michael Windham, who left us far too soon.

List of Tables and figures

Chapter I: Literature review

Introduction

Staphylococcus aureus is a Gram-positive pathogen that causes a host of different human diseases (1), causing greater mortality in the United States per year than HIV (2). *S. aureus* colonizes the human nares, pharynx and skin (3, 4). Indeed, 20-30% of the human population is permanently colonized in the nares with *S. aureus* at any time, with another 30% of the population colonized transiently (5, 6). While this colonization can be asymptomatic (7) colonized individuals are at a greater risk for developing *S. aureus* infections (8, 9). Groups with increased risk for infection with S. *aureus* include military personnel (10, 11), inmates (12), sports teams (13), as well as the young (2, 14), elderly (15, 16) and immune-compromised (17, 18). The introduction of penicillin greatly decreased the mortality rate of *S. aureus* infections; prior to the development of antibiotics, the projected mortality of a patient with *S. aureus* bacteremia was 80% (19). Today, depending on the nature of the infection, the mortality rate of individuals infected with *S. aureus* can reach 40%, (20, 21). Antibiotic treatment has been complicated by the rise of community-acquired and hospital-associated strains of *S. aureus* that are antibiotic resistant (2, 22). Shortly after the introduction of penicillin, antibiotic-resistant *S. aureus* was formally recognized (23). Similarly, the introduction of methicillin was followed by the rise of methicillin resistant *Staphylococcus aureus* (MRSA) (23). Currently the antibiotic of choice to treat MRSA infections is vancomycin, though there are fears that vancomycin resistant *S. aureus* strains may become commonplace (24, 25). With the growing burden of multidrug resistant MRSA strains and fears about current drugs being

rendered ineffective for the treatment of staphylococcal disease, research into new alternative drugs, treatments and a better understanding of how *S. aureus* causes infection is necessary.

Biofilms

A growing concern in *S. aureus* infection is the increase in chronic infections in patients with catheters or implants (1, 26, 27). *S. aureus* can cause chronic infections due to its ability to form biofilms, which are the structured communities of bacteria, held together by a self-produced extracellular matrix (28). Biofilms are formed by many different species of bacteria, whether pathogens or free living organisms (29). It is believed that bacteria form biofilms to localize to food sources and protect themselves from the environment (29). In infections, biofilms afford protection against antibiotics, even if the bacteria do not possess traditional resistance mechanisms (27). Bacteria in biofilms are more resistant to clearance (30) because the biofilm cells are not as easily phagocytized as planktonic cells. Finally, a biofilm can metastasize and spread from the infection site if not properly treated, leading to bacteremia and seeding of other distal sites (29). Studying bacterial biofilms and the mechanisms of their formation and maintenance can therefore lead to a better understanding of how to combat infections.

S. aureus biofilms demonstrate a characteristic sequence of attachment, accumulation/maturation, exodus, tower formation and dispersal (31). How *S. aureus* cells will attach depends on whether the target surface is artificial or host tissue (32). On artificial

surfaces it is believed that the dominant determinants of attachment are hydrophobicity and Van der Waals forces, mediated by surface proteins, autolysins and teichoic acids (32). On host surfaces the bacterium will instead use microbial surface components recognizing adhesive matrix molecules, or MSCRAMMs (32). Once cells are attached to a surface they enter the accumulation/maturation stage. The cells grow and divide, remaining connected to each other by the formation of a biofilm matrix. The continued accumulation is interrupted by the exodus phase (31), where a subpopulation of cells disperses from the biofilm, dependent on the activity of a nuclease produced by *S. aureus* (31). Following exodus is maturation, where the remaining cells continue to accumulate and form microcolonies or tower structures. Maturation is followed by dispersal, where the towers disintegrate and the cells float away. This final stage is characterized by dependence on *agr* and the proteases and nucleases it regulates (33). In an animal host, the dispersal stage can lead to bacteremia and potentially colonization of other parts of the body (29), starting the process over again.

The biofilm matrix

The biofilm matrix is made up of many adhesive molecules, including but not limited to polysaccharides like PIA, extracellular DNA, and assorted proteins (32). What polymer is used and needed can also vary based on the age of the biofilm. The composition of this matrix can be diverse (34), varying between strains (35, 36). The primary focus of the Bayles lab is extracellular DNA, or eDNA, and the regulation of factors that determine when it is released from the bacterial cell. eDNA enters the environment by the

death and lysis of a subpopulation of the cells (36). The living cells surrounding the lysed cells use the eDNA as scaffolding within the extracellular matrix. Mutants deficient in lysis and the release of eDNA are poor biofilm formers, like the murein hydrolase *atl* (37). While there have been reports that suggested that *atl* can act as an adhesin (38, 39), eliminating the enzymatic activity of Atl via point mutations inhibits biofilm formation (40), demonstrating that lysis is required for the biofilm to form. eDNA is most critical for biofilm formation during initial attachment and accumulation but continues to remain important as other matrix molecules come into play (36).

Cell death exhibited by *S. aureus* has been compared to apoptosis in eukaryotes (41, 42). Considering that according to the endosymbiotic theory mitochondria are the remnants of long ago phagocytized bacteria (43), this would suggest that programmed cell death (PCD) in bacteria and apoptosis in eukaryotes share a common evolutionary origin, and the proteins involved, while having little to no homology, fulfill the same role. This raises the rather interesting idea that one of the key components of multicellularity, apoptosis in eukaryotes and PCD exhibited by bacteria, have a common evolutionary origin, and that the processes that govern PCD appeared long before the appearance of truly multi-cellular organisms. It might be counterintuitive that bacteria would have a means to commit suicide, as bacterial cells are typically thought of as unicellular organisms. However, a singular bacterium is part of a clonal population (44), particularly in a biofilm. Low dispersal from sister cells in a biofilm would favor kin selection by means of the limited dispersal hypothesis (45-49). To put it simply, death mechanisms have a cost to the individual, but the benefit to the sister cells around a dead cell outweigh the cost to the individual, leading to its continued selection.

The role of cidABC, lrgAB and alsSD in death and the release of eDNA

The processes of death and lysis in *S. aureus* are influenced by the *cidABC*, *lrgAB* and *alsSD* operons. Previous work performed by the Bayles Lab has demonstrated that expression of CidA can be detrimental to the cell (50, 51). Disrupting *cidA* increases survival of *S. aureus* RN6390 (50) and UAMS-1 (37) strains and decreases resistance to antibiotics (50). Meanwhile, disrupting *lrgAB* has been demonstrated to have the opposite effect; disrupting *lrgAB* transcription increases cell death (52). Investigation into how CidA could kill the cell and LrgA could protect from death, it was found that both proteins are relatively small, possess multiple transmembrane domains, a polar N-terminus and a highly charged C-terminus. Interestingly CidA and LrgA share these features in common with bacteriophage holins (53). Based on these findings it was proposed that CidA and LrgA represent a holin-antiholin system, respectively (37, 50, 52).

First discovered in lytic bacteriophage, holins are proteins that form pores (holes) in the cell membrane of bacteria (54, 55), leading to the death and lysis of the cell. Death is potentiated by the activation of an endolysin/murein hydrolase. There are currently two main models explaining the means by which holins can kill the cell (56). In the lambda endolysin model the oligomerization of the holin forms a large pore in the cellular membrane (57), releasing the endolysin/murein hydrolase from the cytoplasm. Once free of the cell the murein hydrolase breaks down the peptidoglycan, leading to lysis. In the Sar endolysin model, instead of releasing the endolysin/murein hydrolase from the cytoplasm,

the pores formed depolarize the membrane (56), leading to the activation of external murein hydrolases.

The activity of holins are inhibited by antiholins (55). In phage holins and anti-holins share a dual-start motif, or two start codons (58). The antiholin is virtually identical to the holin, typically differing by only the presence of a positively charged amino acid on the N-terminus of the antiholin. This small but important addition allows the antiholin to inhibit the oligomerization of the holin. It is thought that CidA, despite sequence similarity to lambda S holin (56), falls into the Sar endolysin category of holins. It has been proposed that the oligomerization of CidA in the membrane leads to the dissipation of the proton motive force (59) and to the activation of murein hydrolases like *atl* (40). As a putative antiholin, LrgA acts to inhibit the oligomerization of CidA. Therefore, the competition between CidA and LrgA is thought to modulate murein hydrolase activity, with the balance of CidA and LrgA determining the potential for the induction of PCD.

In addition to modulation of cell death by the proposed holin-antiholin system the *cidABC, lrgAB* and *alsSD* operons influence cell death on a metabolic level, through *cidC* and *alsSD*. The *cidC*-encoded pyruvate oxidase (60) contributes to cell death during stationary phase by promoting the acidification of the growth media via the production of acetate (61). The membrane of the cell normally acts as a barrier to the negatively charged acetate in the media (61). If the pH of the environment drops and approaches the isoelectric point of acetate (~4.8) there is an increased percentage of acetate that is protonated to acetic acid. The neutrally charged acetic acid can then freely diffuse across the

membrane into the bacterial cytoplasm. Once across the membrane the protons disassociate from acetic acid.

It is not entirely understood how the influx of acetic acid can kill a bacterial cell. It has been proposed that the increase of intracellular weak acids decreases the cytoplasmic pH, which could lead to the misfolding or unfolding of proteins (61). This theory is supported by the fact that the *clp* genes, involved in protein folding and recycling, are up-regulated when exposed to weak acids (62). It has also been proposed that the acetate reduces the functionality of the electron transport chain (61), potentially creating a bottleneck that leads to the formation of ROS. Of course, the mode of killing by acetate might also be a combination of both mechanisms. However, it is important to remember is that weak acid-induced cell death is an active process that requires the synthesis of RNA and proteins *de novo*. When rifampicin is added to growing cultures at day 1 of a 5-day stationary phase survival assay, no ROS is detected by HPF staining on day 3 (unpublished data). As rifampicin blocks mRNA transcription, these results suggest that the formation of ROS that is normally seen on day 3 during stationary phase was the result of freshly translated proteins. This would mean that the cell death exhibited by *S. aureus* under these conditions (61) is an active process, not unlike the active process of apoptosis in eukaryotes. Interestingly enough, apoptosis features acidification of the cytoplasm (63). Thus, we hypothesize that the *cid* operon mediates cell death via a complex process involving the metabolic potentiation of cell death, possibly mediated by the activation of a holin-like complex associated with the cytoplasmic membrane.

The *alsSD* operon encodes α-acetolactate synthase (*alsS*) and α-acetolactate decarboxylase (*alsD*) (61). AlsSD creates acetoin (61, 64), which can be processed further by acetoin reductase (*butA)* to create 2,3-butanediol (56). The synthesis of acetoin and 2,3-butanediol creates a more neutral intracellular pH by consuming pyruvate, redirecting carbon away from *cidC*. The formation of 2,3-butanediol also acts to replenish NAD^+, allowing redox balancing of the cell. *alsSD* then promotes cell survival, acting as a counterbalance to the cytoplasm acidification promoted by *cidC* (61). Both *cidC* and *alsSD* consume the pyruvate created by glycolysis, acting as part of the carbon overflow mechanisms of the cell (61). Lending further support to the idea that *cidABC* and *alsSD* are acting in concert is the fact that both operons are under the control of the same transcriptional regulator, CidR (61, 64, 65).

Role of central metabolism in CidR-mediated regulation

Because of the importance of excess glucose to *cid*-mediated cell death (64, 65) central metabolism and carbon catabolite repression (CCR) probably play a central role in CidR-mediated regulation. In glycolysis, carbohydrates like glucose are catabolized to form pyruvate. For every molecule of glucose two ATP molecules are formed, as well as two pyruvate and two NADH molecules (66-68). In *S. aureus* the TCA cycle is repressed under nutrient rich conditions (69). Little carbon, in the form of acetyl-coA, enters the TCA cycle during nutrient rich growth (70, 71). Instead, carbon is redirected into carbon overflow pathways. When grown under aerobic conditions most of the carbon is directed

into acetate formation via the *ackA-pta* (72) and *cidC* pathways (60, 61), and into acetoin/2,3 butanediol via *alsSD* and *butA* (61).

By 8 hours of growth in liquid culture the preferred carbon source is exhausted from the media, even with 35 mM glucose (72). *S. aureus* will then switch to the consumption of secondary metabolites to sustain growth, and begin consuming acetate, converting it back to acetyl-CoA by way of AcsA (73) and directing the carbon into the TCA cycle. This is accompanied by an increase in TCA cycle activity and a rapid change in the redox ratio, shifting the $NADH/NAD^+$ ratio in favor of NADH. The oxidation of the influx of NADH requires oxidative phosphorylation via the electron transport chain.

In Gram-positive bacteria like *S. aureus*, CCR is mediated by Hpr and CcpA (74, 75). The preferred carbon source of *S. aureus* is glucose which, like other sugars, enters the cell primarily through the phosphotransferase system (74, 76). During import into the cell the glucose is phosphorylated by the PTS to glucose 6-phosphate. As part of the first steps of glycolysis, glucose 6-phosphate is converted to fructose 1,6 bis-phosphate by glucose 6-phosphate isomerase (*pgi)* and 6-phophofructokinase (*pfkA)*. High levels of fructose 1,6 bis-phophate lead to phosphorylation and activation of HprK kinase (77, 78), which in turn phosphorylates and activates Hpr (74). Fructose-1,6-bisphosphate and glucose-6-phosphate promote the association of phosphorylated Hpr with CcpA (74). The CcpA-Hpr regulates target genes by binding to CRE sites (67). The CRE site is typically found within the transcription initiation or promoter sequences when CcpA acts as a repressor (74), and upstream of the promoter sequence when it acts as a positive regulator.

Effect of oxygen on cidABC and alsSD expression

Under anaerobic or hypoxic conditions the carbon consumed by *S. aureus* will be directed towards lactate via Ldh (61, 79) rather than acetate or acetoin. Metabolically, the reason for redirection of carbon would appear to be redox balance. The formation of 2,3 butanediol and lactate both consume NADH, which would be in excess because of its formation during glycolysis (67, 72). Although carbon is not being directed through the pathways of *cid* and *als*, these operons are, nonetheless, up-regulated under anaerobic and hypoxic conditions (31).

Despite being a facultative anaerobe, the process by which *S. aureus* detects oxygen is poorly understood (80), as *S. aureus* does not possess homologues of the oxygen sensing genes used by other species (81). *S. aureus* must have a means of sensing oxygen to properly determine the route to direct carbon, which would affect the transcription of *cidABC* and *alsSD*. It has been proposed that *S. aureus* detects oxygen via the SrrAB two-component system (81). SrrAB is a homologue of ResDE, known to be essential for anaerobic respiration in many Gram-positive bacteria (80). SrrAB also regulates virulence factors (81, 82), genes involved in cytochrome synthesis and the electron transport chain (83) biofilm formation and protein synthesis (84) and the TCA cycle (67, 79). Despite being considered an oxygen sensor, the exact signal that SrrAB responds to is unknown. Due to its ability to respond to nitric oxide stress and oxygen availability (81, 83) it has been proposed that SrrAB detects changes in the redox status of the electron transport chain by sensing reduced menaquinone, rather than oxygen *per se*. As of yet,

however, this has not been definitively proven. Regardless of the signal, SrrAB is essential for anaerobic growth and respiration (67, 80).

CidR-mediated regulation of cidABC and alsSD transcription

The *cidABC* and *alsSD* operons are positively regulated by CidR (64, 65), a member of the LysR-type transcriptional regulator family of proteins, or LTTRs (65). Formally discovered in 1988 (85), LTTRs currently represent the largest known family of transcriptional regulators (86), with over 800 known members found in all domains of life (87). Few members of the family have been crystallized (88), but it is believed that members of the LTTR family have a very conserved structure (88, 89), displaying strong homology in the helix-turn-helix DNA-binding domain of the N-terminus of these proteins (87). In contrast, the C-terminus of the LTTR has limited homology between members of the protein family (87, 90), likely reflecting the different molecules to which these proteins interact.

As a consequence of the highly conserved N-terminal helix-turn-helix DNA binding domain shared between LTTRs (87) there is a common DNA binding motif. The nucleotide sequence of an LTTR binding site is typically characterized by a T-N_{11}-A sequence motif (87). The N_{11} and surrounding bp, usually arranged within an inverted repeat, give the LTTR binding site its specificity for a specific LTTR protein, though crosstalk between LTTRs is not unknown (91-93). In genes that are positively regulated by an LTTR the binding site typically occurs within 100 bp upstream of the -35 element (87). Another

common feature of LTTR binding sites is that they are usually flanked by AT-rich regions of DNA. AT-rich sections of DNA alter the DNA's intrinsic curvature (87, 94, 95), which in turn facilitates LTTR regulation of its target promoter. The LTTR binding site itself contains two separate elements separated by a few bp, termed the Recognition Binding Site (RBS) and the Activation Binding Site (ABS). The LTTR binds each element as a dimer, and the dimers interact to form a tetramer. It is the tetramer itself that acts to bend the DNA (87). The angle of the bend can vary widely depending on the LTTR, anywhere between 50 and 100 degrees (96). It is thought that the high angle of the bent DNA impedes formation of the RNA transcription bubble. In the presence of a signal, the co-inducer molecule, the LTTR undergoes a conformational change, causing the tetramer to shift on the DNA and relax the degree of the angle. The degree of relaxation is also dependent on the LTTR in question, which can decrease as much as 50 degrees (96). The new angle then allows for the formation of an RNA transcription bubble, and facilitates transcription. This model of LTTR regulation has been termed the 'sliding dimer' model (97).

The signal to which an LTTR responds, the co-inducer, is a small molecular weight compound, which is bound by the C-terminus (87). In LTTRs involved in the regulation of metabolism, the co-inducer is often a product of the genes that the LTTR regulates (87), creating a feedback loop. With CidR it was initially proposed that acetate, the product of CidC could be the co-inducer molecule (98). This has not been confirmed, and furthermore instances in which *cidABC* is induced without the presence of acetate have been found (31, 72, 98, 99). Since induction of *cidABC* and *alsSD* is studied in the context of excess glucose (64, 65), it would seem likely that the co-inducer molecule is a product of

central metabolism. Given that *cidABC* and *alsSD* play a role in carbon overflow metabolism (61, 72) it has been proposed more recently that the co-inducer molecule is pyruvate (100), though **this too has yet to be definitively confirmed.**

Hypothesis and specific aims

Hypothesis – The hypothesis for this dissertation is that the co-inducer of CidR is a metabolite from central metabolism. Given the complexity of central metabolism and the different factors involved, it was decided to approach this from several different avenues. .

Aim 1: Mutagenize the cidABC and alsSD promoter regions to identify the CidR binding site.

Aim 2: Employ transposon mutagenesis to identify metabolic pathways that effect the induction of cidABC transcription.

Aim 3: Use DNA-protein interaction experiments to identify the CidR co-inducer.

Chapter II. Materials and methods

Table 1

Bacterial Strains		
Name	Relevant characteristics	Source
S. aureus		
UAMS-1	Clinical osteomyelitis isolate, *rsb*U+	(101)
JE2	derivative of LAC-13c; cured of cryptic plasmid	(102)
RN4220	Highly transformable strain; restriction defi-cient	(103)
KB1058	UAMS-1 Δ*cidC*	(61)
KB1060	UAMS-1 Δ*cidB,* markerless	(104)
KB1064	UAMS-1 Δ*lrgAB*	Lab stock
KB1065	UAMS-1 Δ$cidA^{\Delta 2\text{-}52}$, markerless	(104)
KB1090	UAMS-1 *cidR::Tet*; Tet^r	(65)
KB5010	UAMS-1 Δ*lytSR*	(105)
KB6001	JE2 Δ*geh::lacZ*	(104)
KB6004	UAMS-1 Δ*srrAB,* markerless	(106)

KB6005	UAMS-1 Δ*srrAB* Δ*cidABC*, markerless	(104)
KB6006	UAMS-1 Δ*srrAB* Δ*cidA*, markerless	(104)
KB6007	UAMS-1 Δ*srrAB* Δ*cidB*, markerless	(104)
KB6008	UAMS-1 Δ*srrAB* Δ*cidC*, markerless	(104)
	UAMS-1 Δ*ccpA::tet;* Tet^r	Lab stock
KB8000	UAMS-1 Δ*ackA::ermB*; Erm^r	(72)
E. coli		
DH5α	Host strain for construction of recombinant plasmids	(107)
BL21	Expression strain, *F-*, *ompT, hsdS* ($r_B^- m_B^-$), gal, dcm (DE3)	Invitrogen
Rosetta 2	F^- *ompT hsdS*$_B$ ($r_B^- m_B^-$) gal dcm pRARE2 (Cam^R)	Invitrogen

396 Table 2: Plasmids

Plasmids		
Name	Relevant characteristics	Source
pAJ22	β-galactosidase reporter plasmid; Cam^r	(108)
pBK*alsSD*	pCR-Blunt derivative, contains promoter from pIHW24lac; ColE1 oriV, kan^R	This study
pBursa	*bursa aurelis* oriV Cam^r Erm^r	(109)
pCL52.2	Temperature-sensitive shuttle vector; Tet^r Sp^r	(110)
pCM12	*E. coli/S. aureus* shuttle vector with P_{sarA}-*sodARBS*-gfp (superfolder); Amp^r Sp^r	(111)
pCM28	Derivative of pDB59; Cam^r	(112)
pCM28-1544	pCM28 with cidABC reporter *lacZ*; Amp^r Cam^r	This study
pCN51	P_{cad}-inducible plasmid; Amp^r Erm^r	(113)
pCR-Blunt	PCR cloning vector; ColE1 oriV, kan^R	Invitrogen
pET24b	IPTG-inducible *E. coli* expression plasmid; kan^R	Invitrogen
pET24b-*ccpA*	pET24b with gene encoding CcpA	This study
pET24b-*cidR*	pET24b with gene encoding CidR	This study
pET24b-*srrA*	pET24b with gene encoding SrrA	(104)
pFA545	mariner transposase	(109)

pIHW5	P_{cad}-inducible *lacZ* reporter plasmid; Amp^r Erm^r	(104)
pIHW7	Promoterless *lacZ* reporter plasmid, derivative of pCN51; Amp^r Erm^r	(104)
pIHW9	*cidABC* reporter plasmid; Amp^r Erm^r, 658 bp	This study
pIHW10lac	*cidABC* reporter plasmid; Amp^r Erm^r, truncation -177 upstream of transcription start site	(104)
pIHW11lac	*cidABC* reporter plasmid; Amp^r Erm^r, truncation -138 upstream of transcription start site	This study
pIHW17lac	*cidABC* reporter plasmid; Amp^r Erm^r, truncation -57 upstream of transcription start site	This study
pIHW22lac	*cidABC* reporter plasmid; Amp^r Erm^r, truncation -93 upstream of transcription start site	This study
pIHW24lac	*alsSD* reporter plasmid; Amp^r Erm^r, truncation -247 upstream of transcription start site	This study
pIHW25	UAMS-1 *geh* allellic exchange with P*cidABC* *lacZ* reporter (pCL52.2); Tet^r Sp^r	this study
pIHW26	pCR-Blunt derivative, contains *cidABC* promoter; ColE1 oriV, kan^R	This study
pIHW32lac	*alsSD* reporter plasmid; Amp^r Erm^r, truncation -116 upstream of transcription start site	This study

pIHW33lac	*alsSD* reporter plasmid; Amp^r Erm^r, truncation -47 upstream of transcription start site	This study
pIHW46	*cidABC* reporter plasmid; Amp^r Erm^r, TAG-TAATACAAA(-65 to -53)AAAAAAAAAAAA	This study
pIHW48	*cidABC* reporter plasmid; Amp^r Erm^r, TAGT(-65 to -61)AAAA	This study
pIHW49	*cidABC* reporter plasmid; Amp^r Erm^r, TACA(-59 to -55)AAAA	This study
pIHW58	*srrAB* complementation plasmid; Tet^r Sp^r	(104)
pIHW62	*alsSD* reporter plasmid; Amp^r Erm^r, TAC(-49 to 46)AAA	This study
pIHW63	*alsSD* reporter plasmid; Amp^r Erm^r, TAGT(-55 to 51)AAAA	This study
pIHW64	*alsSD* reporter plasmid; Amp^r Erm^r, TAGTATTACAAA(-55 to 43)AAAAAAAAAAAA	This study
pJB12	$Temp^S$ UAMS-1 Δ*cidB* plasmid (pCL52.2)	(104)
pJB51	pCN51 with optimized RBS; Amp^r Erm^r	(104)
pJB60	$Temp^S$ allellic exchange plasmid with counter-selection; Amp^r Cam^r	(104)

pJB60-114115	Temp^S UAMS-1 Δ*cidABC* plasmid; Amp^r Cam^r	(104)
pJB61	Temp^S allellic exchange plasmid with counter-selection; Amp^r Cam^r	(104)
pJB66	pJB51 with *gfp* gene from pCM12; Amp^r Erm^r	(104)
pJB67	pCN51 with optimized ribosome binding site; Amp^r Erm^r	(104)
pJB94	*E. coli/S. aureus* shuttle vector; Tet^r Sp^r	(104)
pJB97	UAMS-1 *cidB* complement plasmid; Amp^r Erm^r	(104)
pRN8298	pI258 replicon; Amp^r Erm^r	(113)

Antibiotic abbreviations

Tet - tetracycline

Erm - erythromycin

Cam - chloramphenicol

Kan - kanamycin

Sp - spectinomycin

Amp - ampicillin

404 Table 3: Oligonucleotides

Primers		
Name	Sequence	Source
Buster	GCTTTTTCTAAATGTTTTTTAAGTAAATCAAGT ACC	(109)
Martn-ermR	AAACTGATTTTTAGTAAACAGTTGACGATATTC	(109)
RTPCR alsS F	TTGGATGGCACGTAATTTCA	(99)
RTPCR alsS R	GCCAGCAACGGATACAACTT	(99)
sigA-rt-F	AACTGAATCCAAGTCATCTTAGTC	(99)
sigA-rt-R	TCATCACCTTGTTCAATACGTTTG	(99)
cidA-rt-F	GGGTAGAAGACGGTGCAAAC	(99)
cidA-rt-R	TTTAGCGTAATTTCGGAAGCA	(99)
IW3	gcccgggATGACCATGATTACGGATTCACTGGCCGTC	(104)
IW4	gggcgcgccTTATTTTTGACACCAGACCAACTGGTAATGG	(104)
IW10	gggatccAGCAAATTATCAATGATGAAGTAG	This study

	ATATAGGC	
IW11	ggctagCGCCATCCCTTTCTAAATATGTCTAAATTGTTAC	(104)
IW16	ggatccCTTGGATCATTGAAATAATGAGTGTTTTTTTTG	This study
IW22	ggatccCAAACCATAAAAAAAGAGTATTTTTATATTG	This study
IW27	gaattcTACATCCCTTGCTTATAGACACGATTAGTAATC	This study
IW28	gagctcGAAAAACAACTGCACTTTCAATATAACATGACA	This study
IW29	ctgcagGTGCTACTAACATGGCACGGAAGATATAAGTAG	This study
IW30	aagcttCAACCAACAAAAGGTGCCATTGTCTACATTCAT	This study
IW31	ggatccGAAATTTAGAGAGCGTTTCCATAGAAAATAGTA	This study
IW39	gggatccTTTAAATCGCCAAAAACAGCATTTTCAAAC	This study
IW41	ggctagcTTATATTCATTTCCCTTCAAATGTGATGTG	This study

IW44	ctgcagTGTCACTTTGCTTGATATATGAGAATTATTTAA	This study
IW50	ggatccTCAATCCAACATCCCTTATAATCACTCCCTTCA	This study
IW51	ggatccCAAATAACGATTTTTATTCATCTTACAAAGG	This study
IW52	cacctaggAATTGAATGAGACATGCTACACCTCCGGATA	This study
IW91c	gggaattcGAACAGCGTAGCCAACAATTAATTACTACTGA	(104)
IW92c	ggggatccACATGCTTTTCTTTACAAAAGTATTATATCAC	(104)
IW93c	ggggatccTAAAATTGAATATAGTTATTTCAGAACGCATG	(104)
IW94c	ggtctagaGTAATTGTCTTTAGTGCTAAATAAAGTTGTAA	(104)
IW100	GACGCCTCATGAAGTAAAAGTGATGCGTCA	(104)
IW101	ATAGTTGATATTCGCAAAAACCCTAAACCC	(104)

IW110	biotin-AGTGAAATTTAGAGAGCGTTTCCATAGAAAATAGTAATACAAACCATAAAAAAAGAGTAT	This study
IW111	AGTGAAATTTAGAGAGCGTTTCCATAGAAAATAGTAATACAAACCATAAAAAAAGAGTAT	This study
IW112	biotin-ATACTCTTTTTTTATGGTTTGTATTACTATTTTCTATGGAAACGCTCTCTAAATTTCACT	This study
IW113	ATACTCTTTTTTTATGGTTTGTATTACTATTTTCTATGGAAACGCTCTCTAAATTTCACT	This study
IW114	ggctagcTGATTGAAAGGTTATCACAATTGAATTGAA	(104)
IW115	ggggtcgacCCAGAACGGTGAATAGAAAATATGATGTAA	(104)
IW116c	ggctagcGAGGAAATTATGACAGTTACTATATATGATGTAGC	This study
IW117cc	ggctcgagTTTTGTAGTTCCTCGGTATTCAATTCTGTGTGG	This study
IW118cc	ggctagcGTGGGAGGTATGACCTGTATGTCG	(104)

	AACG	
IW119ccc	gctcgagTTTAGCCGGCTCATCATTAGATTTAACCTCAAATTTATACC	(104)
IW128cc	gggctagcGTGGATATCAAACATATGAAATATTTTATT	This study
IW129cc	ggctcgagGCCTAAACGATCTTTCAAAAATTCTATCCA	This study
IW130	GAGCATCGACTCGCAAAATA	This study
IW131c	CAAAGCCAACGTTTTTAGCA	This study
IW132	CGGGTCAACAAATGGATTTAGATGAATTCCAAGC	This study
IW133	CGCTCAACCTGGTCGAGCAAGTGGTTTTTGTATATAC	This study
IW135	biotin-TCAAAATCTACTCATGCATTTTTGGAATACTTAGTATTACAAATAACGATTTTTATTCAT	This study
IW136	ATGAATAAAAATCGTTATTTGTAATACTAAGTATTCCAAAAATGCATGAGTAGATTTTGA	This study
IW137		This study

	TCAAAATCTACTCATGCATTTTTGGAATACTTAGTATTACAAATAACGATTTTTATTCAT	
IW138	ggagctcACAATAACAGAAGGTCGTAATCGTCAAGTC	(104)
IW139	gggatccTTATTCTGGTTTTGGTAGTTTAATAATAAA	(104)
IW141	/5phos/TTTTGGAATACTTAGTAATACAAATAACGATTTTT	This study
IW142	/5phos/ATGCATGAGTAGATTTTGAAGGGAGTGATT	This study
IW145	GTGTCGCGTGTTGTTAATGG	This study
IW146	GTCCACGAGCAAGTTGTGAA	This study
IW147	ggggatccGTGGGAGGTATGACCTGTATGTCGAACG	(104)
IW15	ggatccCATATTAATAAAGCACTCATTATTTGTGATTCC	(104)
IW152	ggggtcgacTTTAGCCGGCTCATCATTAGATTTAACCTCAAATTTATACC	(104)
IW154	GCTTATGAACTTGCAATGGAG	(104)

IW155	CAGTTGATACTCATGTTAAACGAC	(104)
IW156	GGGCTCATCTCAAACATATATTTTG	(104)
IW157	CGGAAATGCGTGATTTAGAAATG	(104)
IW162	AGTGAAATTTAGAGAGCGTTTCCATAGAAAACATATTAATAAACCATAAAAAAAGAGTAT	This study
IW163	ATACTCTTTTTTTATGGTTTATTAATATGTTTTCTATGGAAACGCTCTCTAAATTTCACT	This study
IW166	TCAAAATCTACTCATGCATTTTTGGAATACTTAGTATTACAAATAACGATTTTTATTCAT	This study
IW167	ATGAATAAAAATCGTTATTTGTAATACTAAGTATTCCAAAAATGCATGAGTAGATTTTGA	This study
IW168	biotin-ATAGTTATTGTAACAATTTAGACATATTTAGAAAGGGATGGCGCCATGCACAAAGTCCAA	(104)
IW169	TTGGACTTTGTGCATGGCGCCATCCCTTTCTAAATATGTCTAAATTGTTACAATAACTAT	(104)

IW170	ATAGTTATTGTAACAATTTAGACATATTT AGAAAGGGATGGCGCCATGCACAAAGTC CAA	(104)
IW170	ATAGTTATTGTAACAATTTAGACATATTT AGAAAGGGATGGCGCCATGCACAAAGTC CAA	This study
IW171	/5phos/TTTTGGAATACTTAGTATTAAAAAT AACGATTTTT	This study
IW172	/5phos/TTTTGGAATACTAAAAATTACAAAT AACGATTTTT	This study
IW173	/5phos/TTTTGGAATACTAAAAAAAAAAAA TAACGATTTTT	This study
IW174	biotin-TTTAAATCGCCAAAAACAGCATTTTCAAA C	This study
IW175	biotin-CATAGAAAAAAAAAATACAAACCATAAA AAAAGAGTATTT	This study
IW176	CATAGAAAAaaaaAATACAAACCATAAAAA AAGAGTATTT	This study
IW177	AAATACTCTTTTTTTATGGTTTGTATTTTTT	This study

	TTTTCTAT	
IW178	biotin-CATATTAATAAAGCACTCATTATTTGTGATTCCTCATTACTTGGATCATTGAAATAATGA	This study
IW179	CATATTAATAAAGCACTCATTATTTGTGATTCCTCATTACTTGGATCATTGAAATAATGA	This study
IW180	TCATTATTTCAATGATCCAAGTAATGAGGAATCACAAATAATGAGTGCTTTATTAATATG	This study
IW181	Biotin-AAAAAGAGTATTTTTATATTGTGTACGCCATCTTTATAATAGTTATTGTAACAATTTAGA	This study
IW182	AAAAAGAGTATTTTTATATTGTGTACGCCATCTTTATAATAGTTATTGTAACAATTTAGA	This study
IW183	TCTAAATTGTTACAATAACTATTATAAAGATGGCGTACACAATATAAAAATACTCTTTTT	This study

IW184	/5phos/TTTTGGAATACTTAGTATAAAAAATAACGATTTTT	This study
IW193	gggagctcACATTTTTCAACAAATGCAATTGATATTTG	This study
IW194	ggggatccTTATTTTGTAGTTCCTCGGTATTCAATTCT	This study
JBCACOMP1	cggatCCGCATGCAAATTATCAATGATGAAGTAGATATAGGC	(104)
JBCDALAC3	cgtcgacCCATGCTTGTAATGCTTTAACTAATGCTTC	(104)
JBGFP4	cgaattcttaTTTGTAGAGCTCATCCATGCCATGTG	(104)
JBGFP8	CCATATGCCCGGGagcaaaggagaagaacttttcactgg	(104)
JBI258ORI1	*ccagatc*tggcgaatggcgccgttttatcttcatcac	(104)
JBI258ORI2	*GGTGTACA*GGGCCCTCGATGATTACCAGAAGTTCTCAC	(104)

Bacterial strains and growth conditions

All the bacterial strains used in this study are listed in Table 1. *S. aureus* strains were grown in tryptic soy broth (TSB; Difco Laboratories, Detroit, MI) or filter-sterilized NZY broth (3% [wt/vol] N-Z Amine A [Sigma Chemical Co., St. Louis, Mo.], 1% [wt/vol] yeast extract [Fisher Scientific, Fair Lawn, N.J.] adjusted to pH 7.5). *Escherichia coli* DH5α was grown in Luria-Bertani medium (Fisher Scientific). Liquid *S. aureus* cultures were grown in Erlenmeyer flasks at 37°C with shaking (250 rpm) in a volume that was no greater than 10% of the flask volume. Hypoxic conditions were performed using the same media in 3:5 media volume to flask ratio with shaking at 60 rpm. All antibiotics were purchased from either Sigma Chemical Co. or Fisher Scientific and were used at the following concentrations: kanamycin, 50 $\mu g \cdot ml^{-1}$; chloramphenical, 10 $\mu g \cdot ml^{-1}$; ampicillin, 100 $\mu g \cdot ml^{-1}$; and erythromycin, 5 $\mu g \cdot ml^{-1}$.

DNA manipulations

Genomic DNA was isolated from *S. aureus* using the Wizard Plus kits from Promega, Inc. (Madison, Wis.). Restriction endonucleases, DNA polymerases and T4 DNA ligase used in this study were purchased from either New England Biolabs (Beverly, Mass.) or Invitrogen Life Technologies (Carlsbad, Calif.). Recombinant plasmids were isolated using the Wizard Plus SV Minipreps DNA purification system (Promega Corporation, Madison, WI). PCR was performed using primers purchased either from Integrated DNA Technologies (Coralville, IA) or Eurofins Operon (Louisville, KY), a KOD polymerase

kit (Novagen, Madison, WI), and an Applied Biosystems GeneAmp PCR System 9700 (Life Technologies Corporation, Carlsbad, CA). DNA fragments were recovered using the DNA Clean and Concentrator-5 Kit (Zymo Research, Orange, CA) and recombinant DNA plasmid products were sequenced at the University of Nebraska Medical Center DNA Sequencing Core facility and analyzed using Vector NTI (Invitrogen, Carlsbad, CA).

The *lacZ* reporter plasmid to monitor *cidABC* expression was created by first PCR amplifying the *gfp* gene of pCM12 (111) using primers JBGFP4 and JBGFP8. The resulting PCR was cloned into the NdeI and EcoRI sites of pJB51, a derivative of pCN51 containing an optimized RBS, to yield the plasmid pJB66. An internal EcoRI digest was performed which removed the *gfp* gene, leaving the desired construct pJB67. The *lacZ* gene in pAJ22 (108) was amplified by PCR using the primers, IW3 and IW4, and cloned into the SmaI and AscI restriction sites of pJB67 to produce the plasmid pIHW5. The cadmium inducible promoter of pIHW5 was removed by digestion with SphI and PstI, treatment with Klenow and self-ligated to produce the *lacZ* vector plasmid pIHW7. The *cidABC* promoter was PCR amplified off of the UAMS-1 genome using the primers, IW11 and IW15, and cloned into the BamHI and NheI cut sites to yield the final reporter product pIHW10lac. The *alsSD* reporter pIHW24lac was constructed by using the pIHW7 plasmid backbone. The primers IW39 and IW41 were used to clone the *alsSD* promoter fragment, which was then cloned into the BamHI and NheI cut sites to yield the reporter.

A nested set of DNA fragments spanning the *cidABC* promoter region was generated by PCR using a series of primer pairs that generated successively shortened fragments at the 5' end but common 3' ends. The 3' primer used (IW11) generated a BamHI recognition site, while the 5' primers (IW15, IW16, IW31 and IW22; see Table X) generated NheI recognition sites. Each PCR promoter fragment generated was digested with BamHI and NheI and cloned into pIHW4 or pIHW7, yielding the plasmids pIHW10(lac), pIHW11(lac), pIHW22(lac) and pIHW17(lac), respectively. A similar process was used to generate nested deletions in the *alsSD* promoter region. The primer, IW41, determined the 3' end of the *alsSD* promoter fragment and was used in conjunction with the primers, IW39, IW50 and IW51, to generate the different 5' ends. As above, the PCR products generated were digested with BamHI and NheI and ligated into pIHW4 or pIHW7 to produce the plasmids, pIHW24(lac), pIHW32(lac) and pIHW33(lac), respectively. All of the deletion constructs truncations were generated such that the -35 and -10 elements, as well as the untranslated regions (UTRs) of the *cidABC* and *alsSD* transcripts remained intact.

Point mutations in the *cidABC* promoter region were generated following the protocol described by Bose et al. (40). The template used for these experiments was pIHW26, a derivative of the pCRblunt plasmid from the Zero Blunt PCR Cloning Kit (Invitrogen, Carlsbad, CA) containing the *cidABC* promoter. PCR products were self-ligated and then treated with DpnI to remove any methylated template DNA that remained. After digestion, the DNA was transformed into DH5α, and kanamycin-resistant colonies were minipreped and potential plasmids screened by digest and sequenced. Plasmids containing the desired point mutations were digested with BamHI and NheI, and the promoter fragment cloned into pIHW7 (Table 1). The same strategy was used to construct point

mutations in the *alsSD* promoter using the template plasmid pBK*alsSD*, also a derivative of pCRblunt.

Chromosome mutants were generated as previously described (40). Briefly, an in-frame deletion plasmid for *cidB* was generated by amplifying approximately 1,000 bp of DNA flanking the *cidB* gene from the UAMS-1 chromosome. Subsequent cloning of the PCR products into pCL52.2 (110) yielded a plasmid, pJB12, which contains *cidB* gene replaced by an XhoI site. A similar strategy was used for *cidA*. Due to the presence of a *cidBC* promoter in the *cidA* open reading frame, an in-frame deletion of *cidA* was constructed such that the 5' 150 bp (38%) of the *cidA* gene was removed, but leaving the *cidBC* promoter intact. This construct would produce a CidA protein lacking the first 50 amino acids after the start codon. The *cidC* mutant was published previously (60). The *srrAB* knockout strain was constructed as described previously (106). To create a markerless *cidABC* knockout strain, UAMS-1 genomic DNA was used as a template for PCR using the primers, IW114 and IW115 (Table 1), to isolate the 3' region of the *cidABC* operon. The PCR products were digested with SalI and NheI and ligated into the vector, pJB60, to produce the *cidABC* knockout plasmid, pJB60-114115. Deletion of the *cidABC* operon in UAMS-1 was then generated by allelic replacement as described previously (114).

A *srrAB* complementation plasmid was generated by PCR amplifying the low-copy, pI258 replicon from pRN8298 (115) using the primers, JBI258ORI1 and JBI258ORI2. The PCR product was then ligated into the BglII and BsrGI sites of pCL52.2 (116), replacing the temperature-sensitive origin of replication to create the plasmid, pJB94. The

primers, IW138 and IW139, were used to amplify the *srrAB* operon, including its promoter region, using UAMS-1 genomic DNA as a template. The PCR product was then ligated into the SmaI site of pJB94 in a blunt-end ligation reaction. The resulting plasmid, pIHW58, was confirmed to contain the proper DNA insert by DNA sequencing. A *cidB* complement plasmid was generated by PCR amplifying *cidB* from the UAMS-1 chromosome using the primers JBCACOMP1 and JBCDALAC3. The PCR product was digested with SphI and ligated into the same site of pCN51 to produce the plasmid pJB97.

To create a markerless *cidABC* knockout strain the UAMS-1 genome was used as a template for PCR using the primers IW114 and IW115 to isolate the 3' region after *cidABC*. The PCR was digested with SalI and NheI and cloned into the vector pJB60 to produce the *cidABC* knockout plasmid pJB60-114115. Deletion of the *cidABC* operon in UAMS-1 was then generated by allelic replacement as described previously (114).

For easy use of a *cidABC* reporter in the Nebraska Transposon library mutants a new reporter plasmid had to be created as the *erm* resistant of the pIHW6 or 9 plasmids was incompatible with the transposon mutants. PCR of the *cidABC* promoter and *lacZ* was performed off of pIHW9 using the primers IW15 and IW44. The PCR product was digested with BamHI and PstI and cloned into pCM28 to yield pCM28-1544, which was then used in all NE Transposon Mutants that were tested.

Transposon mutagenesis

512 It was decided to integrate the reporter into the *geh* gene so that integration could be
513 confirmed by lipase activity assays. Primers IW27 and IW28 were used to clone the 5'
514 region upstream of *geh*. The PCR products were digested with the restriction enzymes
515 EcoRI and SacI and ligated into the plasmid pCL52.2 to produce the plasmid pIHW20.
516 Primers IW29 and IW30 were used to clone the 3' region downstream of *geh*. The PCR
517 product was digested with the enzymes PstI and NheI and ligated into pIHW20 to pro-
518 duce the plasmid pIHW21. Finally, primers IW10 and IW44 were used to clone the
519 *cidABC* promoter, *lacZ* reporter and blazTT off of pIHW9. The PCR product was then
520 digested with PstI and BamHI and ligated into pIHW21 to produce the integration plas-
521 mid pIHW25.

522 The reporter strain was made by first streaking out UAMS-1 containing the plasmid
523 pIHW25 onto TSA + 10 μM · ml^{-1} tetracycline. The plate was then grown at 45°C over-
524 night. The plate was then restruck and grown at 45°C overnight again. Colonies were
525 picked and used to inoculate 5 mL of TSB. Cultures were then grown at 30°C 250 rpm
526 overnight. Cultures were diluted 1 to 1000 into fresh TSB daily for 3 days. Beginning the
527 fourth day dilution plating was also performed. Colonies from the dilution plating were
528 patched onto TSA and TSA + tet, both containing 35 mM glucose and 50 μg · ml^{-1} X-gal.
529 Colonies that turned blue and were tetracycline sensitive were confirmed by PCR to have
530 integrated properly to produce the strain KB6001.

531 The *mariner*-based transposon (Tn) *bursa aurealis* was used to generate random Tn
532 insertion mutations in *S. aureus* strain JE2 essentially as described by Bae et al. (109).
533 First, bacteriophage φ11 was used to transduce the *bursa aurealis* delivery plasmid

pBursa into JE2 containing the transposase-encoding plasmid pFA545, with selection on TSA medium containing chloramphenicol (Cam) (10 μg · ml^{-1}) and Tet (5 μg · ml^{-1}). After growth for 48 h at 30°C to allow for transposition events, one colony was resuspended in 100 μl of prewarmed 45°C water and then plated onto TSA plates containing erythromycin (Erm) (25 μg · ml^{-1}) and grown at 45°C for 12 to 24 h. Resulting colonies, irrespective of colony size, were then screened for loss of the temperature-sensitive plasmids pBursa and pFA545 by patching them on TSA-Erm (25 μg · ml^{-1}), TSA-Cm (10 μg · ml^{-1}), and TSA-Tet (5 μg · ml^{-1}). Those colonies that were Cm and Tet susceptible but resistant to Erm were grown in 5 mL of TSB-Erm (5 μg · ml^{-1}) and grown at 37°C overnight.

After overnight growth, the Wizard genomic DNA purification kit (Promega) was used to isolate genomic DNA from the cultures with the following modifications. Briefly, after centrifugation at 4,100 rpm for 5 min in a Sorvall (Newtown, CT) Legend tabletop centrifuge, supernatants were removed, the content of each well was resuspended in 110 μl of 50 mM EDTA (pH 8.0), and 5 μl of 10-mg/ml lysostaphin was added. After incubation at 37°C for 60 min, 600 μl of Nuclei Lysis solution was added and the genomic DNA was collected according to the manufacturer's instructions. After resuspension in Tris-EDTA (TE) buffer, the genomic DNA was digested with 10 units of AciI (New England Biolabs) at 37°C for 4 h. AciI was then heat inactivated at 65°C for 30 min; T4 DNA ligase (200 U) (Monserate Biotechnologies, San Diego, CA) was then added to each sample and ligated overnight at 4°C, followed by heat inactivation at 65°C for 30 min. DNA fragments spanning the *bursa aurealis* insertion sites in each sample were amplified using the Buster (5= GCTTTTTCTAAATGTTTTTTAAGTAAATCAAGT ACC 3=)

and Martn-ermR (5= AAACTGATTTTTAGTAAACAGTTGAC GATATTC 3=) primer set. PCR conditions included 30 cycles with an annealing temperature of 63°C and an extension time of 3 min. Once amplified, samples of the DNA products were separated in a 1% agarose gel by electrophoresis, and the remainder was purified for sequencing using Exo-SAP-IT (GE Healthcare) according to the manufacturer's instructions. Finally, determination of the nucleotide sequences of the genomic DNA flanking the transposons was achieved using the Buster primer at the DNA Microarray and Sequencing Core Facility at the University of Nebraska Medical Center.

β-galactosidase assays

β-galactosidase assays were performed based on protocols previously described (105). Briefly**,** 1.0 ml of cell cultures was centrifuged and the cell pellet was resuspended in 1 ml Z-buffer (60 mM Na_2HPO_4, 40 mM NaH_2PO_4, 10 mM KCl, 1 mM $MgSO_4$, 50 mM β-mercaptoethanol, pH 7.0) and disrupted using a FastPrep FP120 (MP Biomedicals, Santa Ana, California). Cellular debris was pelleted by centrifugation and 700 µl of the supernatant was transferred to a 1.5 ml microcentrifuge tube. After the addition of 140 µl of ONPG (4 mg ml^{-1}), the samples were incubated at 37°C until they turned slightly yellow (under OD_{420} 1.0). To stop the reactions, 500 µl of 1 M sodium carbonate was added and the OD_{420} was measured. Protein concentrations were determined by performing Bradford Assays using the Protein Assay Dye Solution (Bio-Rad, Hercules, California). Miller units were calculated using protein concentration instead of OD_{600} (117).

Expression of recombinant protein

To produce purified CidR for analysis, the *cidR* gene was PCR-amplified using the primers, IW128cc and IW129cc, and UAMS-1 genomic DNA as a template. The PCR product was ligated into the NheI and XhoI sites of pET24b and the DNA sequence confirmed by sequencing the cloned product. The resulting plasmid (pET24b-*cidR*) was transformed into the rare-codon enhanced *E. coli* strain BL21 derivative Rosetta 2 (Novagen, Madison, WI) for protein expression. For CcpA, the *ccpA* gene was isolated from the UAMS-1 genome via PCR using the primers, IW116 and IW117, and ligated into pET24b as above. The resulting plasmid (pET24b-*ccpA*) was transformed into the *E. coli* strain BL21 (Novagen, Madison, WI) for expression. To produce purified SrrA for analysis, the *srrA* gene was PCR-amplified using the primers, IW147 and IW152, and UAMS-1 genomic DNA as a template. The PCR product was ligated into the NheI and XhoI sites of pET24b and the DNA sequence confirmed by sequencing the cloned product. The resulting plasmid (pET24b-*srrA*) was transformed into BL21 (Novagen, Madison, WI) for protein expression.

To purify CidR, the Rosetta 2 **(**pET24b-*cidR*) strain was grown in 1 L of LB media containing kanamycin and chloramphenicol at 37°C until the culture reached mid-exponential phase. IPTG was added to a final concentration of 0.4 mM to induce expression of CidR. The culture was transferred to a 20°C incubator and grown overnight. To purify CcpA, a similar approach was utilized, with the exception that the overnight cultures were grown at 30°C. To express and purify SrrA, the BL21**(**pET24b-*srrA*) strain was grown in 1 L of LB media containing kanamycin at 37°C until the culture reached

mid-exponential phase. IPTG was added to a final concentration of 0.4 mM and *srrA* was expressed at 30°C overnight. The cells of all cultures were collected by centrifugation and resuspended in 50 mL lysis buffer (100 mM phosphate, 300 mM NaCl) containing PMSF (1.0 mM) to inhibit protease activity. Cells were lysed via serial passage through an Emulsiflex-C3. The proteins were then purified using HisPur™ Cobalt Purification Kit columns (Pierce Biotechnology, Rockford, IL) according to the manufacturer's instructions. The proteins were then desalted via ultrafiltration using an exchange buffer (100 mM Tris-HCl, pH 8.0, 150 mM KCl, 1 mM EDTA, and 0.1 mM dithiothreitol). The purified protein was stored at -20°C in the exchange buffer containing 40% glycerol.

Protein-DNA interactions

The binding of purified proteins to target DNA was demonstrated by electrophoretic mobility shift assays (EMSAs) using a Lightshift Chemiluminescent Kit (Pierce Biotechnology, Rockford, IL) according to the manufacturer's instructions. The target DNA used for the CidR and CcpA EMSAs were made by annealing 60 bp primers, IW110 and IW113 for *cidABC*, and IW135 and IW136 for *alsSD*, together. Mutant specific competitor DNA was made from primers, IW162 and IW163 for the 4 bp mutation promoter, and primers IW176 and IW177 for the complete replacement of the CidR binding site. The target DNA used for the SrrA EMSAs were made by annealing the 60-bp primers, IW168 and IW169. The binding reaction mixture for each sample contained 10 mM Tris, pH 7.5, 50 mM KCl, 1 mM DTT, 2.5% glycerol, 1 µg of salmon sperm DNA, 5 mM $MgCl_2$, 0.05% NP-40, 10 mM EDTA and 5 fmol of labeled DNA in a total volume of 20 µL. Competitor

DNA was added in 200-fold excess according to the manufacturer's instructions. After 30 minutes incubation at room temperature, the protein-DNA mixtures were separated in a 6% TBE gel in 0.5 TBE buffer at 85 volts. The DNA was then transferred from the gel to a nylon membrane and cross-linked to the nylon membrane using a UV Stratalinker® 1800 (Stratagene ®) cross-linker instrument. The labeled DNA fragments were then imaged using an SRX-101a Imager (Konica Minolta, Wayne, NJ).

Quantification of the mRNA transcripts

RNA isolation was carried out as described previously (118). Quantitative real-time PCR was performed using the *sigA*-, *cidA*- and *alsS*-specific primers listed in Table 3. Total RNA (500 ng) was converted to cDNA using the Quantitect Reverse Transcription Kit (Qiagen). The samples were then diluted 1:50, and the cDNA products were amplified using the LightCycler DNA Master SYBR green I kit (Roche Applied Science) following the manufacturer's protocol. The relative transcript levels were calculated using the comparative threshold cycle (*CT*) method (119) with normalization to the amount of *sigA* transcripts present in the RNA samples.

Flow cytometry

Flow cytometry was performed as previously described (61). Briefly, a BD LSRII flow cytometer (Beckton and Dickinson, San Jose, California) was used to perform anal-

yses using 1- and 3-day old stationary phase cultures of *S. aureus*. Cell samples were washed twice and diluted to a final concentration of 10^7 cells per ml in PBS and then stained for 30 min with 5-cyano-2,3-ditolyl tetrazolium chloride (CTC, 5 mM) and 3-(p-hydroxyphenyl) fluorescein (HPF, 15 mM). FACS analyses were performed at a flow rate of 1,000 cells per second. A total of 10,000 events were collected for each sample. Bacteria were discriminated from background using a combination of forward scattered light (FSC) and side scattered light (SSC). Samples were excited at 488 nm using an argon laser and HPF emission was detected at 530 $\pm$ 30 nm (with a 505 nm long-pass mirror) whereas CTC emission was detected at 695 $\pm$ 40 nm (with a 685 nm long-pass mirror). Raw data were analyzed using FlowJo software.

Metabolite analyses

For these analyses, bacterial growth was allowed to proceed at 37°C and 250 rpm in flasks containing TSB (35 mM glucose) in a 1:10 flask to volume ratio. Metabolite excretion profiles were determined from culture supernatants that were harvested at 1 and 3 days of incubation. Acetate was measured using commercial kits (R-Biopharm, Marshall, MI), according to the manufacturer's instructions.

Acetoin assays were performed as previously described (120). Briefly, Acetoin assay was performed as follows. 200 µL of supernatant was mixed with 140 µL 0.5% creatine, 200 µL 5% α-napthol, and 200 µL 40% KOH. The sample was incubated for 15 to 30 minutes. The OD_{560} was measured and used to determine the concentration of acetoin.

Chapter III. A direct link between glycolysis and *cid*-mediated *Staphylococcus aureus* cell death

Introduction

Many *Staphylococcus aureus* infections are thought to involve biofilms, a structured community of bacteria held together by an extracellular matrix created by the bacterial population (28). The composition of this matrix is diverse in nature and critical for adherence between cells and adherence to surfaces (34). Many different molecules are part of the matrix, including carbohydrates, proteins, and extracellular DNA (eDNA). In *S. aureus*, it has been demonstrated that eDNA is an important component, released by the lysis of a subpopulation of cells in the biofilm via a process termed bacterial programmed cell death (PCD) (32, 121). The surviving cells benefit from the death of the subpopulation by using the eDNA as part of the scaffolding of the matrix.

Although the mechanism(s) controlling cell death are not fully understood, this process is known to involve the products of the *cidABC, lrgAB* and *alsSD* operons (42, 61, 64). In the past we have demonstrated that disruption of the *cidA* gene resulted in decreased antibiotic-induced death and lysis (50), whereas disruption of the *lrgAB* operon had the opposite effect (52). Additionally, CidA and LrgA were found to share sequence similarities with bacteriophage holins (50), proteins well-known for their role in the control of death and lysis. Based on these findings a model was proposed in which CidA and LrgA represent a bacterial holin-antiholin system that is the foundation of bacterial PCD (42). CidA oligomerizes and forms pores in the cytoplasmic membrane, leading to membrane depolarization, activation of murein hydrolase activity, and cell lysis (56). LrgA is

envisioned as an antiholin (52), opposing the activity of CidA by interfering with its ability to depolarize the membrane and cause subsequent death and lysis (50). More recently other effectors of cell death have been discovered. The *cidC*-encoded pyruvate oxidase (60) was shown to potentiate cell death during stationary phase and biofilm development by promoting cytoplasmic acidification through the production of acetate (61). At the same time the *alsSD* operon encodes α-acetolactate synthase (*alsS*) and α-acetolactate decarboxylase (*alsD*) which synthesize acetoin which has been found to have a role in promoting cell survival (61, 64). Though it might at first appear that *cidC* and *alsSD* have opposing functions, both operons consume the pyruvate created by glycolysis. It therefore seems likely that *cidC* and *alsSD* act as part of the carbon overflow mechanisms of the cell (61, 100).

The regulation of *cidABC* and *alsSD* expression is known to be mediated by CidR (61, 64, 65), which is required for the induction of transcription during growth in excess glucose (50). CidR is a member of the LysR type transcriptional regulator (LTTR) family of proteins (65), which have a common mechanism of regulation and key motifs that appear in their target sequence. While we know that CidR-mediated regulation responds to excess glucose (64, 65) and low oxygen (99) we do not know the sequence of the CidR binding site.

In the current chapter, we sought to better define the mechanisms of the regulation of cell death in *S. aureus*. We used genetic techniques to create truncations and mutations in the *cidABC* and *alsSD* promoters to ultimately define the sequence of the CidR binding site, 5'-TAGTA-A/T-TACAAA-3'. While creating our truncations we found that another

transcriptional regulator, CcpA, plays a direct role in the regulation of *cidABC* and *alsSD*, demonstrating a role for CCR in *cidABC* and *alsSD* induction that was not previously anticipated. To uncovered further metabolic modulators of *cidABC* induction we also performed Transposon Mutagenesis (Tn). EMSAs confirmed the regulation to be direct. The data we present here sheds light on the complicated regulation of *cid* and *als*, creating a more complete picture of PCD in *S. aureus*.

Results

Identification of cis-acting elements important for CidR-inducible gene expression

In a first step to defining the regulatory interactions associated with CidR-mediated regulatory control, we sought to identify the *cis*-acting DNA sequences important for binding of CidR to the promoter regions of the only two known targets of CidR regulation, the *cidABC* and *alsSD* operons. Although LTTR binding sites typically encompass the consensus sequence T-N_{11}-A (87), the AT-rich nature of *S. aureus* DNA made the identification of putative CidR-binding sites within the *cidABC* and *alsSD* promoter regions difficult. We therefore constructed a nested set of truncations (Fig. 3.1) of the sequences spanning both promoter regions, fused them to the *lacZ* reporter gene, and introduced these reporter plasmids into the *S. aureus* wild-type strain, UAMS-1. As both *cidABC* and *alsSD* transcription has been shown to exhibit CidR-dependent glucose-inducible expression (51, 64), we grew each reporter strain in the presence of 35 mM glucose and measured β-galactosidase activity after six hours of growth. Consistent with previous results (65), glucose-inducible expression of both full-length *cidABC* and *alsSD* reporter constructs was shown to be abolished in the *cidR* mutant strain (data not shown), indicating that the *cis*-acting elements important for CidR-mediated control were intact. As can be seen in Fig. 3.2, removal of the regions 5' to the nts -177, -138, and -93 upstream of the transcription start site had a minimal effect on *cidABC*-inducible expression, indicating the absence of elements important for glucose-inducible expression. In contrast, the -57 construct abolished induction, suggesting that a *cis*-acting element was present

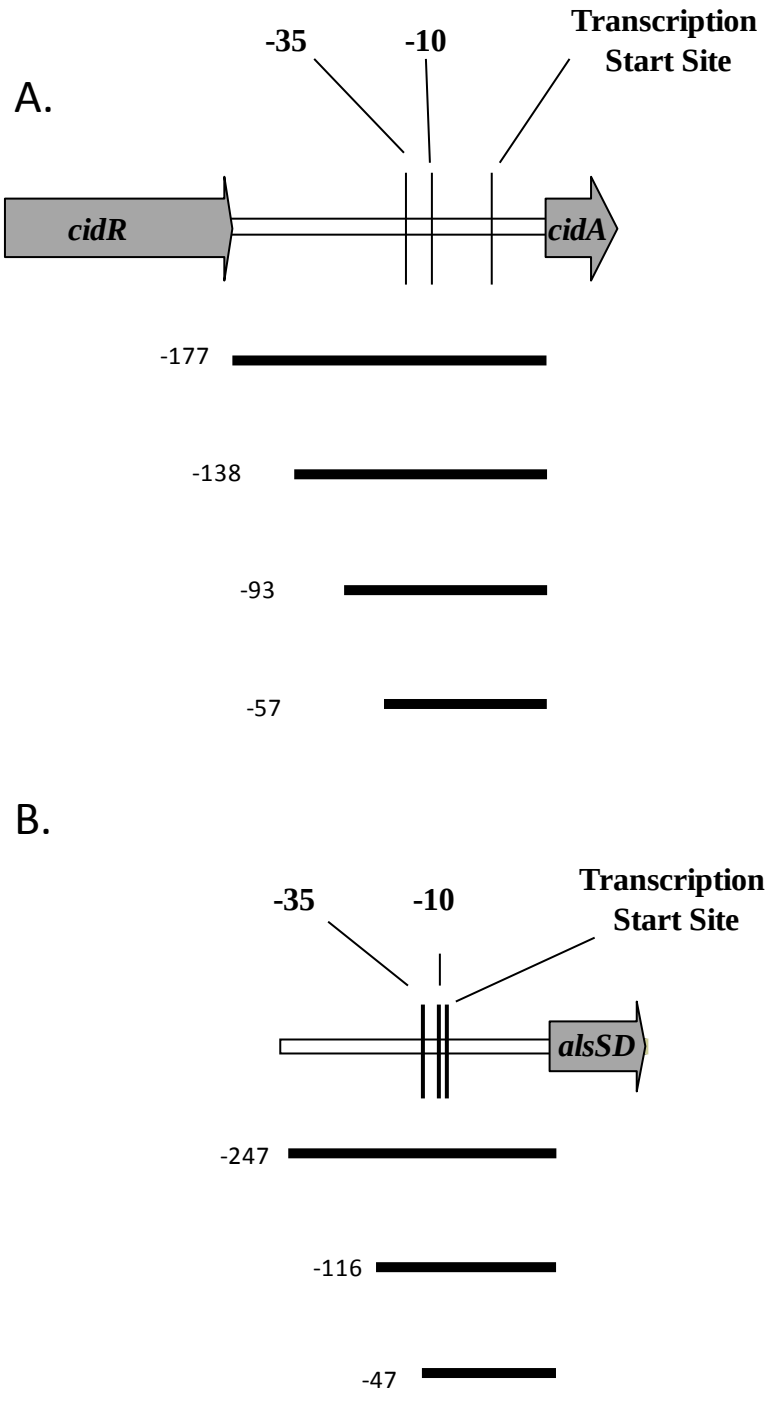

734

735 **Figure 3.1: Truncations of the *cidABC* and *alsSD* promoters.** Truncations created for *lacZ* reporter
736 plasmids in the A. *cidABC* and B. *alsSD* promoters. Truncations are denoted by numbers indicating bp be-
737 fore the transcription start site. All resulting reporter plasmids contain the native -35, -10 and transcription
738 start site elements.

739 between nts -93 and -57. Analysis of the *alsSD* reporter constructs revealed that the re-
740 moval of the regions 5' of nt -116 had little effect on glucose-inducible expression. How-
741 ever, the elimination of sequences 5' of nt -47 resulted in a dramatic reduction in glucose-
742 inducible expression, indicating the presence of an important *cis*-acting regulatory ele-
743 ment between nts -116 and -47. Inspection of the DNA sequence of both promoters in
744 this region revealed almost identical 12-bp elements, 5'-TAGTA-A/T-TACAAA-3', be-
745 tween the two promoter regions. Interestingly, this sequence was in roughly the same re-
746 gion relative to the *cidABC* and *alsSD* transcription start sites identified previously (50).
747 This conserved element identified is one bp short of the consensus LTTR binding site.

748 To specifically test the importance of these potential *cis*-acting elements, we generat-
749 ed mutations in both the *cidABC* and *alsSD* promoter reporter plasmids that altered the
750 sequences of these elements. For example, mutations were generated that replaced 4 bp
751 of the 5' half site with AAAA, changed the only non-adenine bp in the 3' half site to ade-
752 nine, and replaced the elements entirely. The reporters were then assessed for CidR-
753 dependent promoter activity as performed above. We found that all the mutations gener-
754 ated in both the *cidABC* (Fig. 3.3A) and *alsSD* (Fig. 3.3B) promoter regions eliminated
755 expression, confirming their role in the induction of transcription of these operons.

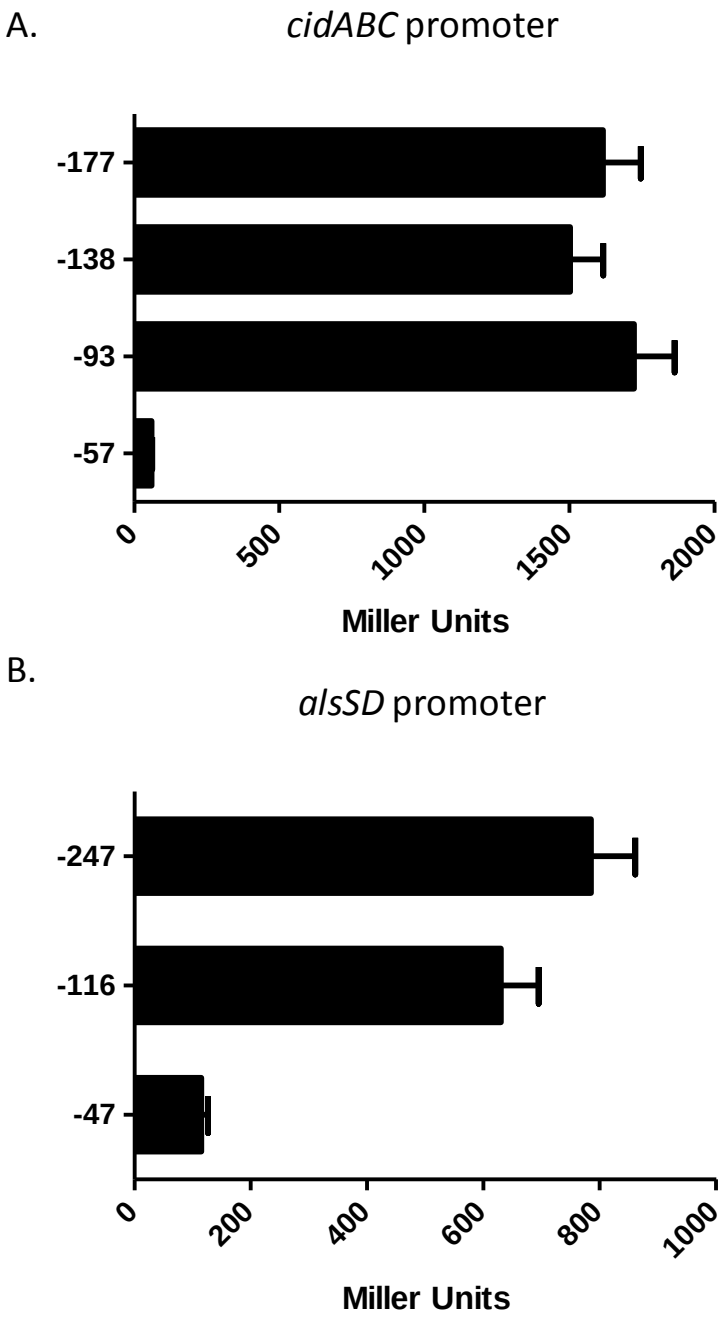

Figure 3.2: Deletion analysis of the *cidABC* and *alsSD* promoters. Truncations made in the *cidABC* (A) and *alsSD* (B) promoters and the effect on induction. Cultures were grown in flasks containing NZY + 35 mM glucose at a 1:10 media to volume ratio. After six hours of growth samples of the cultures were spun down, lysed and assayed for B-galactosidase activity. Data are the average of three separate experiments (each experiment N=3). No expression was seen in a *cidR* mutant for any truncation (data not shown).

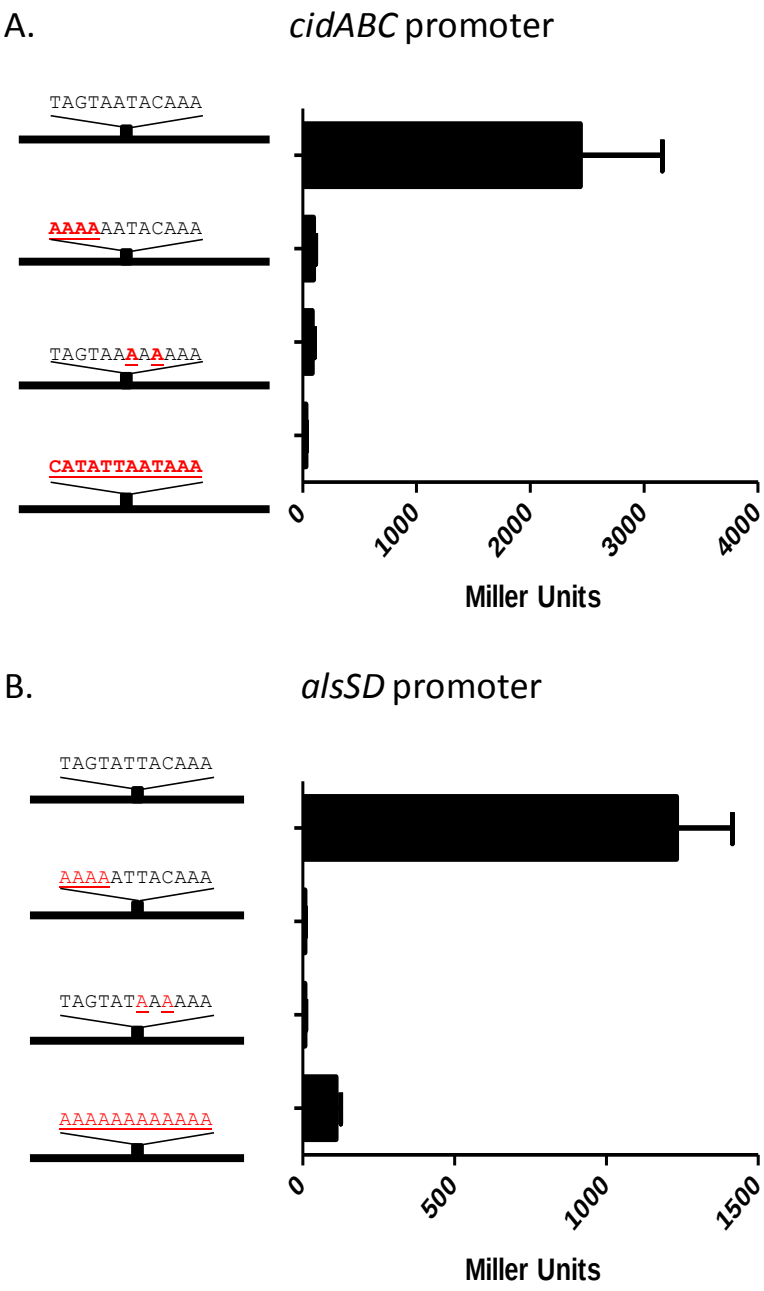

764

765 **Figure 3.3: Mutation analysis of the *cidABC* and *alsSD* promoters.** Mutations made in the *cidABC*
766 (A) and *alsSD* (B) promoters and the effect on induction. Cultures were grown in flasks containing NZY +
767 35 mM glucose at a 1:10 media to volume ratio. After six hours of growth samples of the cultures were
768 spun down, lysed and assayed for B-galactosidase activity. Data are the average of three separate experi-
769 ments (each experiment N=3). No expression was seen in a *cidR* mutant for any truncation (data not
770 shown).

771

CidR binds to the promoters of cidABC and alsSD

Although the mutagenesis data demonstrated that the 5'-TAGTA-A/T-TACAAA-3' sequence is important for glucose-inducible expression of the *cidABC* and *alsSD* operons, these results are not sufficient to demonstrate that these sequences are binding sites for CidR. To address this, we performed electrophoretic mobility-shift assays (EMSAs) using C-terminal His tag-labeled CidR protein and biotin-labeled DNA fragments from the *cidABC* and *alsSD* promoter regions. As shown in figure 3.4, incubation of purified CidR protein with either the *cidABC* (panel A) or *alsSD* (panel B) fragments resulted in a dose-dependent shift in the migration of the target DNA. The addition of 200-fold excess unlabeled specific competitor DNA effectively blocked the formation of higher order CidR-DNA complexes, indicating that the binding of CidR to the target DNA was specific.

To demonstrate that the sequence we uncovered was the CidR binding site we then tested regions upstream and downstream of the sequence from the cidABC promoter (Fig. 3.5A). CidR binding was not observed in these regions of DNA, demonstrating the specificity of these protein-DNA interactions. Finally, we exploited the findings of our mutagenesis experiments to test the sequences that altered *cidABC* expression in our EMSAs (3.5D). Complete replacement of the CidR binding site sequence with a random sequence in the competitor DNA eliminated competition, even at concentrations that were 200-fold excess of the labeled target DNA. This demonstrates the essentiality of the 5'-TAGTA-A/T-TACAAA-3' sequence is for CidR binding. Interestingly, we found that one of the mutations we made, 5'-AAAAAATACAAA-3', eliminates induction (Fig. 3.3A) but does not block CidR binding (Fig. 3.5B).

794

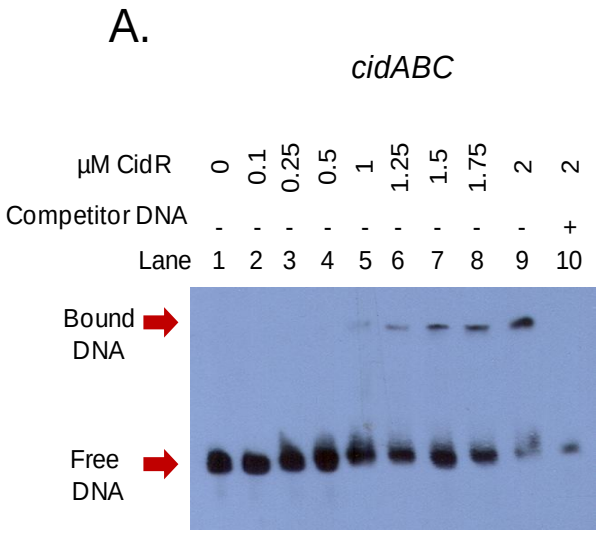

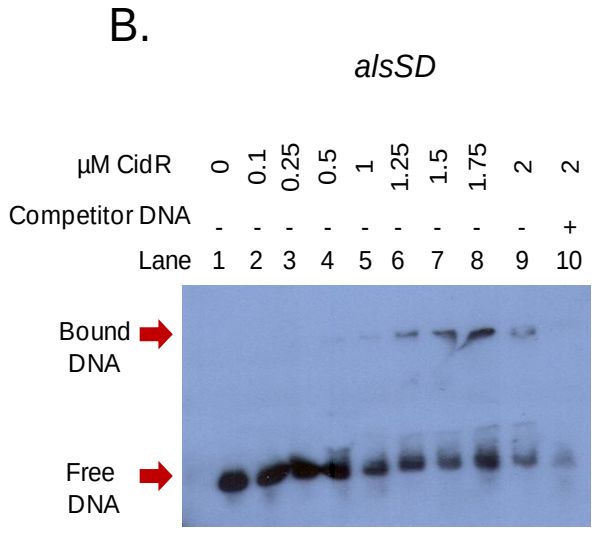

795

796 **Figure 3.4: CidR binds to the *cidABC* and *alsSD* promoters.** A. *cidABC* and B. *alsSD*. Electropho-
797 retic Mobility-Shift Assays (EMSAs) were performed using increasing amounts of purified CidR protein
798 and biotin-labeled *cidABC* promoter DNA as a target. Reaction mixtures were incubated for 30 minutes at
799 room temperature and separated in a 6% TBE polyacrylamide gel. DNA was then transferred to a nylon
800 membrane and developed as per the manufacturer's instructions. Lanes 1 and 10 contain a no-protein con-
801 trol and 200-fold excess of unlabeled competitor DNA control, respectively.

802

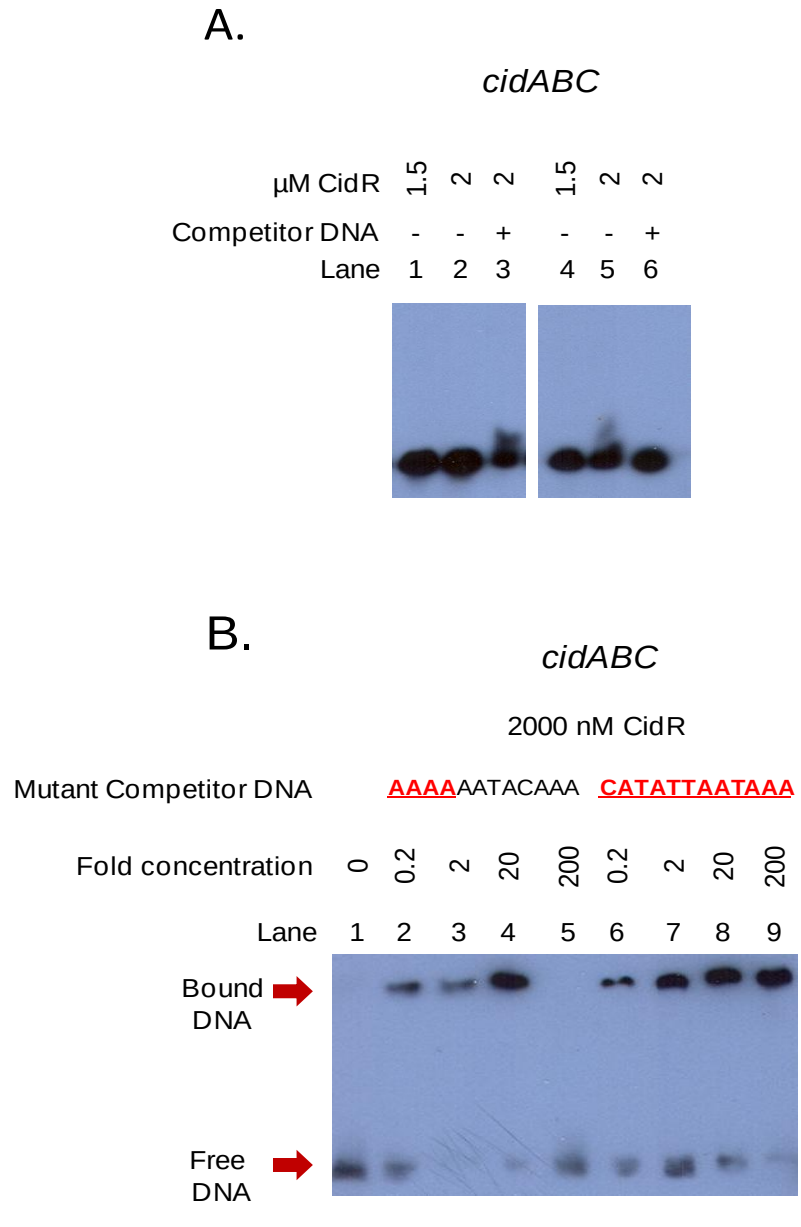

803

804 **Figure 3.5: Intact 12 bp element is required for CidR binding.** A. Biotin-labeled primers were con-
805 structed for downstream (Lanes 1-3) and upstream (Lanes 4-6) of the putative CidR binding site. B. Com-
806 petitor DNA containing mutations was added in increasing amounts (range 0.2 to 200 fold excess) to 2000
807 nM purified CidR incubated with biotin-labeled DNA. Mutations were made in the sequences shown.

These data demonstrate that the 5'-TAGTA-A/T-TACAAA-3' element is a critical binding site for CidR-mediated control of *cidABC* and *alsSD* expression.

CcpA directly regulates cidABC and alsSD induction

In addition to the CidR binding site, we noticed the presence of a putative CcpA recognition site, so-called "CRE site", directly upstream of the CidR-binding site in both the *cidABC* and *alsSD* promoter regions. It had previously been reported that disrupting CcpA altered biofilm formation and *cidABC* expression (122), though it wasn't known if this effect was due to direct regulation by CcpA, nor if CcpA affected *alsSD* expression. We therefore assessed expression of both promoters in a Δ*ccpA* mutant. In agreement with the previous report (122), we found that both *cidABC* and *alsSD* expression was reduced in a Δ*ccpA* mutant under inducing conditions (Fig. 3.6A). Quantitative RT-PCR confirmed that alteration of the expression of *cidR* was statistically insignificant in the Δ*ccpA* mutant, thus ruling out that the reduced induction exhibited by *cidABC* and *alsSD* was due to altered CidR expression (Fig. 3.6B). To determine whether CcpA-mediated regulation of *cidABC* and *alsSD* was direct we performed EMSA experiments as described above (Fig. 3.7). C-terminal His tag-labeled CcpA was affinity purified and incubated with the same 60-bp biotin-labeled *cidABC* and *alsSD* promoter fragments that were used to assess CidR binding (Fig. 3.4). Analysis of the EMSA clearly showed that CcpA bound the target DNA in a dose-dependent manner for both promoters. Furthermore, the addition of 200-fold excess unlabeled specific competitor DNA effectively

A.

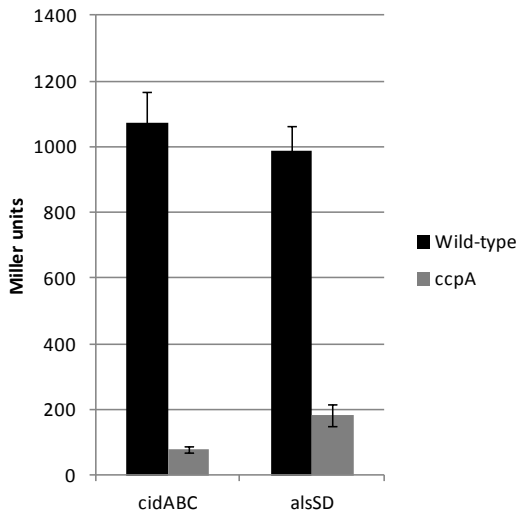

B.

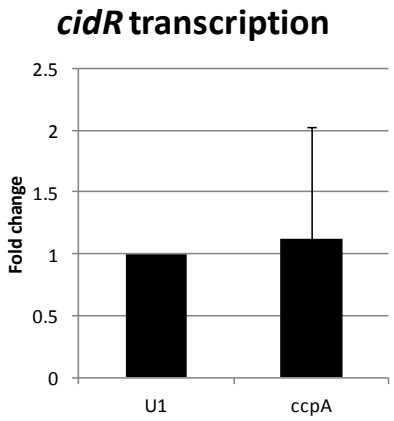

829

830 **Figure 3.6: Effect of disruption of *ccpA* on *cidABC* and *alsSD* induction.** A. Induction of *cidABC* and
831 *alsSD* in the wild-type and *ΔccpA* background. Cultures were grown in flasks containing NZY + 35 mM
832 glucose at a 1:10 media to volume ratio. After six hours of growth samples of the cultures were spun down,
833 lysed and assayed for B-galactosidase activity. Data are the average of three separate experiments (N=3). B.
834 Transcription of *cidR* in the UAMS-1 and isogenic *ccpA* background. Cultures were grown for 3 hours in
835 NZY + 35 mM glucose before mRNA isolation. Total RNA (500 ng) was converted to cDNA using the
836 Quantitect Reverse Transcription Kit (Qiagen). The samples were then diluted 1:50, and the cDNA prod-
837 ucts were amplified using the LightCycler DNA Master SYBR green I kit (Roche Applied Science) follow-
838 ing the manufacturer's protocol. The relative transcript levels were calculated using the comparative
839 threshold cycle (*CT*) method (119) with normalization to the amount of *sigA* transcripts present in the RNA
840 samples.

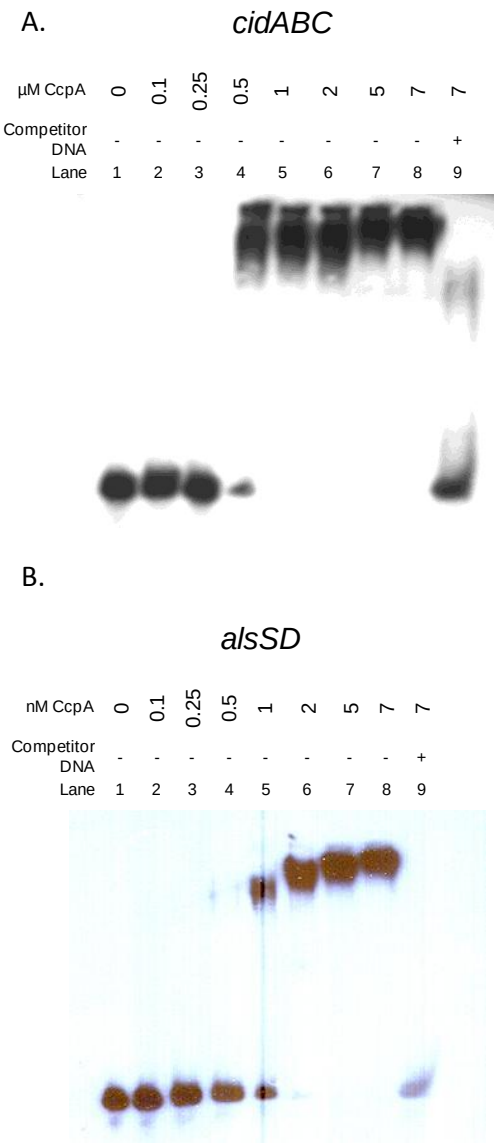

841

842 **Figure 3.7: Binding of CcpA to the *cidABC* and *alsSD* promoters.** Purified CcpA was added in increas-
843 ing concentrations (range 100 to 7000 nM) to biotin labeled target DNA for the *cidABC* (A) and *alsSD* (B).
844 Reaction mixtures were incubated for 30 minutes at room temperature and separated on a 6% TBE poly-
845 acrylamide gel. DNA was then transferred to a nylon membrane and developed as per the manufacturer's
846 instructions. Lanes 1 and 9 contain a no-protein control and 200-fold excess of unlabeled competitor DNA
847 control, respectively.

848

A. *cidABC* promoter

CATATTAATAAAGCACTCATTATTTGTGATTCCTCATTACTTGGATCATTGAAA

TAATGAGTGTTTTTTTTGTGAAAATGAAGTGAAATTTAGAGAG**CGTTTCCA**TAG

CRE

AAAA**TAGTAATACAAA**CCATAAAAAAAGAGTATTTTTATATTGTGTACGCCATC

CidR **-35**

TTTATAATAGTTATT**G**TAACAATTTAGACATATTTAGAAAGGGATGGCGCCATG

-10 *****

B. *alsSD* promoter

TTTAAATCGCCAAAAACAGCATTTTCAAACCGTCATAAAACAGCATTTTCAGCC

CGCCATAAAACGACAATTTCAAACCGTCATTGACTAAAGACCTCATTCTCAAAT

ATGCTAACAATCCTCCACACCAATCAATCCAACATCCCTTATAATCACT**CCCTT**

CRE

CAAAATCTACTCATGCATTTT**TGGAATAC**T**TAGTATTACAAA**TAACGATTTTTA

CRE **CidR** **-35**

TTCATCTTACAAAGGATATATAATGTACTGA**A**GGCAATTTTTATGTATCACAAA

-10 *****

TCTAATTGTATATGTAAAGTTTTGATAAATATCATTAATTTTACATAACTATCA

TTAGATTACAAATCACAATGTAATTACATGTAATACACATCTACACATCACATT

TGAAGGGAAATGAATATAAATG

Figure 3.8: Nucleotide sequences of the *cid* and *als* promoters. A. *cidABC* and B. *alsSD* promoters. Truncations created are denoted by numbers indicating bp before the transcription start site. The CidR and CcpA binding sites are underlined and labeled. First methionine of CidA and AlsS are colored green.

blocked the formation of higher order CcpA-DNA complexes, indicating that the binding of CcpA to the target DNA was specific. These data demonstrate that CcpA directly regulates *cidABC* and *alsSD*. The sequence of the *cidABC* and *alsSD* promoters, with the CidR and CRE sites marked can be seen in figure 3.8.

CidR and carbon catabolite repression are necessary for the induction of cidABC and alsSD

Because *ccpA* is the primary regulator of CCR in Gram positives (74), we tested what effect other carbon sources would have on the induction of *cidABC* and *alsSD*. Our hypothesis was that a carbon source whose catabolism did not result in the formation of glucose 6-phosphate and fructose 1,6 bis-phosphate would not result in induction of *cidABC*. We grew wild-type cultures in media containing either glucose (35 mM), fructose (42 mM) or glycerol (70 mM) as a carbon source. Like glucose, fructose was found to cause induction of both *cidABC* and *alsSD* (Fig. 3.9). The addition of glycerol did not promote induction from either promoter. The possibility that *S. aureus* was not consuming glycerol as a carbon source was discounted by measuring the pH. By six hours growth all cultures grown with an extra carbon source had a decrease in pH below 5.5 (data not shown), suggesting that acetate was being produced. Utilization of glycerol will not lead to the formation of glucose 6-phosphate and fructose 1,6 bis-phosphate, and thus will not promote CCR. These experiments demonstrate that CCR is a necessity for *cidABC* and *alsSD* induction.

We also confirmed this by performing a second experiment to observe the effect of disrupting *ccpA* in an *ackA* mutant background. Our lab has shown that an *ackA* mutant has increased induction of *cidABC* (72). Importantly, this occurs without the addition of 35 mM of glucose or the acidification of the media, thus giving another means of determining the contribution of CcpA-mediated CCR to *cidABC* induction. As can be seen in figure 3.10, the disruption of *ccpA* in the *ackA* background eliminates induction to the same extent as disrupting *cidR* in the *ackA* background. This demonstrates the need for CcpA even when CCR is not active.

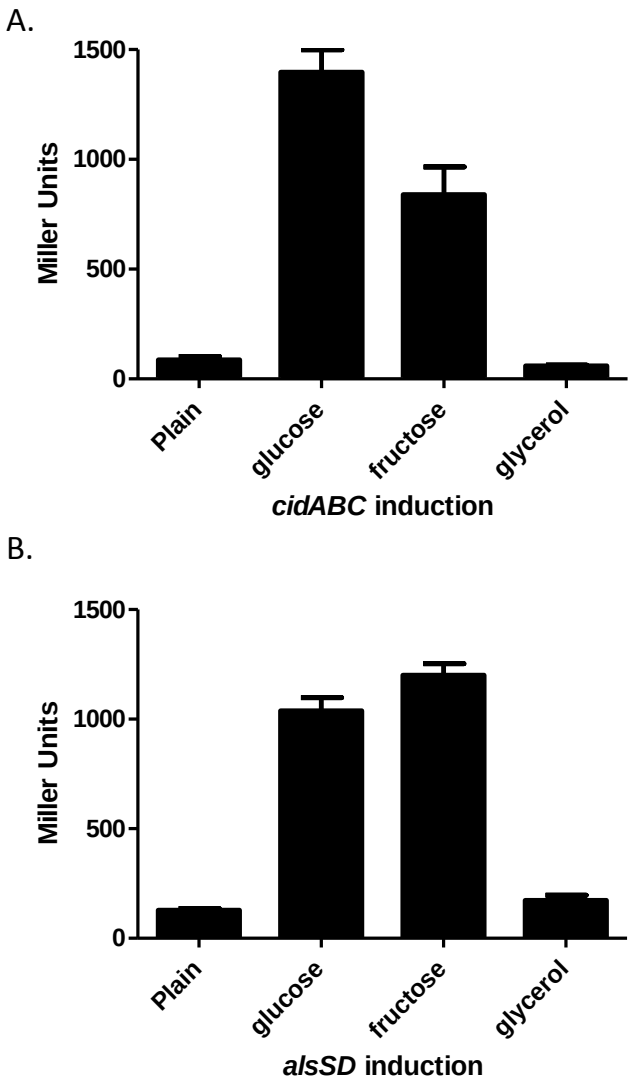

882

883 **Figure 3.9: Effect of alternative carbon sources on *cidABC* and *alsSD* induction.** Cultures containing
884 the A. *cidABC* reporter or B. the *alsSD* reporter were grown in flasks at a 1:10 media to volume ratio. Me-
885 dia was NZY with no additives, + 35 mM glucose, + 42 mM fructose or + 70 mM glycerol. After six hours
886 of growth samples of the cultures were spun down, lysed and assayed for B-galactosidase activity. Data are
887 the average of two separate experiments.

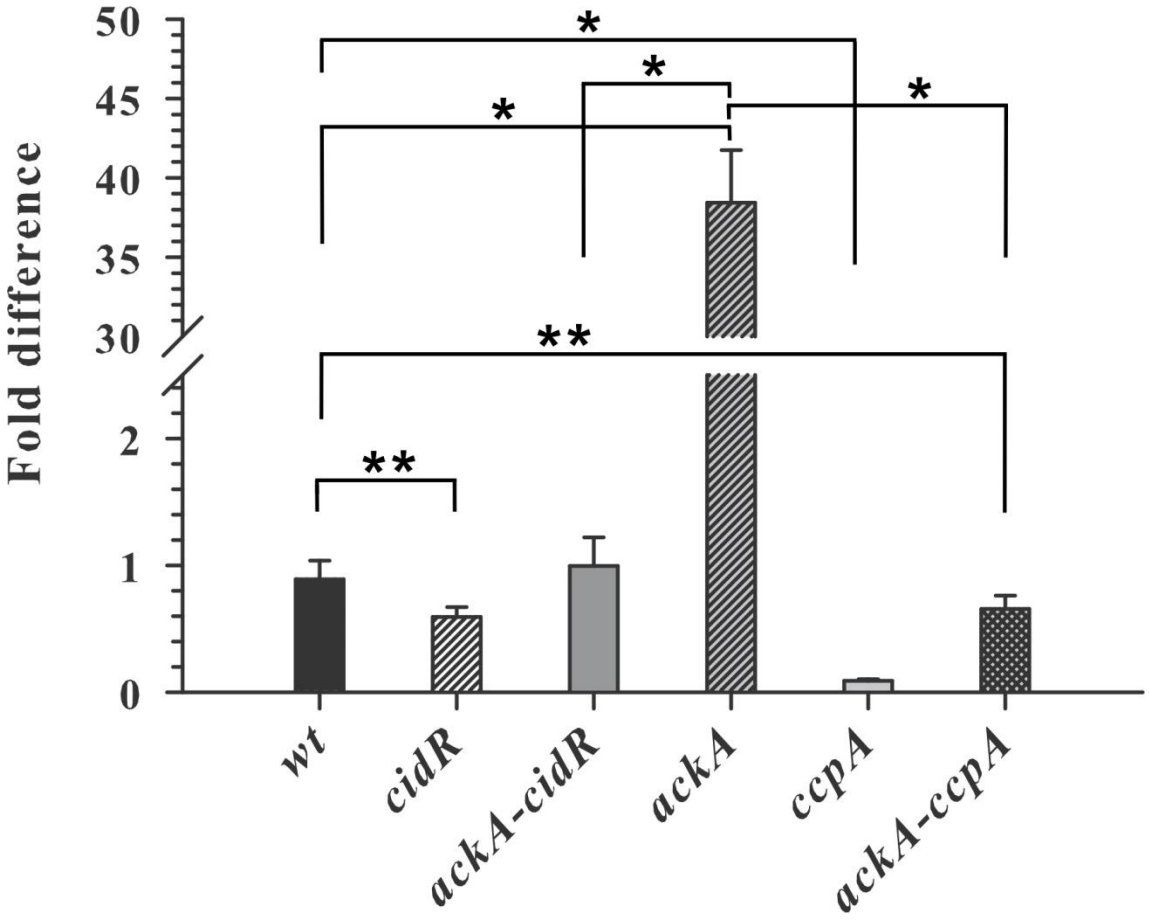

Figure 3.10: CidR and CcpA are required for full induction of *cidABC*. Transcription of *cidA* in the wild-type, Δ*cidR*, Δ*ackA* Δ*cidR*, Δ*ackA*, Δ*ccpA*, and Δ*ackA* Δ*ccpA* backgrounds. Cultures were grown for 3 hours in TSB + 35 mM glucose before mRNA isolation. Total RNA (500 ng) was converted to cDNA using the Quantitect Reverse Transcription Kit (Qiagen). The samples were then diluted 1:50, and the cDNA products were amplified using the LightCycler DNA Master SYBR green I kit (Roche Applied Science) following the manufacturer's protocol. The relative transcript levels were calculated using the comparative threshold cycle (*CT*) method (119) with normalization to the amount of *sigA* transcripts present in the RNA samples. (*P<0.001. **p<0.05)

Identification of other potential effectors of cidABC expression

Having established the roles of CidR and CcpA in the regulation of *cidABC* and *alsSD* expression, along with the findings that the SrrAB two-component system plays an important role in the regulation of *cidABC* expression, we next sought to identify metabolic effectors that influence the expression of this operon. To accomplish this, we designed an unbiased, transposon mutagenesis approach to identify additional factors/metabolic pathways that influence *cidABC* expression. We first generated a reporter strain derivative of *S. aureus* JE2 (102) that contained a chromosomally encoded P_{cidABC}::*lacZ* fusion construct that was inserted in the *geh* gene (strain KB6001). As above, we demonstrated that expression of *lacZ* was inducible by growth under glucose-excess conditions in a *cidR*-dependent fashion (data not shown), thus, giving confidence that this reporter construct reflected the normal control of the *cidABC* promoter. We then performed transposon mutagenesis as has been described previously (102) on KB6001 and screened for colonies that displayed altered *cidABC* expression. In one screen, we surveyed for mutants that caused an increase in *cidABC* expression (increased blue color) under non-inducing conditions. In another we surveyed for mutants that caused a decrease in *cidABC* expression (decreased blue color) under inducing conditions. The results of the plate screen are displayed in Table 4. Using this method we found two potential effectors of positive *cidABC* induction; acetate kinase (*ackA*) and phosphoglucosemutase/phosphomannomutase (*pgcA*). Our lab has reported previously that disrupting *ackA* increases *cidABC* induction (72), indicating that the screen was working as predicted.

We then took those mutants recovered on TSA plates and confirmed altered *cidABC* induction by quantitative beta-galactosidase assays to verify positive hits. Figure 3.11 displays the remaining potential mutants. Of particular interest to us from this screen were the *ptsH* and *ptsI* mutants; phosphocarrier protein HPr and phosphoenolpyruvate-protein phosphotransferase, respectively. As these genes are part of the PTS system and CCR, they influence CcpA binding, further demonstrating that the screen could identify effectors of *cidABC* transcription.

926 Table 4. Results of transposon mutagenesis screen

Locus	Description	Gene Name
Increase		
SAUSA300_1657	acetate kinase	*ackA*
SAUSA300_2433	phosphoglucomutase/phosphomannomutase family protein	*pgcA*
Decrease		
SAUSA300_1327	cell surface protein	*ebh*
SAUSA300_0659	sugar efflux protein, MFS family, sugar:cation symporter	
SAUSA300_0352	ABC transporter, ATP-binding protein	
SAUSA300_2645	glucose-inhibited division protein A	*gidA*
SAUSA300_0983	phosphocarrier protein HPr	*Hpr*
SAUSA300_0984	phosphoenolpyruvate-protein phosphotransferase	*ptsI*
SAUSA300_0388	inosine-5'-monophosphate dehydrogenase	*guaB*
SAUSA300_0984	phosphoenolpyruvate-protein phosphotransferase	*ptsI*
SAUSA300_0388	inosine-5'-monophosphate dehydrogenase	*guaB*
SAUSA300_1507	glucokinase	*glk*
SAUSA300_2059	ATP synthase F1, gamma subunit	*atpG*
SAUSA300_0495	hypothetical protein	
SAUSA300_1902	Conserved hypothetical protein, Lactonase	
SAUSA300_0552	Conserved hypothetical protein, LmbE family protein	
SAUSA300_2059	ATP synthase F1, gamma subunit	*atpG*
SAUSA300_1624	upstream of MutT/nudix family protein	
SAUSA300_0192	Conserved hypothetical protein	*murQ?*
Intergenic	metallopeptidase	
SAUSA300_2588	preprotein translocase	*SecY*
Intergenic	upstream of rrsC, 16s ribosomal RNA	
SAUSA300_1393	phiSLT ORF2067-like protein, phage tail tape measure protein	
SAUSA300_1015	cytochrome oxidase assembly protein	*ctaA*
SAUSA300_0764	ribonuclease R	*rnr*
SAUSA300_1259	ImpB/MucB/SamB family protein; DNA damage repair	
SAUSA300_0123	siderophore biosynthesis protein, IucC family	

SAUSA300_1286	aspartate kinase	

927

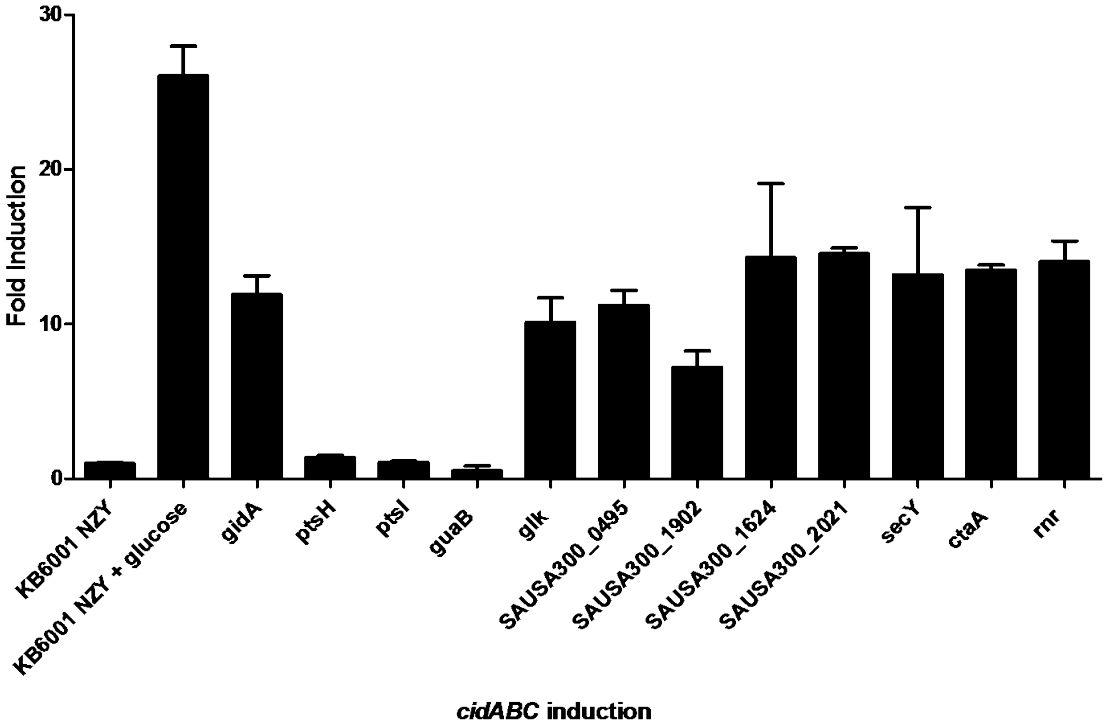

928

929 **Figure 3.11: *cidABC* induction in isolated transposon mutants**. Transposon mutants listed in Table 4
930 were tested for *cidABC* induction in planktonic culture. Cultures were grown in flasks containing NZY + 35
931 mM glucose at a 1:10 media to volume ratio. After six hours of growth samples of the cultures were spun
932 down, lysed and assayed for β-galactosidase activity. Data are the average of at least two separate experi-
933 ments. Mutants shown are remaining mutants after eliminating false positives.

Discussion

In this study we sought to better understand the regulation of the *cidABC* and *alsSD* operons. Our lab has demonstrated the necessity of CidR for their induction (64, 65). However, it was unknown what DNA sequence to which CidR binds, and thus whether or not CidR-mediated regulation of *cidABC* and *alsSD* was direct or through an intermediate transcriptional regulator. CidR is a member of the LTTR family of proteins (65), which have a characteristic binding sequence termed the T-N_{11}-A motif (87). However, the promoters of *cidABC* and *alsSD* are AT-rich and contain an abundance of potential T-N_{11}-A motifs (Fig. 3.8), so a homologous sequence with a T-N_{11}-A motif between the promoters of *cidABC* and *alsSD* that could be the CidR-binding site was not readily apparent. As it has previously been shown that disrupting out *cidR* eliminates *cidABC* and *alsSD* induction (64, 65) we created a series of nested truncations that removed all or part of the CidR binding site. Examination of expression from the truncations revealed a region of the DNA that was essential for induction in both promoters (Fig. 3.2). Upon examination of the DNA sequence, a conserved element was noted, 5'-TAGTA-A/T-TACAAA-3'. Mutations made in this sequence eliminated induction in both the *cidABC* and *alsSD* promoters (Fig. 3.3), further demonstrating the importance of this element. EMSAs performed (Fig. 3.4 and 3.5) confirmed that CidR directly binds to this element.

CidR has been demonstrated to regulate only the *cidABC* and *alsSD* operons (64), despite the fact that LTTRs are usually thought of as global transcriptional regulators (87). Using the newly discovered CidR binding sequence we performed a search for other potential CidR-binding sites in the UAMS-1 genome. The 5'-TAGTA-A/T-TACAAA-3'

motif occurs in only 4 other locations in hypothetical genes, and is not found in the promoters of genes or operons other than *cidABC* and *alsSD* (data not shown). This makes us confident that the 5'-TAGTA-A/T-TACAAA-3'element is the target of CidR binding.

Interestingly, we found that one of the mutations we made, 5'-AAAAAATACAAA-3', eliminates induction (Fig. 3.3) but does not block CidR binding (Fig. 3.5B). The canonical LTTR binding region contains two separate binding sites separated by a few bp, termed the Recognition Binding Site (RBS) and the Activation Binding Site (ABS). The LTTR binds each site as a dimer, the dimers interact to form a tetramer, and the tetramer acts to bend the DNA (87). It is thought that the high angle of the bent DNA impedes formation of the RNA transcription bubble. In the presence of a signal the LTTR undergoes a conformational change, causing the tetramer to shift on the DNA and relax the angle. The new angle then allows for the formation of an RNA transcription bubble, and facilitates transcription. This model of LTTR regulation has been termed the 'sliding dimer' model (97). By replacing four bp of the 5' half site with adenines, it would appear that we have made it so that CidR can still bind the DNA but cannot bend the DNA into a conformation that would lead to induction of *cidABC* transcript.

Our lab had also proven previously that SrrAB acts as a direct regulator of *cidABC* expression (104), so we were curious what other transcriptional regulators besides CidR and SrrAB would play a direct role in the regulation of *cidABC* and *alsSD*. While producing truncations we noticed the presence of putative CRE sites directly upstream of the CidR-binding site in both the *cidABC* and *alsSD* promoter regions. We therefore assessed expression of both promoters in a Δ*ccpA* mutant. We found that both *cidABC* and *alsSD*

978 expression was reduced in a Δ*ccpA* mutant under inducing conditions (Fig. 3.6A), and
979 that this regulation was direct (Fig. 3.7). While it had previously been reported that dis-
980 rupting CcpA altered biofilm formation and *cidABC* expression (122), these results con-
981 firm that this is due to direct regulation by CcpA. This is also the first report of CcpA-
982 mediated regulation of *alsSD* expression in *S. aureus*.

983 Our transposon mutagenesis screen suggested that CCR could play a role beyond me-
984 tabolism, so we investigated the transcriptional regulator CcpA, as it has been suggested
985 before that CcpA plays a role in *cidABC* induction (122). Here we show that CcpA is re-
986 quired for the induction of *cidABC* and also *alsSD* (Fig. 4A). Importantly, CcpA binds
987 both promoters (Fig. 4B-C), demonstrating for the first time that CcpA-mediated regula-
988 tion of *cidABC* and *alsSD* is direct.

989 In conclusion, our work here demonstrates two novel findings concerning *cid*-
990 mediated cell death in *Staphylococcus aureus*. We used genetic techniques to create trun-
991 cations and mutations in the *cidABC* and *alsSD* promoters to ultimately define the se-
992 quence of the CidR binding site, 5'-TAGTA-A/T-TACAAA-3'. We have also found that
993 *cid*-mediated cell death is directly linked to the phosphotransferase system and central
994 metabolism through CcpA-mediated transcription. Our transposon mutagenesis screen
995 revealed other potential modulators for further study. Our work here expands our under-
996 standing of cell death in bacteria.

997

Chapter IV. SrrAB modulates *Staphylococcus aureus* cell death through regulation of *cidABC* transcription

Introduction

A fundamental aspect of bacterial biofilms is the synthesis of self-produced extracellular matrix molecules that are critical for intercellular adherence and binding to surfaces (34). These molecules are diverse in nature and include specific carbohydrates, proteins, and extracellular DNA (eDNA). In *Staphylococcus aureus,* it has been demonstrated that eDNA is released as a consequence of the death and lysis of a subpopulation of cells in the biofilm via a process termed bacterial programmed cell death (PCD) (32, 41, 121). The surviving cells derive benefit from the death of the subpopulation by using the eDNA as part of the scaffolding of the matrix. Although the mechanism(s) controlling cell death remain to be elucidated, this process is known to involve the products of the *cidABC* and *lrgAB* operons, which share many features in common with the regulatory components known to regulate PCD in more complex eukaryotic organisms (41, 56, 123).

The current model for the role of the *cidABC* and *lrgAB* operons in cell death is based on the functions of holins and antiholins in the control of cell death and lysis during the lytic cycle of a bacteriophage infection (50). Similar to holins, CidA is thought to have the capacity to form pores in the cytoplasmic membrane by oligomerization, leading to depolarization of the membrane and cell death, followed by the activation of murein hydrolase activity and cell lysis (56). LrgA, as an anti-holin (52), is envisioned to oppose the activity of CidA, interfering with its ability to depolarize the membrane and cause subsequent death and lysis (50). Thus, the balance between CidA and LrgA is thought to

determine whether a cell will live or die. Indeed, both CidA and LrgA have been shown to associate with the cytoplasmic membrane and oligomerize into high molecular weight complexes (53). More recently, *cidC*-encoded pyruvate oxidase (60) was shown to promote cell death during stationary phase and biofilm development by producing acetate and promoting the acidification of the growth media (61). Thus, we hypothesize that the *cid* operon influences cell death both by affecting murein hydrolase activity and by acidifying the local environment.

The regulation of *cidABC* expression is known to be mediated by CidR, which is required for the induction of expression during growth in excess glucose (50) or low oxygen (31). Recent studies have also demonstrated that *cidABC* expression is influenced by the SrrAB two-component system, known to be important for anaerobic growth and survival (81). Disruption of *srrAB* resulted in enhanced cell death and decreased biofilm thickness (83, 84), likely as a result of the role this regulatory system has in adaptation to an anaerobic environment. In the current study we demonstrate that the increased death exhibited by the *srrAB* mutant is a function of increased *cidABC* expression caused by the *srrAB* mutation. However, in contrast to our expectations, the increased death observed was not a function of increased acetate accumulation. Rather, death was associated with *cidB*-dependent increased reactive oxygen species (ROS) accumulation. Thus, these results are the first to demonstrate a positive role for CidB in cell death.

Results

Disruption of srrAB enhances weak acid-dependent death

Previous studies have demonstrated a pronounced cell death phenotype associated with the Δ*srrAB* mutation (83, 84). Given that transcription profiling experiments suggested that the SrrAB regulatory system has a negative effect on *cidABC* transcription (83), and that media acidification due to the accumulation of acidic fermentative metabolites can influence cell fate (61), we initially tested the hypothesis that increased *cidC*-dependent acetate production was responsible for the decreased survival of a *S. aureus* Δ*srrAB* mutant relative to the wild-type strain. Thus, we monitored the survival of the wild-type strain and the Δ*srrAB* mutant in stationary phase following growth in tryptic soy broth (TSB) supplemented with excess glucose (35 mM) as previously described (61). Indeed, the Δ*srrAB* mutant exhibited an increased rate of cell death in the presence of 35 mM glucose compared to the wild-type strain, but demonstrated similar survival in stationary phase when grown in the presence of 14 mM glucose (Fig. 4.1A) indicating that acidification is necessary for cell death to occur. Additionally, consistent with a role for acetate in modulating the rate of cell death associated the Δ*srrAB* mutant during stationary phase, cell viability of both the wild-type and mutant strains was dramatically increased when grown in media (TSB supplemented with 35 mM glucose) buffered to a pH of 7.4 with 50 mM MOPS (Fig. 4.5A), most likely due to the inability of acetate (pK_a = 4.8) to permeate cells and acidify the cytoplasm under relatively neutral conditions (61). Much to our surprise, however, measurements of acetate production and culture pH revealed that the *srrAB* mutant produced nearly identical amounts of acetate compared to

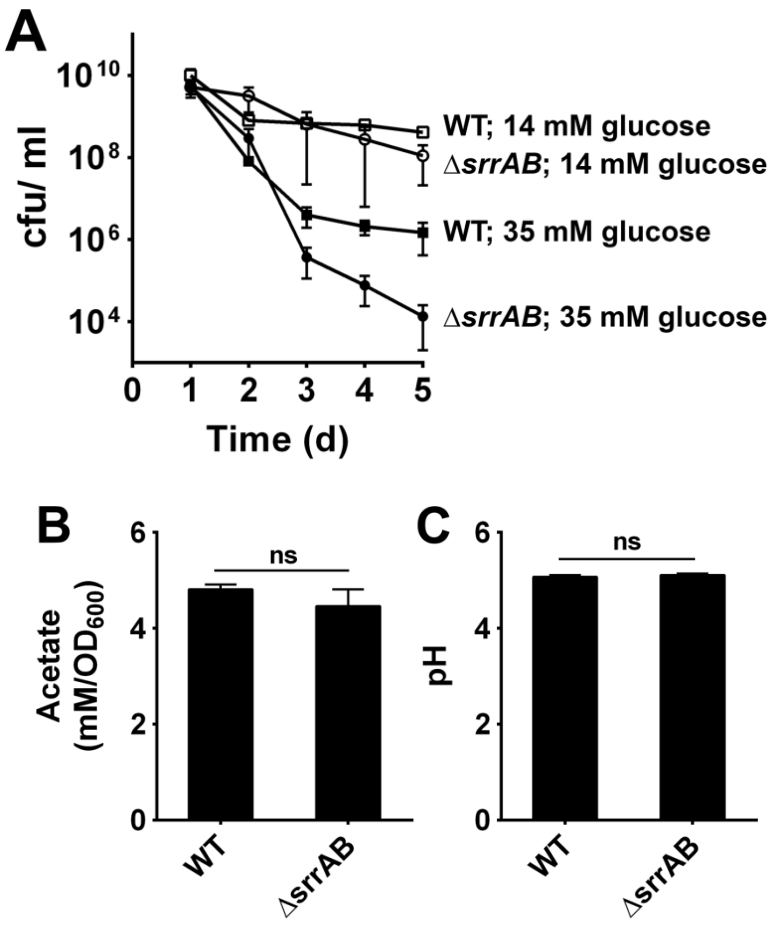

1062

1063 **Figure 4.1. Acidic conditions adversely affect survival of the Δ*srrAB* mutant in stationary phase. A.** *S.*
1064 *aureus* UAMS-1 (WT) and the isogenic Δ*srrAB* mutant cell viabilities (cfu/ml, mean ± SEM) were moni-
1065 tored every 24 h over a period of five days in TSB + 14 mM glucose or TSB + 35 mM glucose. Cultures
1066 were grown at 37°C under aerobic conditions. **B.** Acetate levels accumulated in *S. aureus* UAMS-1 (WT)
1067 and the isogenic Δ*srrAB* mutant culture supernatants were measured after 24 h of growth in TSB + 35 mM
1068 glucose using a commercially available kit (R-biopharm). **C.** The corresponding pH values of the culture
1069 supernatants from panel B.

1070

1071

the wild-type strain (Fig. 4.1B) and exhibited similar culture pH values (Fig. 4.1C) when grown in the presence of 35 mM glucose. Thus, in contrast to our hypothesis, these data indicate that the decreased viability of the Δ*srrAB* mutant during stationary phase is not due to the increased production and release of acetate.

Decreased srrAB mutant viability is dependent on enhanced cidABC transcription

Although the increased death of the Δ*srrAB* mutant in stationary phase did not correlate with acetate excretion, *cidABC* expression was still involved in this process. As shown in Figure 4.2A, survival of the *srrAB* mutant during stationary phase was dramatically improved by disruption of the *cidABC* operon, to levels similar to that associated with cells containing the *cidABC* mutation alone, as well as to those observed previously for an *S. aureus* strain containing the *cidC* deletion alone (61). To confirm that disruption of *srrAB* results in increased *cidABC* transcription, we engineered a reporter construct, pIHW10lac, that contained the *cidABC* promoter fused to a *lacZ* reporter. Both the wild-type and the Δ*srrAB* mutant strains containing the reporter plasmid were grown in media containing 35 mM glucose and assayed for β-galactosidase activity. As shown in Figure 4.2B, *srrAB* disruption resulted in an approximately 4-fold increase in *cidABC* expression compared to the wild-type strain, consistent with previously published results (83). Complementation of *srrAB in trans* under the control of its native promoter restored *cidABC* promoter activity to wild-type levels (Fig. 4.2B). To determine whether SrrA directly binds the *cidABC* promoter region, we performed electrophoretic mobility shift assays (EMSA) (Fig. 4.2C). C-terminal His tag-labeled SrrA was affinity purified and incubated

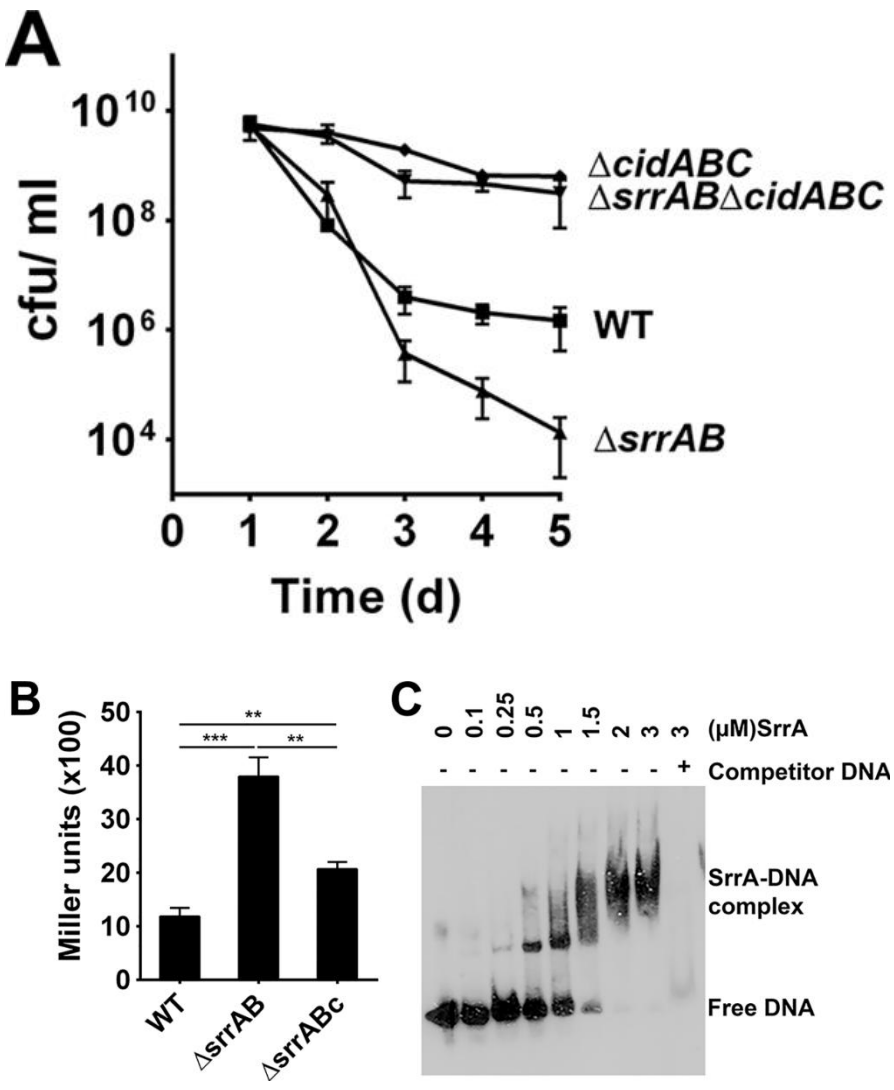

1094

1095 **Figure 4.2. The Δ*srrAB* phenotype requires *srrAB*-dependent *cidABC* expression. A.** *S. aureus* UAMS-
1096 1 (WT) and the isogenic Δ*srrAB*, Δ*cidABC*, and Δ*srrAB*Δ*cidABC* mutant cell viabilities (cfu/ml, mean ±
1097 SEM) were monitored every 24 h over a period of five days in TSB + 35 mM glucose. Cultures were grown
1098 at 37°C under aerobic conditions. **B.** *S. aureus* cells containing a *cidABC* promoter fused to *lacZ* were
1099 grown to post-exponential phase and assayed for β-galactosidase activity. **C.** Electrophoretic Mobility-Shift
1100 Assays (EMSAs) were performed using increasing amounts of purified SrrA protein and biotin-labeled
1101 *cidABC* promoter DNA as a target. Reaction mixtures were incubated for 30 minutes at room temperature
1102 and separated in a 6% TBE polyacrylamide gel.

with 60-bp biotin-labeled DNA fragments of the *cidABC* promoter region including the putative SrrA binding site (Fig. 4.5B). Analysis of the EMSA clearly showed that SrrA bound the target DNA in a dose-dependent manner. Furthermore, the addition of 200-fold excess unlabeled specific competitor DNA effectively blocked the formation of higher order SrrA-DNA complexes, indicating that the binding of SrrA to the target DNA was specific. Taken together, these data demonstrate that SrrA acts as a direct repressor of *cidABC* transcription, and that the decreased viability of the *srrAB* mutant in stationary phase is a function of enhanced *cidABC* expression, but not a result of increased production of CidC-mediated acetate excretion into the culture medium.

The ΔsrrAB mutant generates increased levels of reactive oxygen species

Given that death induced by weak acids is associated with the inhibition of respiration and the production of reactive oxygen species (ROS) in *S. aureus* (61), we also tested the hypothesis that the decreased survival of the *srrAB* mutant in stationary phase was due to increased sensitivity to ROS. Both the wild-type strain and Δ*srrAB* mutant were grown in TSB supplemented with 35 mM glucose and co-stained with cyano-2, 3-ditolyl tetrazolium chloride (CTC) and 3'-(*p*-hydroxyphenyl) fluoroscein (HPF) at 24 h and 72 h, which have previously been used to distinguish between respiring bacterial populations and those generating deleterious hydroxyl radicals (124, 125). As expected under these conditions, both the wild-type strain and Δ*srrAB* mutant exhibited respiring populations at 24 h (Fig. 4.3A). However, these populations declined by 72 h and were replaced by a ROS-generating population (HPF positive) (Fig. 4.3A). Interestingly, the mutant

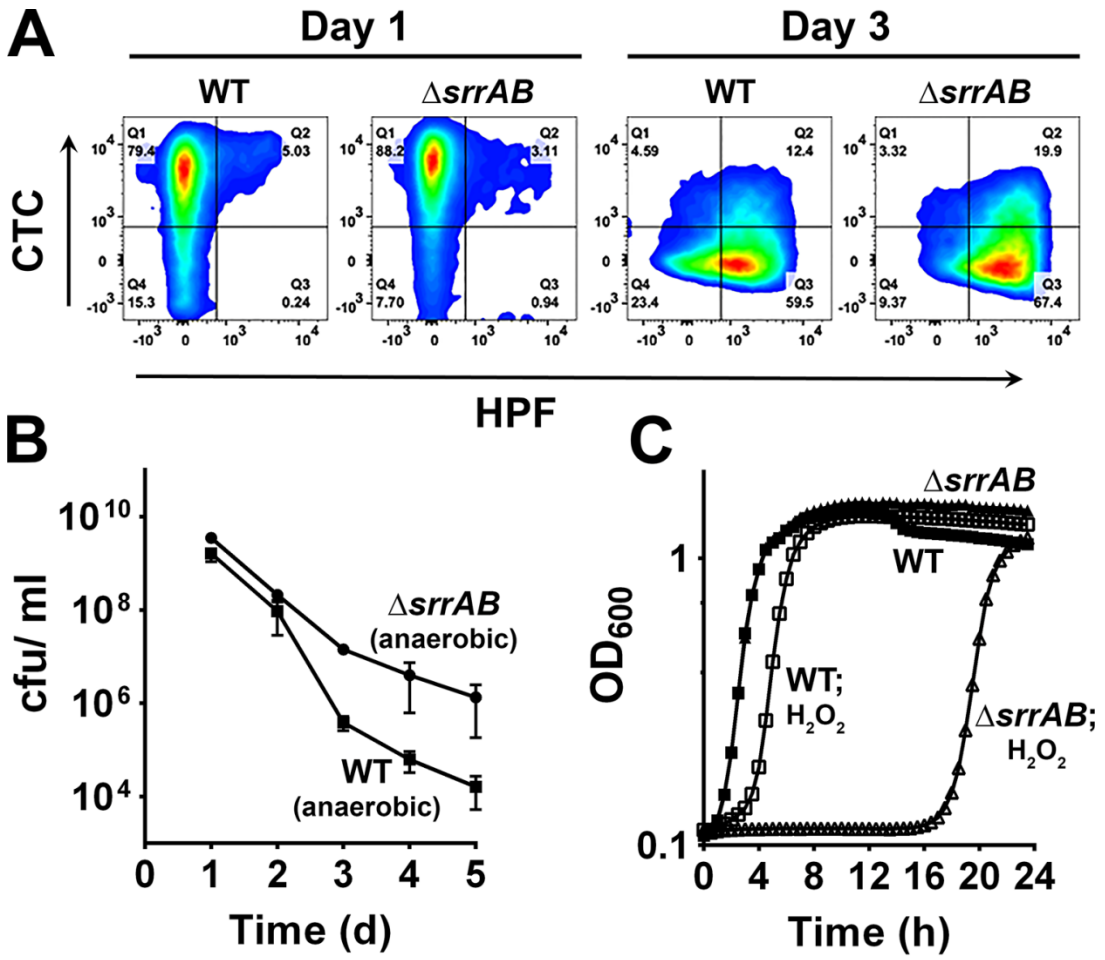

1125

1126 **Figure 4.3. Effect of the Δ*srrAB* mutation on ROS production and survival. A.** *S. aureus* UAMS-1
1127 (WT) and isogenic Δ*srrAB* mutant cells were collected at one and three days of growth in TSB + 35 mM
1128 glucose at 37°C under aerobic conditions, stained with CTC and HPF, and then analyzed by flow cytometry.
1129 **B.** Aerobically grown cells of UAMS-1 and Δ*srrAB* mutant (TSB-35 mM glucose) were shifted to an an-
1130 aerobic chamber after 24 hours of growth and monitored for cell viability every 24 h over a period of five
1131 days in TSB + 35 mM glucose. **C.** Growth of *S. aureus* UAMS-1 (WT) and Δ*srrAB* mutant cultures con-
1132 taining 5 mM H_2O_2 were monitored for 24 h at 37°C in a Tecan infinite 200 spectrophotometer under max-
1133 imum aeration.

produced 15% more HPF-positive cells at 72 h of growth compared to the wild-type strain (Fig. 4.3A). These observations suggest that increased cell death observed in the Δ*srrAB* mutant may be a consequence of ROS accumulation. Evidence supporting this hypothesis was obtained by shifting the Δ*srrAB* mutant to anaerobic conditions following 24 h of aerobic growth in TSB supplemented with 35 mM glucose (Fig. 4.3B). This strategy allowed the cells to remain under weak acid stress, but devoid of the ROS observed at 72 h of growth due to the anoxic growth conditions. Consistent with a significant role for ROS in catalyzing cell death of the Δ*srrAB* mutant, we observed that a shift to anaerobiosis improved the survival of the Δ*srrAB* mutant, even beyond that observed for the wild-type strain. Finally, to test the relative sensitivity of the Δ*srrAB* mutant to oxidative stress, we performed growth experiments in the presence and absence of hydrogen peroxide. As shown in Figure 4.3C, analysis of cell growth (OD_{600}) revealed that the Δ*srrAB* mutant was more sensitive to hydrogen peroxide challenge (5 mM) than the wild-type strain. Together, these data suggest a role for SrrAB in negatively regulating cell death under acidic conditions by decreasing the generation of ROS while at the same time increasing resistance to these toxic molecules, possibly by modulating antioxidant activities.

*Inactivation of cidB rescues the Δsrr**AB** mutant from stationary phase cell death*

Although a role for the SrrAB regulon in an adaptive response to anaerobiosis has been demonstrated, its ability to modulate ROS sensitivity has not been reported. Since disruption of *cidABC* increased stationary phase survival (Fig. 4.2A), and since CidA is a

integral membrane protein that has holin-like properties proposed to be involved in the control of cell death, we reasoned that its expression in the context of the *srrAB* mutant background may affect stationary phase survival. To test this hypothesis, in-frame and isogenic deletion mutants (Δ*srrAB*Δ*cidA*, Δ*srrAB*Δ*cidB* and Δ*srrAB*Δ*cidC*) were generated and monitored for their survival relative to the Δ*srrAB* mutant. Consistent with our previous studies of a Δ*cidC* mutant, a triple mutant in which both *srrAB* and *cidC* were disrupted (Δ*srrAB*Δ*cidC*) exhibited a decrease in ROS generation and increased population of respiring cells at day 3 (Fig. 4.4A), resulting in increased stationary phase survival (Fig. 4B). This was due to reduced acetate excretion (Fig. 4.4C). Interestingly, despite generating higher acetate levels than the Δ*srrAB*Δ*cidC* mutant (Fig. 4.4C), as well as a lower pH (Fig. 4.4D), the Δ*srrAB*Δ*cidB* mutant phenocopied the Δ*srrAB*Δ*cidC* mutant in terms of survival (Fig. 4.4B) and the presence of a healthy respiring population and reduced generation of ROS relative to the wild-type strain (Fig. 4.4A). A polar effect of *cidB* mutation on the *cidC* allele was ruled out as trans-complementation of *cidB* in the Δ*srrAB*Δ*cidB* mutant restored the rates of cell death (Fig 4.5C) to levels observed in the Δ*srrAB* mutant. Consistent with its decreased ROS production and similar to the Δ*srrAB*Δ*cidC* mutant, the Δ*srrAB*Δ*cidB* mutant was more resistant to oxidative stress upon hydrogen peroxide challenge (Fig. 4.4E), a phenotype that could also be complemented in the latter strain by expressing *cidB* in trans (Fig 4.5D). Taken together, these data suggest that over-expression of CidB in the Δ*srrAB* mutant induces cell death by enhancing ROS production and increasing sensitivity to oxidative stress. In contrast, although the *cidA* gene is co-expressed with *cidB* and *cidC*, the Δ*srrAB*Δ*cidA* mutant exhib-

ited phenotypes similar to that of the Δ*srrAB* mutant with respect to ROS production, acetate generation and survival in stationary phase (Fig. 4.4A-D).

Role of superoxide dismutase and catalase in the increase sensitivity of srrAB to ROS

When *srrAB* is transferred to anaerobic conditions after 24 hours aerobic growth it demonstrates improved survival compared to the wild-type, demonstrating that the *srrAB* mutant has increase sensitivity to ROS (Fig. 4.3B). Since *cidB* would appear to reduce the production of reactive oxygen species (Fig. 4.4A) we reasoned that the Δ*cidB* mutation would not rescue the Δ*srrAB* mutant under anaerobic conditions. To test this hypothesis we grew our mutants (Δ*srrAB* Δ*cidA,* Δ*srrAB* Δ*cidB* and Δ*srrAB* Δ*cidC*) for 24 hours aerobically before transferring the cultures to an anaerobic chamber, and monitored their survival relative to the Δ*srrAB* mutant via cfu count (Fig. 4.6A). The *srrAB cidC* mutant displays improved survival compared to the *srrAB* mutant, consistent with decreased acidic stress due to lower concentrations of acetate within the first 24 hours. The *srrAB cidA* mutant demonstrates decreased survival compared to the *srrAB* mutant, a result consistent with the increased acetate concentration that results with the disruption of *cidA*. In keeping with our hypothesis, disrupting *cidB* does not rescue *srrAB* to the extent that as disruption of *cidC* under anaerobic conditions, confirming that CidB plays a role in ROS sensitivity. Interestingly, Δ*srrAB* Δ*cidB* demonstrated an intermediate phenotype between Δ*srrAB* Δ*cidC* and Δ*srrAB* for the first 3 days, before experiencing massive die off on the 4^{th} day, ending the experiment with a population comparable to that Δ*srrAB* Δ*cidA*. This

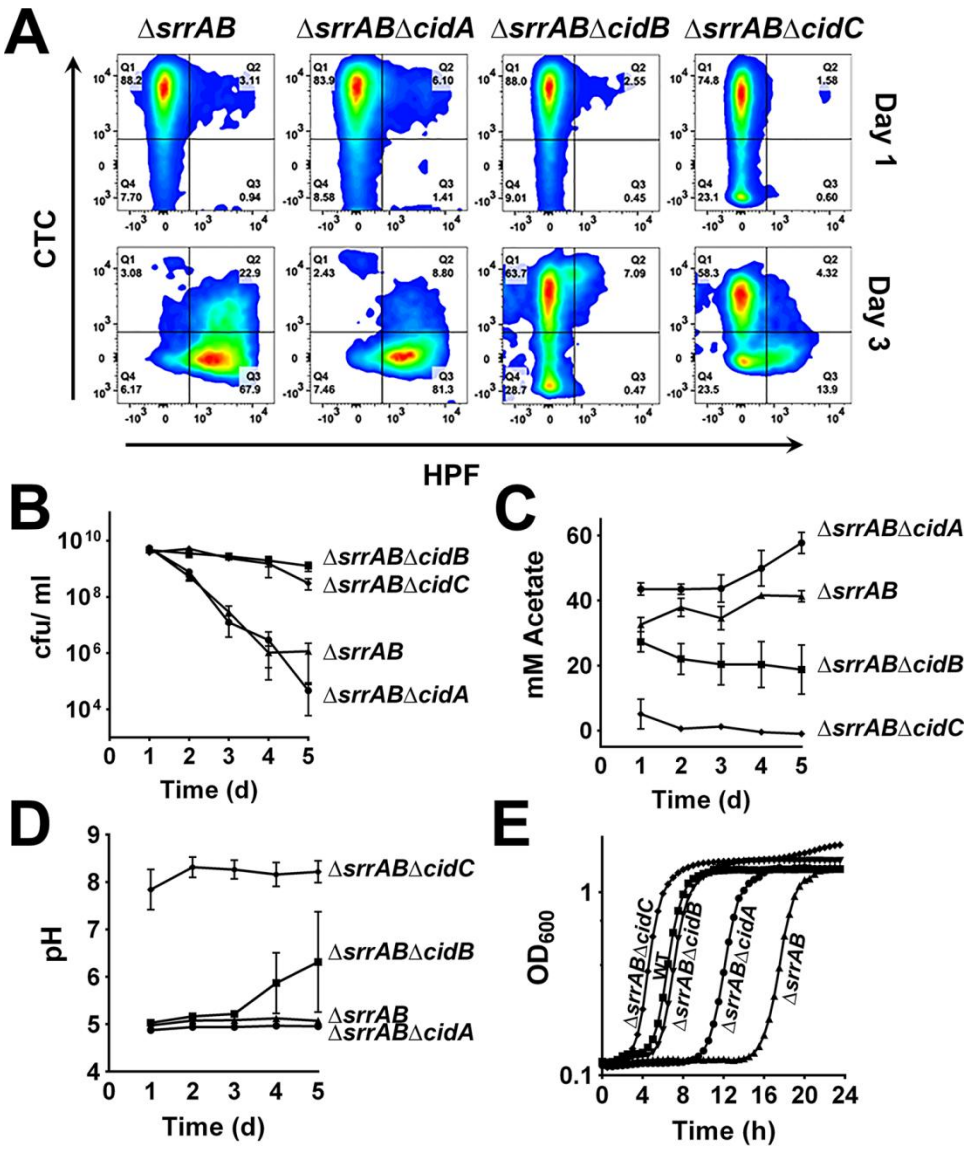

1199

1200 **Figure 4.4. Role of the *cidABC* genes on ROS production and survival. A.** *S. aureus* Δ*srrAB*,
1201 Δ*srrAB*Δ*cidA*, Δ*srrAB*Δ*cidB*, and Δ*srrAB*Δ*cidC* mutants were collected at one and three days of growth in
1202 TSB + 35 mM glucose at 37°C under aerobic conditions, stained with CTC and HPF, and then analyzed by
1203 flow cytometry. **B.** Cell viabilities (cfu/ml, mean ± SEM) were monitored every 24 h over a period of five
1204 days in TSB + 35 mM glucose. **C.** Acetate concentrations in culture supernatants were measured every 24 h
1205 over a period of five days using a commercially available kit (R-biopharm). **D.** The pH of the culture su-
1206 pernatants. **E.** Overnight cultures were resuspended to an OD_{600} of 0.06 in TSB. Growth of the *S. aureus*
1207 mutants in the presence of 5 mM H_2O_2 were monitored for 24 h at 37°C in a Tecan infinite 200 spectropho-
1208 tometer under maximum aeration.

would suggest that CidB plays not only a role in sensitivity to ROS, but also a role in acid resistance.

Given that the *srrAB* mutant displayed increased sensitivity to ROS (Fig. 4.3B) it seemed likely that disrupting *srrAB* had altered transcription of superoxide dismutase or catalase. When the transcription of these genes was investigated, however, there was no significant alteration in the expression of the genes encoding these enzymes in the Δ*srrAB* mutant (Fig. 4.6B). Thus, the sensitivity to ROS demonstrated by the Δ*srrAB* mutant is the result of something other than an inability to detoxify increased ROS.

SrrAB-mediated repression of the alsSD promoter

We reasoned that because the synthesis of 2,3-butanediol from acetoin consumes NADH + H^+, which could potentially be used for redox balance and cytoplasmic pH homeostasis SrrAB would not repress *alsSD*. This hypothesis is supported by the lack of a change in *alsSD* induction in a *srrAB* mutant under aerobic conditions with excess glucose (Fig. 4.7A). Interestingly, when the concentration of acetoin in the supernatant was measured during stationary phase survival, the *srrAB* mutant demonstrated a statistically significant increase in acetoin concentration compared to wild-type (Fig. 4.7B). Given our other data it would seem most likely that disrupting *srrAB* had altered metabolism to redirect carbon into acetoin rather than affecting transcription of *alsSD* directly. However, for our assays we measured induction of *alsSD* at 6 hours growth with excess glucose, and could not discount the possibility that *alsSD* induction was altered at later time points.

To determine if *alsSD* was under SrrAB-mediated regulation we decided to perform EMSAs with our purified SrrA protein.

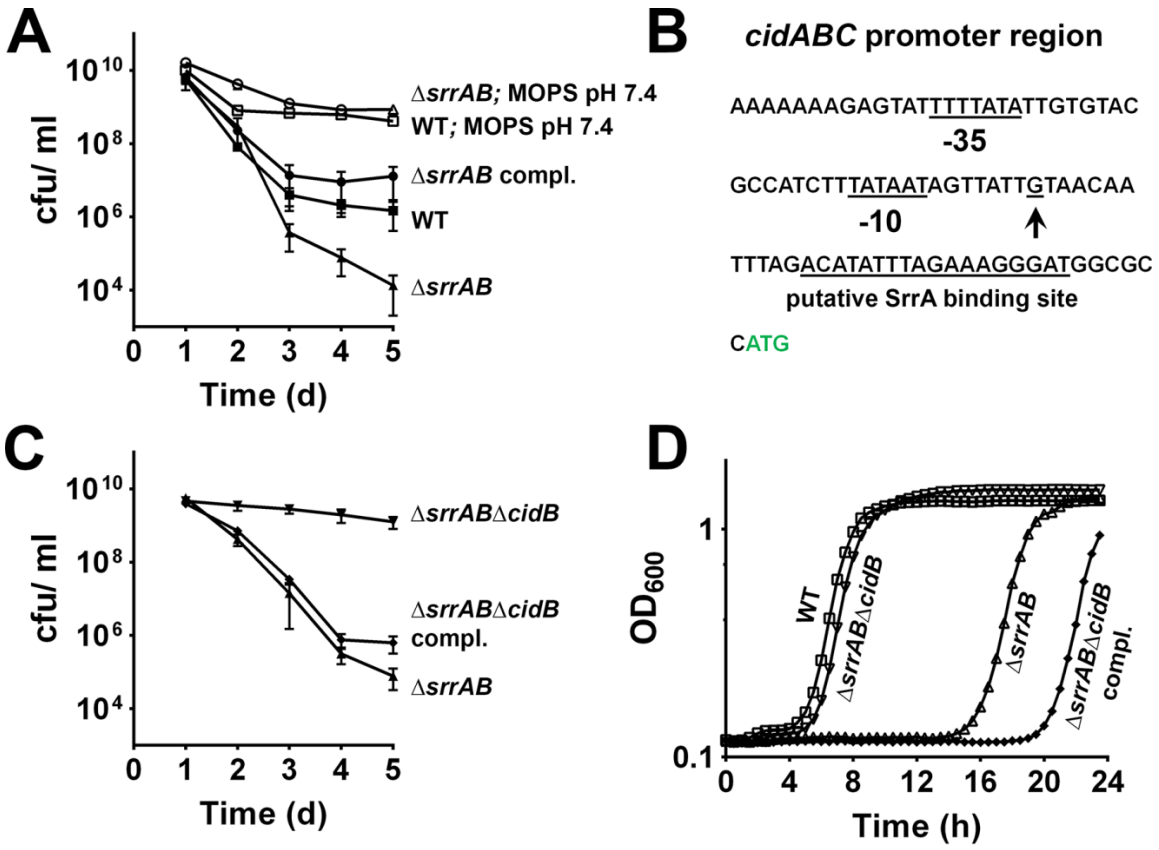

1232

1233 **Figure 4.5. Complementation of CidB phenotypes.** A. Stationary phase viabilities were monitored for
1234 cultures following growth in TSB-35 mM glucose over a period of 5 days. B. Sequence of the *cidABC*
1235 promoter. -35 and -10 are underlined. Transcription and translation start sites are denoted by an arrow and
1236 asterisk, respectively. The putative SrrA binding site is underlined and in bold C. Stationary phase viabili-
1237 ties were monitored for cultures following growth in TSB-35 mM glucose over a period of 5 days. D.
1238 Overnight cultures were resuspended to an OD_{600} of 0.06 in TSB. Cultures were challenged with 5 mM
1239 H_2O_2 and growth was monitored for 24 hours at 37°C in a Tecan infinite 200 spectrophotometer under
1240 maximum aeration.

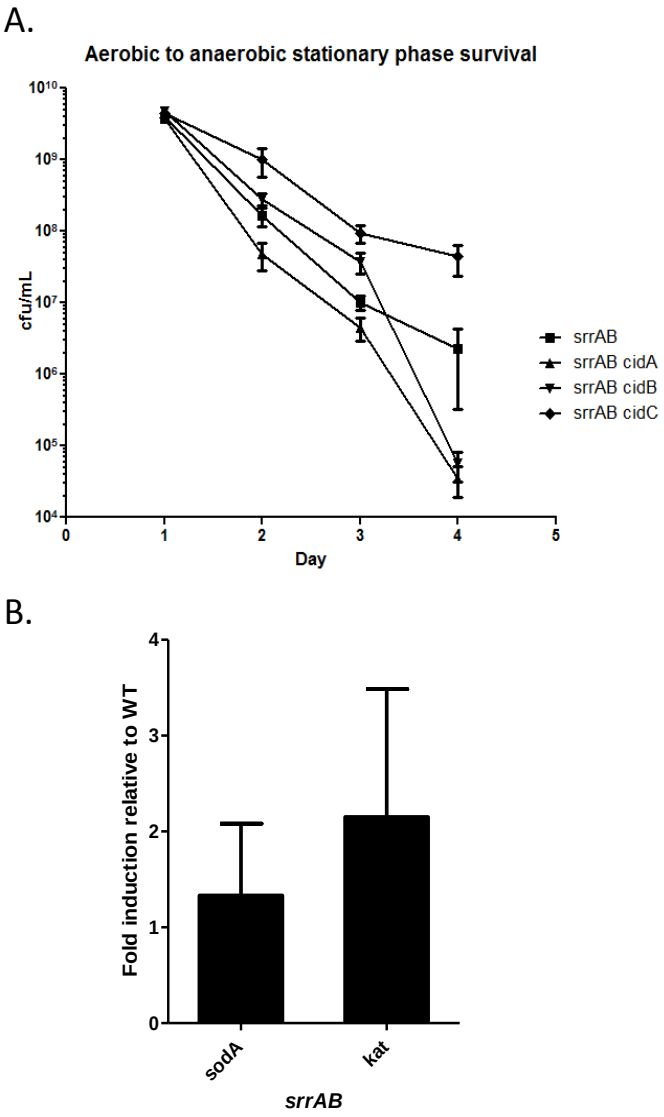

Figure 4.6. Effect of anaerobic conditions on stationary phase survival of individual *cidABC* mutations in the Δ*srrAB* mutant background. A. Aerobically grown cells of Δ*srrAB*, Δ*srrAB*Δ*cidA*, Δ*srrAB*Δ*cidB* and Δ*srrAB*Δ*cidC* (TSB-35 mM glucose) were shifted to an anaerobic chamber after 24 hours of growth and monitored for cell viability every 24 h over a period of five days in TSB + 35 mM glucose. B. Transcription of superoxide dismutase (*sodA*) and catalase (*kat*) in the Δ*srrAB* mutant. Cultures were grown to an OD_{600} of 0.4 in a 3 to 5 media to flask ratio to imitate microaerobic conditions. The cultures were then exposed to 10 mM hydrogen peroxide for 10 minutes and then isolated for mRNA for RT-PCR. Data are the average of two separate experiments.

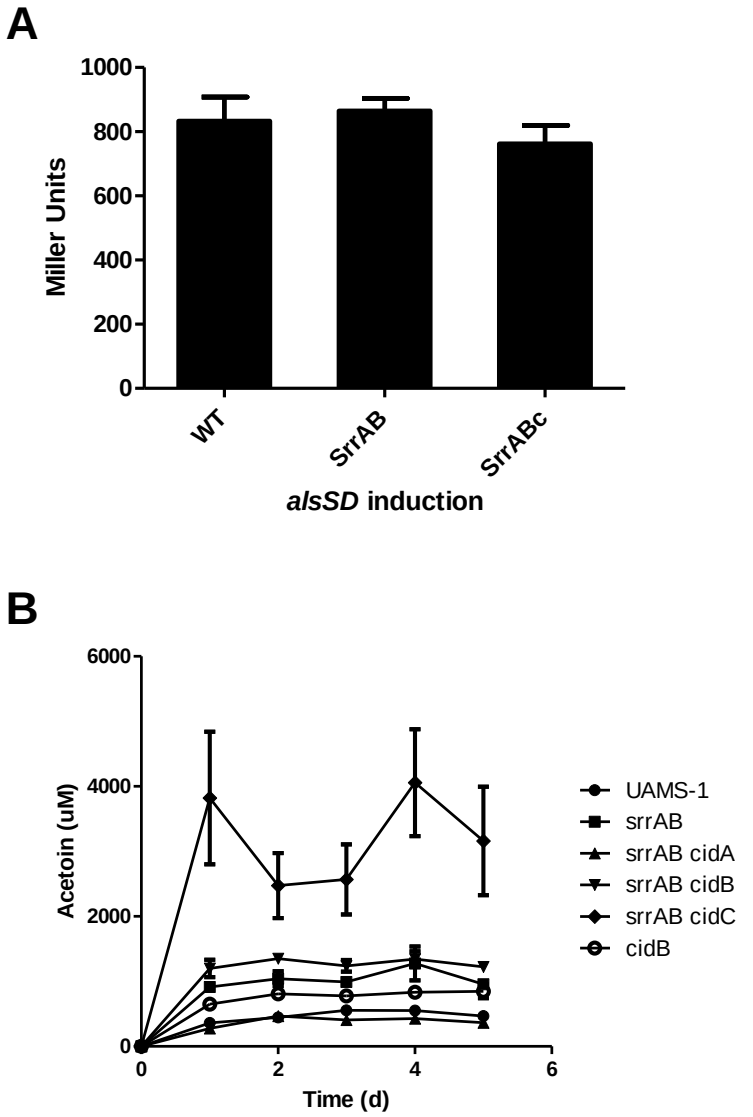

1250

1251 **Figure 4.7. Effect of disruption of *srrAB* on *alsSD* transcription**. A. *S. aureus* cells containing an *alsSD*
1252 promoter fused to *lacZ* were grown to post-exponential phase and assayed for β-galactosidase activity. B.
1253 Acetoin concentrations in culture supernatants were measured every 24 h over a period of five days. 200
1254 µL of supernatant was mixed with 140 µL 0.5% creatine, 200 µL 5% α-napthol, and 200 µL 40% KOH.
1255 The sample was incubated for 15 to 30 minutes. The OD_{560} was measured and used to determine the con-
1256 centration of acetoin.

1257

1258

1259

A

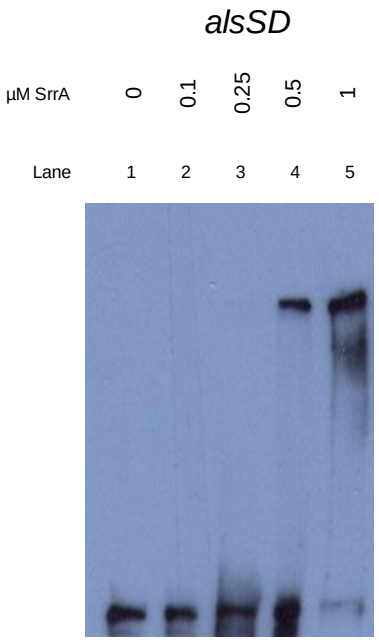

B *alsSD* promoter

CAAAATCTACTCATGCATTTTTGGAATACTTAGTATTACAAATAACGATTTTTA

-35

TTCATCTTACAAAGGATATATAATGTACTGA**A**GGCAATTTTTATGTATCACAAA

-10 *****

TCTAATTGTATATGT**AAAGTTTTGATAA**ATATCATTAAT**TTTACATAACTAT**CA

SrrA **SrrA**

TTAGATTACAAATCACAATGTAATTACATGTAATACACATCTACACATCACATT

TGAAGGGAAATGAATATAAATG

1260

1261 **Figure 4.8. SrrA binds to the promoter of *alsSD*.** A. Electrophoretic Mobility-Shift Assays (EMSAs)
1262 were performed using increasing amounts of purified SrrA protein and biotin-labeled *alsSD* promoter DNA
1263 as a target. Reaction mixtures were incubated for 30 minutes at room temperature and separated in a 6%
1264 TBE polyacrylamide gel. B. Nucleotide sequence of the alsSD promoter displaying putative SrrA binding
1265 sites.

To our surprise SrrA bound the DNA (Fig. 4.8A). Upon review of the sequence of the *alsSD* promoter we found several putative SrrA binding sites downstream of the -35 and -10 elements, suggesting that SrrA binding in that location could disrupt transcription, acting as a repressor. We reviewed our data to find a reason for the discrepancy between SrrA binding and a lack of an effect on *alsSD* transcription. SrrAB can act as a regulator during aerobic conditions (84), as evidenced by the results of our stationary phase survival assays and beta-galactosidase assays. Nonetheless SrrAB is traditionally considered to be an anaerobic regulator (67, 81, 83). We reasoned then that since SrrAB activity would be more pronounced under conditions of low oxygen (84), SrrAB mediated repression of *alsSD* transcription would be more apparent under microaerobic conditions (Fig. 4.9). We found that when grown microaerobically with excess glucose, the induction of *alsSD* is not affected in a significant manner by disruption of *srrAB* (Fig. 4.9A). However, when grown without excess glucose under microaerobic conditions *alsSD* finally demonstrated a SrrAB-dependent phenotype. These results indicate that SrrAB does act as a repressor of *alsSD*, albeit in a very weak fashion.

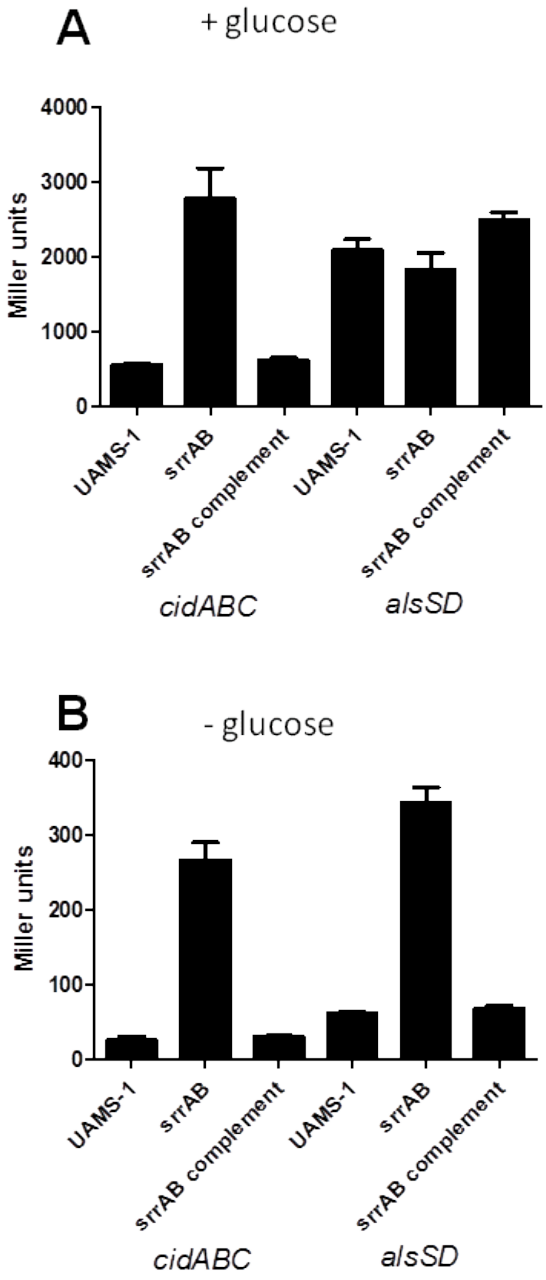

Figure 4.9: SrrAB represses *cidABC* and alsSD under microaerobic conditions. The expression of *cidABC* and *alsSD* in the *srrAB* mutant background under microaerobic conditions, 3 to 5 media to flask ratio for 24 hours before samples were assayed for β-galactosidase activity. A. Cultures were grown in NZY + 35 mM glucose. B. Cultures were grown in NZY (no glucose). Data are the average of at least two separate experiments.

The lrgAB and lytSR operons play a role in sensitivity to exogenous ROS

It has been demonstrated that disruption of the Δ*lrgAB* and Δ*lytSR* operons in *Streptococcus mutans* results in increased sensitivity to H_2O_2 (83). We reasoned that Δ*lrgAB* and Δ*lytSR* mutants would show the same phenotype in *S. aureus*. Indeed, our investigations of the *S. aureus* Δ*lrgAB* and Δ*lytSR* operons revealed a similar increase in sensitivity to this ROS (Fig. 4.10). Since Δ*cidA* and Δ*cidB* decrease sensitivity to ROS in a Δ*srrAB* mutant (Fig. 4.4E), it is interesting then that *cidAB* and *lrgAB* have opposing phenotypes when it comes to sensitivity to exogenous ROS.

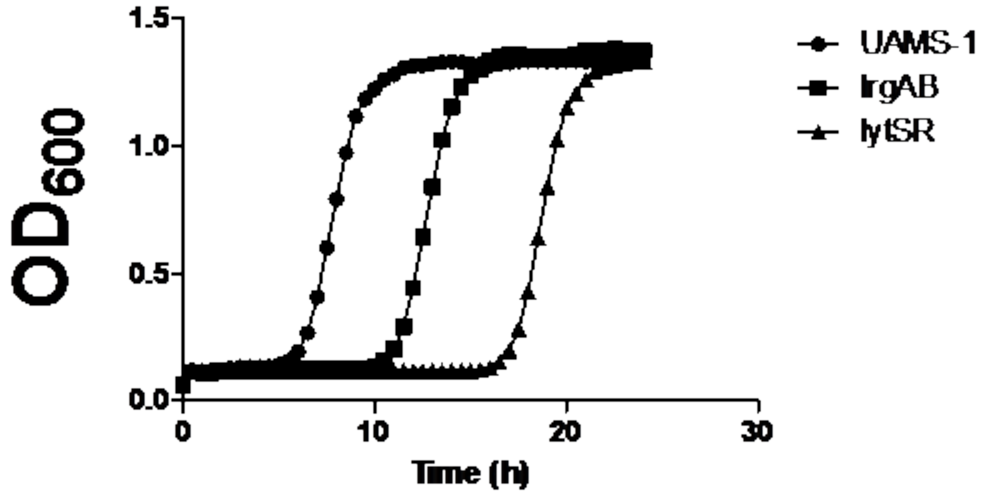

Figure 4.10. UAMS-1 Δ*lrgAB* and Δ*lytSR* mutants display increased sensitivity to ROS. Overnight cultures were resuspended to an OD_{600} of 0.06 in TSB. Cultures were challenged with 5 mM H_2O_2 and growth was monitored for 24 hours at 37°C in a Tecan infinite 200 spectrophotometer under maximum aeration.

Discussion

The results generated in this study demonstrate that the SrrAB two-component system functions to directly repress expression of the *cidABC* operon under conditions of excess glucose (Fig. 4.2B-C), resulting in the suppression of cell death. The decreased stationary phase survival of the *srrAB* mutant is not due to changes in the levels of acetate or changes in the pH (Fig. 4.1B-C), but instead the result of increased sensitivity of this strain to acetate-dependent ROS (Fig. 4.3). Importantly, this study revealed for the first time the critical role of *cidB* in this process.

Previous studies performed by our laboratory have reported that the *S. aureus cidC*-encoded pyruvate oxidase plays a critical role in cell death during stationary phase under excess glucose conditions (60) by producing acetate and promoting the acidification of the growth media (61). Thus, given that *cidABC* transcription was enhanced in a Δ*srrAB* mutant (Fig. 4.2B) (83), we initially hypothesized that the decreased survival of these cells was due to increased acetate, which would in turn lead to cytoplasmic acidification and ROS accumulation. However, the results of the current study revealed that this phenotype was clearly not associated with increased acetate accumulation or decreased pH of the culture medium (Fig. 4.1B-C). Instead, experiments where the cultures were switched to anaerobic conditions (Fig. 4.3B) suggested that the decreased stationary phase survival of the Δ*srrAB* mutant was due to increased sensitivity to the acetate-dependent generation of ROS.

Acetate potentiates cell death via a complicated process (61). When the pH of the environment surrounding the cell is higher than the pK_a of acetate (~4.8), most of the ace-

tate is unprotonated and has a negative charge (61), allowing the cell membrane to act as a barrier to entry. As the extracellular pH decreases and approaches the pK_a of acetate there is an increased percentage of acetate that is protonated to acetic acid. Now neutrally charged, the acetic acid can diffuse across the membrane into the bacterial cytoplasm. Once across the membrane the protons disassociate from acetic acid, leading to a decrease in the intracellular pH and, through an unknown mechanism, an increase in the accumulation of ROS. Over time, this leads to increasing amounts of cellular damage and cell death. It has been suggested that acetate may contribute to a bottleneck in electron transport by reducing the functionality of the respiratory chain and catalyzing the reduction of oxygen, resulting in the production of ROS (61), but it is not clear how acetate initiates ROS production at the molecular level. Interestingly, the disruption of *cidB* improved both stationary phase survival (Fig. 4.4B) and sensitivity to H_2O_2 (Fig. 4.4E), implicating the involvement of *cidB* in these processes. Importantly, any involvement of catalase or superoxide dismutase seems unlikely as there was no alteration in the expression of the genes encoding these enzymes in the Δ*srrAB* mutant (Fig. 4.6B). Thus, the Δ*srrAB* mutant background may be an important genetic context in which the role of CidB manifests itself as a direct mediator of cell death in the response to ROS.

Although the model for CidAB and LrgAB function up to now has focused primarily on the CidA and LrgA proteins as a holin and antiholin, respectively, the results presented here, as well as recent data generated by our laboratory, has cast this system in a different light. Although an early report suggested that the *cidB* gene can affect the expression/activity of a 25-30 kDa murein hydrolase (126), little is known about CidB and LrgB, other than that they are predicted to be ~25 kDa membrane-associated proteins (50, 126).

The results of the current studies indicate that in the context of the Δ*srrAB* mutation, disruption of *cidB* has a dramatic effect on stationary phase survival (Fig. 4.4B), but only a modest effect on acetate secretion (Fig. 4.4C) and culture pH (Fig. 4.4D). Importantly, ongoing studies in our laboratory indicate that CidB plays a positive role in the regulation of CidC activity and acetate secretion (unpublished data). Combined with the studies presented here, these results suggest that CidB may have a more impactful role in the cell death pathway and acetate metabolism than had been previously recognized.

The survival of the Δ*srrAB* Δ*cidB* mutant under anaerobic conditions confirms that CidB plays a role in sensitivity to ROS (Fig. 4.6). Growth under anaerobic conditions allows us to differentiate between the effects of ROS and the effects of acid stress concerning cell death. The Δ*srrAB* Δ*cidC* and Δ*srrAB* Δ*cidB* do not display the same phenotype under anaerobic conditions, demonstrating that over-expression of CidB leads to sensitivity to ROS in the *srrAB* background. Interestingly, on the 4th day of stationary phase the Δ*srrAB* Δ*cidB* mutant experiences a sudden decrease in viability, after which the viability of the Δ*srrAB* Δ*cidB* mutant is indistinguishable from the Δ*srrAB* Δ*cidA* mutant. Under aerobic conditions the Δ*srrAB* Δ*cidB* shows an increase in the pH within this time frame (Fig. 4.4D). This could indicate that CidB plays an important role in resistance to weak acid stress at this time point. This would make some sense given that it has been proposed that CidB acts as a transporter for the acetate produced by CidC (work in progress by Vinai Thomas). It could be that the presence of the acetate transporter is required for long term resistance to weak acid stress under anaerobic conditions.

In addition to the effect of the *cidB* mutation on H_2O_2 sensitivity, this study revealed that the disruption of *cidA* also decreased the sensitivity of the Δ*srrAB* mutant to H_2O_2 (Fig. 4.4E). In contrast to these findings, disruption of the *Streptococcus mutans* Δ*lrgAB* and Δ*lytSR* operons were previously shown to cause increased sensitivity to H_2O_2 (83). Our investigations of the *S. aureus* Δ*lrgAB* and Δ*lytSR* operons revealed a similar increase in sensitivity to this ROS (Fig. 4.10). With respect to the H_2O_2 phenotype, it is interesting to note that SrrAB and LrgAB have a negative effect on *cidABC*; SrrAB represses *cidABC* expression at the transcriptional level, and LrgA has been proposed to inhibit CidA activity as an antiholin (42). Although we did not observe altered ROS sensitivity resulting from *cidA* or *cidB* mutations in the wild-type background (data not shown), this is likely due to the fact that *cidABC* expression is repressed by the SrrAB regulatory system in this genetic context. Overall, these results are consistent with the model in which the *cid* and *lrg* operons play opposing roles in cell death

Although we noted that *cidABC* expression is increased nearly four-fold in the Δ*srrAB* mutant background (Fig. 4.2B), a corresponding increase in extracellular acetate levels was not observed (Fig. 4.1B). One explanation for this is that under these conditions an alternative pathway, the *pta-ackA* pathway (72), produces most of the acetate in the Δ*srrAB* mutant. Alternatively, while we have focused on *cidABC* transcription in this study, the *cid* operon also produces a *cidBC* transcript, whose expression is regulated by sigma factor B, independently of CidR (51). Since the *cidBC* transcript is highly elevated when there is excess glucose (51), it is possible that the increase in *cidABC* transcription does not result in a significant increase in CidC protein levels and as a result, acetate production. The elevated *cidBC* transcript could also be the reason that there is a large dif-

ference in the ROS detected in Δ*srrAB*Δ*cidA* mutant compared to the Δ*srrAB*Δ*cidB* and Δ*srrAB*Δ*cidC* mutants (Fig. 4.4A). These possibilities are currently under investigation.

It is also interesting to note that while the Δ*srrAB* mutant has previously been shown to exhibit poor growth under anaerobic conditions (81), we have demonstrated that it survives better in stationary phase under these conditions compared to the wild-type strain (Fig. 4.3B). These data suggest that SrrAB necessary for anaerobic growth, but conversely may be detrimental to survival within an anaerobic environment. It has been suggested that the decreased expression of genes involved in anaerobic metabolism may be responsible for the altered growth and survival of the Δ*srrAB* mutant under these conditions (84). For example, the discrepancy between growth and survival could be explained by the deregulation of the *nrdDG* and *nar* operons (83). The *nrdDG* operon encodes ribonucleoside-triphosphate reductase, essential for anaerobic growth (127); thus, the decreased expression of *nrdDG* in a Δ*srrAB* mutant (83) would lead to poor growth under low oxygen conditions. On the other hand, the *nar* genes (nitrate reductase) are repressed by SrrAB (83), so increased expression could lead to greater consumption of nitrate, a more active electron transport chain and more energy for the cell, potentially allowing for better survival during stationary phase under anaerobic conditions in a Δ*srrAB* mutant.

Given that our initial data would suggest that SrrAB does not regulate *alsSD* (Fig. 4.7A), the discovery that disrupting *srrAB* increased acetoin concentration in the supernatant was interpreted as a redirection of carbon and not necessarily *alsSD* transcription. However, we found that SrrA binds the *alsSD* promoter (4.8A). Further investigation revealed that SrrAB represses *alsSD*, but only under microaerobic conditions without ex-

cess glucose (Fig. 4.9). The answer to this confusing result is suggested by comparing the EMSAs of SrrA binding between the two promoters. SrrA creates a shift in the *cidABC* promoter at 0.25 µM (Fig. 4.2C), whereas the *alsSD* shift does not occur until 0.5 µM of purified SrrA (Fig. 4.8B). While we have not performed experiments looking into the dissociation constant of SrrA to its target DNA, these EMSAs would suggest that SrrA has lower affinity for the *alsSD* promoter compared to the *cidABC* promoter. The affinity is so weak that repression is easily overpowered by CcpA and CidR-mediated up-regulation of *alsSD,* so SrrAB-mediated regulation of *alsSD* is noticeable only when there is no glucose and the signal to which SrrAB responds is strong. By contrast then, SrrAB-mediated repression in the *cidABC* promoter would not be as easily overpowered, making a sizable difference in *cidABC* induction even under aerobic conditions when CidR and CcpA are active.

In conclusion, our results indicate that the disruption of the *srrAB* regulatory operon in *S. aureus* results in reduced stationary phase viability due to the increased production and sensitivity to ROS. The ROS are formed in the presence of acetic acid produced by CidC encoded by the *cidABC* operon, which is repressed by SrrAB. Furthermore, we demonstrate that the increased cell death observed in the Δ*srrAB* mutant is dependent on *cidB.* These results are the first to demonstrate a role for *cidB* in cell death and provide greater insight into the functions of the *cidABC*-encoded proteins, as well as the transcriptional control of this cell death regulatory system.

Chapter V. Concluding remarks

cidABC

The *cid* operon consists of the *cidA*, *cidB* and *cidC* genes, organized into two overlapping transcripts, the *cidABC* transcript (3.0 Kb) and the *cidBC* transcript (2.7 kb). It has been published previously that *cidABC* expression is positively regulated by CidR (31, 50). Experiments performed for this dissertation found that *cidABC* transcription is also under positive regulation by CcpA (Chapter 3), and negative regulation by SrrAB (Chapter 4). The binding site of CcpA, the *cre* site, lies -80 to -73 bp upstream of the transcription start site. The CidR binding site is located 7 bp downstream of the *cre* site. The SrrA binding site lies downstream of the transcription start site, suggesting that repression is the result of impeding the activity of RNA polymerase. The production of the *cidBC* transcript is up-regulated by sigma factor B (51). As a result the increase in induction from the *cidABC* promoter does not significantly change the expression of the *cidB* and *cidC* genes (work in progress by Vinai Thomas). This could indicate that SrrAB-mediated repression effectively decreases the expression of the *cidA* gene only. If true, this suggests that SrrAB-mediated repression of *cidABC* transcription is to reduce stress to the cell created by CidA.

The genes of the *cid* operon are involved in the modulation of cell death. In our current understanding, CidA is a holin, based on its sequence similarities with bacteriophage holins and holin-like properties (50, 53). It has been theorized that CidA localizes to the cell membrane, forming pores by oligomerization. These pores have been proposed to lead to membrane depolarization, activating murein hydrolase activity and leading to cell

lysis (56). The *cid* operon also influences cell death metabolically through CidC, a pyruvate oxidase (60) that potentiates cell death during stationary phase and biofilm development through the production of acetic acid (61). Due to the results of the experiments detailed in this dissertation it was discovered that CidB also plays a role in influencing staphylococcal cell death (104). Disruption of *cidB* restored the viability of the Δ*srrAB* mutant culture in stationary phase (Fig. 4.4B) and sensitivity of the Δ*srrAB* mutant to exogenous ROS (Fig. 4.4E). Unusually, disruption of *cidB* in the wild-type background does not produce as strong a phenotype. Acetate production was slightly decreased, but the effect on stationary phase survival, ROS production and ROS sensitivity was not observed (data not shown). These results suggest that the *srrAB* mutant background provides a genetic context in which the function of CidB manifests itself.

alsSD

Like *cidABC*, the transcription of *alsSD* is also positively regulated by CidR (64), and the experiments performed in this dissertation found that positive regulation by CcpA and negative regulation by SrrAB. The *alsSD* promoter contains multiple *cre*-like sites that CcpA could potentially bind, the first from -90 to -83, and the second from -64 to -57 bp upstream of the putative transcription start site. The *alsSD* promoter also has two putative SrrA binding sites downstream of the transcription start site. Like the SrrA binding site in the *cidABC* promoter, the binding sites in the *alsSD* promoter are in a position that suggests binding could interfere with RNA polymerase function.

The genes in the *alsSD* operon, organized into a single 2.5 Kb transcript, play a role in modulating cell death. The genes in the *als* operon are α-acetolactate synthase (*alsS)* and α-acetolactate decarboxylase (*alsD*). AlsS and AlsD synthesize acetoin, which has a role in promoting cell survival (61, 64). Since the activity of both AlsSD and CidC act to deplete pyruvate pools, it therefore seems likely that AlsSD and CidC act as part of the carbon overflow mechanisms of the cell (61, 100).

Individual regulators

CidR

CidR is an LTTR, a LysR-type transcriptional regulator (65). LTTRs are often thought of as global transcriptional regulators (87), controlling metabolic genes (128), virulence determinants and quorum sensing (129). However, microarrays performed to determine the regulatory targets of *S. aureus* CidR found that disrupting the *cidR* gene affected expression of only the *cidABC* and *alsSD* operons (64). In agreement with this finding, the 5'-TAGTA-A/T-TACAAA-3' sequence occurs only in the promoters of *cidABC* and *alsSD* in the *S. aureus* genome (data not shown). Despite controlling only two operons, CidR is widely conserved. A study was conducted screening for homologs of all 125 transcriptional regulators in *S. aureus* across more than 1,200 different Gram-positive and Gram-negative bacterial species genomes (130). It was determined that CidR was the third most common transcriptional regulator, after sigma factor A and HU. These results suggest that the processes that CidR controls have deep ancestral roots and under-

score the need to understand the operons it controls and the signals to which CidR responds.

CcpA

CcpA is the primary mediator of CCR in Gram-positive bacteria like *S. aureus* (74, 75), affecting the expression of hundreds of genes (73, 74). CcpA responds to fructose-1,6-bisphosphate and glucose-6-phosphate levels, which promote the association of phosphorylated Hpr with CcpA (74). The CcpA-Hpr complex then regulates target genes by binding to *cre* sites (67). Though the process is termed CCR (the "R" referring to "repression"), CcpA can act as a positive regulator when it binds to a *cre* site upstream of the promoter (74), as is the case with *cidABC* and *alsSD*. In *S. aureus* CcpA represses the TCA cycle in the presence of glucose (67, 73, 131), leading to the accumulation of pyruvate and acetyl-CoA. CidC and AlsSD act to deplete pyruvate pools (60), while Pta/AckA deplete acetyl-CoA (72), suggesting that the up-regulation of *cidABC* and *alsSD* is a component of the response to carbon overflow within the cell (61, 100).

SrrAB

SrrAB is a homologue of the two-component system ResDE, essential in many Gram-positive bacteria for anaerobic respiration (67, 80). Despite being essential for anaerobic respiration, the exact signal that SrrAB responds to is unknown. Due to the fact that de-

creased menaquinone production results in decreased *srrAB* expression (132) and that SrrAB responds to both nitric oxide stress and oxygen availability (81, 83), it has been proposed that SrrAB detects changes in the redox status of the electron transport chain by sensing reduced menaquinone, though this has not yet been proven. Under anaerobic conditions, to restore redox balance *S. aureus* produces lactate via L-lactate dehydrogenase (*ldh*) (61, 79), consuming NADH. This suggests that repression of *cidABC* (104) and *alsSD* expression (Chapter 4) is a means of redirecting carbon to lactate. This is consistent with the fact that although the creation of 2,3-butanediol by acetoin reductase (*butA)* also consumes NADH (56), *S. aureus* does not synthesize acetoin under anaerobic conditions (data not shown).

Current understanding

The current understanding of what is occurring in *cid*-mediated cell death is depicted in Figure 5.1. To begin, glucose enters the cell via the phosphotransferase system (67, 74, 76). During translocation into the cell, glucose is phosphorylated to glucose 6-phosphate to enter glycolysis. Glucose 6-phosphate is then converted to fructose 1,6 bis-phosphate. High levels of fructose 1,6 bis-phosphate lead to phosphorylation and activation of HprK kinase (77, 78), which then phosphorylates Hpr (74). Fructose 1,6-bisphosphate and glucose 6-phosphate then promote the association of the phosphorylated Hpr and CcpA. Once associated, the CcpA-Hpr complex can then bind to *cre* sites to mediate CCR.

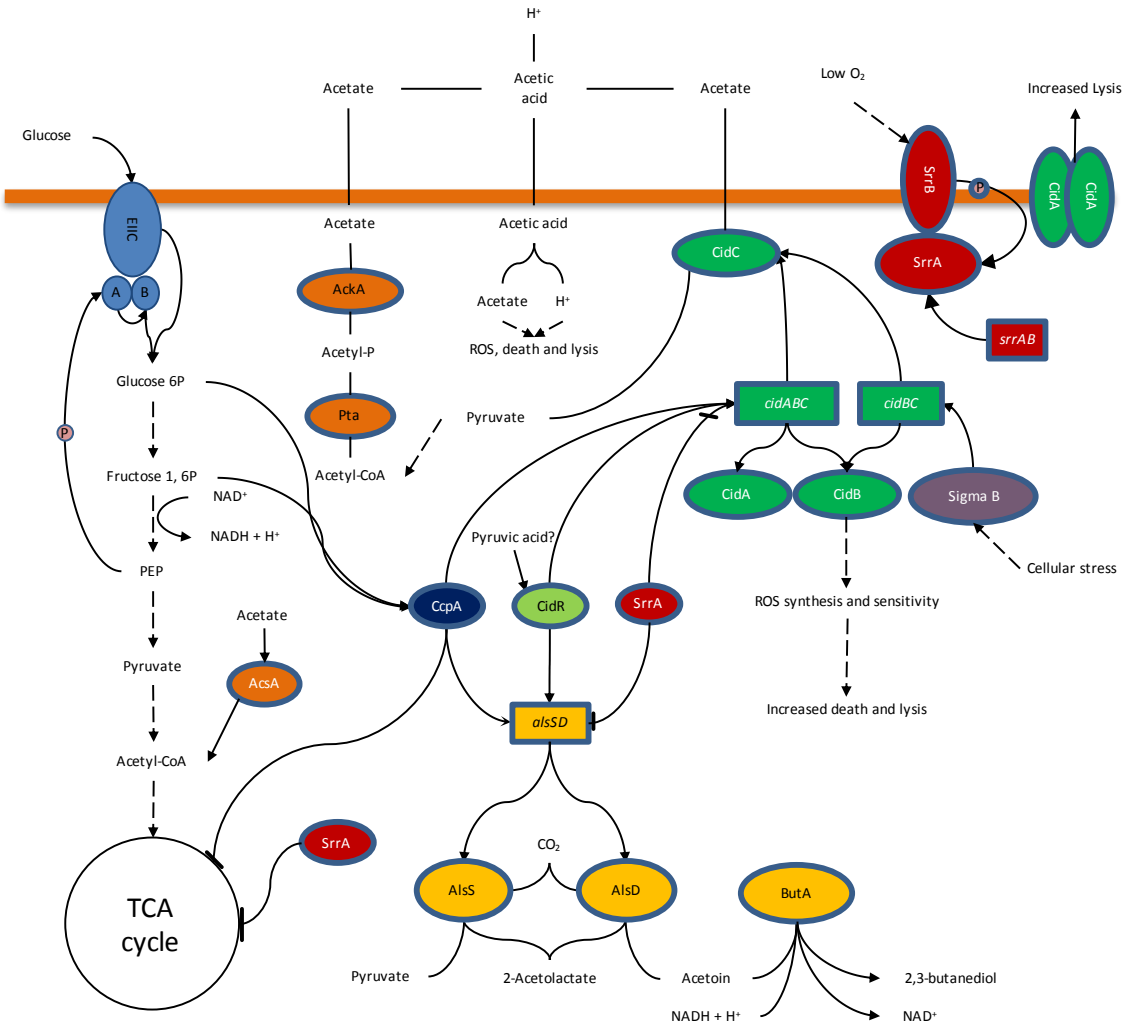

1537

1538 **Figure 5.1. Current understanding of the process of *cid*-mediated cell death.** Depicted are the *cidABC*
1539 and *alsSD* operons, the proteins produced by these operons and their known function, the transcriptional
1540 factors involved in regulation of *cidABC* and *alsSD* and the stimuli they respond to. Due to the importance
1541 of excess glucose and CCR to induction of *cidABC* and *alsSD*, the phosphotransferase system, glycolysis
1542 and the TCA cycle are included. Acetate and its role in cell death (61) are included. For more in depth de-
1543 scription see the main text.

1544

1545

1546

1547

In *S. aureus*, one of the processes repressed by CCR in the presence of glucose is the TCA (67, 73, 131), leading to the accumulation of pyruvate and acetyl-CoA. The pools of pyruvate and acetyl-CoA must be depleted to continue glycolysis, so carbon overflow mechanisms are activated, including CidC and AlsS/AlsD. The activity of CidC and AlsS/AlsD acts to consume pyruvate by converting it to acetate (60) and acetoin, respectively. Acetyl-CoA is converted to acetate by Pta/AckA (72). Once generated, the acetate and acetoin are excreted from the cell to be consumed later.

The breakdown of excess glucose leads to the induction of the *cidABC* operon through CidR-mediated regulation responding to increasing concentrations of an unknown co-inducer molecule. While CidC acts to deplete pyruvate, the *cidABC* operon contributes to the overall stress of the cell. The current model suggests that CidA localizes to the cell membrane, oligomerizing and forming pores. These pores lead to membrane depolarization, which activates murein hydrolase activity, leading to cell lysis (56). The role of CidB during this time period is unclear because the mechanism of CidB is not yet understood. Nonetheless, our data suggests that CidB plays a role in creating ROS sensitivity in the cell, which could also lead to stress and ultimately lysis.

In addition, glycolysis results in increased cytoplasmic levels of NADH (67). Since elevated levels of NADH can inhibit biosynthetic pathways (67), the redox balance must be restored. This can be partially accomplished by AlsS/AlsD; the acetoin produced from pyruvate can be processed further by acetoin reductase to create 2,3-butandiol and NAD^+ (56). This can partially restore redox balance, but to convert high concentrations of NADH to NAD^+ requires increasing the activity of the electron transport chain. However,

increased respiration also produces increased ROS (133-135), which in turn leads to increased cell stress.

Cellular stress also comes from the acetate released into the environment. The increased levels of acetate produced by CidC in the presence of excess glucose lowers the extracellular pH. As the pH of the extracellular environment decreases and approaches the isoelectric point of the weak acid, an increasing percentage of the acetate molecules become protonated to acetic acid (61), and can diffuse across the cell membrane. Once inside the acetic acid causes acidification of the cytoplasm and increased ROS formation, further contributing to stress that can lead to the death of the cell.

In a biofilm the cellular stresses created by *cidABC* are further modulated by the heterogeneity of the biofilm. The rapid mixing of metabolites observed in liquid culture does not occur in a biofilm because the diffusion of metabolites in a biofilm is reduced by microbial cells and the extracellular matrix (136). This creates localized niches that exhibit variable metabolite concentrations throughout the biofilm. The altered diffusion leads to localized pockets of high concentrations of glucose, acetate, and low pH, resulting in increased cell death in these regions. Therefore in a biofilm one would predict that thicker regions of the biofilm provides more opportunities for metabolite accumulation and greater induction of *cidABC* and *alsSD*, leading to increased cell death and lysis and release of eDNA into the environment. This prediction is supported by the induction of *cidABC* is increased in the thick towers formed by a biofilm, which also correlates with the presence of eDNA (99).

The heterogeneous environment within a biofilm also effects the diffusion and consumption of oxygen. Oxygen is consumed by the surface layer of cells, resulting in hypoxic conditions deeper within the biofilm (99). Reduced oxygen conditions promotes glycolysis in the deeper cells (137) if glucose penetrates deep enough, leading to increased CCR and *cidABC* induction and cell lysis. Low oxygen also leads to increased repression by SrrAB (81) potentially reducing *cidABC* and *alsSD* induction.

Remaining questions and future directions

The identity of the co-inducer molecule of CidR

Despite the efforts detailed within this dissertation, the identity of the co-inducer molecule of CidR remains unknown. The original planned approach included three specific aims: 1) mutagenize the *cidABC* and *alsSD* promoter regions to identify the CidR binding site; 2) employ transposon mutagenesis to identify metabolic pathways that effect the induction of *cidABC* transcription; and 3) use DNA-protein interaction experiments to identify the CidR co-inducer. While Aims 1 and 2 led to the discovery of the CidR binding site and CCR as an affecter of *cidABC* and *alsSD* expression, the attempts at Aim 3 so far have not proven successful. Despite attempting multiple potential co-inducer molecules under multiple conditions the EMSA experiments performed have not revealed the identity of the co-inducer molecule (data not shown). As stated above, LTTRs regulate the target promoter by bending the DNA (87). An EMSA proving the identity of the co-inducer molecule is predicated on the LTTR making a big enough change in DNA bend-

ing in the presence of the co-inducer that this would be noticeable in an EMSA (97). If the bend is not big enough, the EMSA will not be sensitive enough to determine the identity of the co-inducer molecule. In a more sensitive experiment, a DNase I footprinting assay the LTTR binding the co-inducer molecule would be visualized as a change in the footprint position. An alternative to DNase I footprinting would be to use an *in vitro* transcription assay. Purified CidR, CcpA and RNA polymerase would be added to purified plasmid containing the *cidABC* promoter. Putative co-inducer molecules would be added to determine which molecule increases *cidABC* transcription.

Another alternative strategy to identify the CidR co-inducer would be to use a gel filtration analysis of CidR in the presence of different candidate molecules. It was recently demonstrated that the LTTR, CcpE, oligomerizes in the presence of its co-inducer molecule, citrate (128). Ordinarily, CcpE exists in solution as a 66 kDa dimer. However, when citrate is added, CcpE oligomerizes to form a 132 kDa tetramer. The same experiment could be attempted with CidR with potential co-inducer molecules at varying concentrations. Although this approach would inform us about the effects of these molecules on the oligomerization state of CidR, additional experiments would be required to demonstrate that these physical changes are sufficient to induce transcription.

An additional alternative would be to crystallize CidR and determine what molecule is bound in the co-inducer binding domain of this protein. While this technique has been used for some LTTRs (138, 139), protein crystallization is a long and intensive process, made worse by the fact that LTTRs are notoriously difficult to crystallize (87, 140).

Although attempts to identify the co-inducer for CidR have been unsuccessful thus far, there is conflicting evidence to suggest that it is pyruvate. Disruption of the *ackA/pta* genes results in a more than 40-fold increase in *cidABC* transcription, which correlates with 4-fold increase in pyruvate concentration (72). The experiment shown in Figure 3.9 demonstrates that a carbon source that does not induce CCR does not induce *cidABC* or *alsSD* transcription. One explanation for this is that CCR represses the TCA cycle, leading to an increase in intracellular pyruvate and the induction of CidR-mediated transcriptional control. Given that *cidC* and *alsSD* appear to play a role in carbon overflow by depleting pyruvate pools (72), it would make sense that pyruvate would act as the signal for CidR to begin upregulation of the operons that would lead to pyruvate's depletion. On the other hand, it was found that the addition of acetic acid or lactic acid can increase *cidABC* expression, but pyruvic acid did not (141). Ultimately, success with the proposed experiments described above will be required to determine the identity of the co-inducer molecule.

The difficulty encountered in identifying a co-inducer molecule for CidR raises the possibility that CidR does not possess one. There are LTTRs for which this is known to be the case (87, 142). However, this is unlikely for CidR since the up-regulation of target genes by a co-inducerless LTTRs require that expression of the LTTR be variable and CidR is constitutively expressed (65). Furthermore, the timing of *cidABC* induction suggests that there is a co-inducer molecule. CCR starts within 30 minutes of the addition of glucose (143). CcpA would then be bound to the DNA of the *cidABC* and *alsSD* promoters. However, *cidABC* induction is not seen until three to four hours of growth with ex-

cess glucose (98). Since *cidR* is constitutively expressed (65), there must be another factor involved.

Physical interaction between CidR and CcpA

Chapter 3 demonstrated that both CcpA and CidR directly bind and up-regulate expression of the *cidABC* and *alsSD* promoters (Fig. 3.4 and 3.6). In both promoters *cre* sites are located upstream of the CidR-binding sites. The close proximity of the binding sites raises the possibility that the two proteins physically interact with one another, that physical interaction between CcpA and CidR is required for up-regulation of *cidABC* and *alsSD* transcription. In at least one instance it has been proposed that an LTTR physically interacts with another protein for induction (144). If this is indeed the case for CidR it would be the second known LTTR to do so. Yeast two-hybrid assays could be employed to determine if these physical interactions occur. Alternatively, *in vivo* crosslinking analysis or *in vitro* pulldown assays could be employed.

The role of CidB in acetate metabolism, ROS sensitivity and cell death

Disrupting *cidB* restored the viability of the Δ*srrAB* mutant culture in stationary phase (Fig. 4.4B), as well as rescued the increased sensitivity of this mutant to exogenous ROS (Fig. 4.4E). Restoration of the normal Δ*srrAB* mutant phenotypes by expressing *cidB* from a plasmid (Fig. 4.5C) indicated that the phenotypes displayed were in fact due

to CidB and not a polar effect on *cidC*. In contrast, disrupting the *cidB* gene in the wild-type background alters acetate production, but does not have an effect on ROS production, ROS sensitivity, and stationary phase survival (data not shown). These results suggest that the *srrAB* mutant background provides a genetic context in which the CidB protein functions.

The identification of a genetic context in which *cidB* function manifests itself provides an opportunity to study its function in greater detail. Studies will be conducted to determine the function of CidB. For example, *cidB* could be overexpressed in wild-type cells to determine if over-expression of *cidB* alone, and not altered expression of other genes in the SrrAB regulon, results in increased sensitivity to hydrogen peroxide and poor stationary phase survival. In addition, one could determine if the proteins of the *cidABC* operon interact with each other, using yeast two-hybrid assays *in vivo* crosslinking analysis or *in vitro* pulldown assays. This type of experiment could be used to determine how CidA and CidB effects acetate production and consumption.

Why does Δ*srrAB exhibit increased sensitivity to ROS?*

Chapter 4 demonstrated that the Δ*srrAB* mutant displayed an increased sensitivity to ROS (Fig. 4.3C). One possibility that was considered was that the Δ*srrAB* mutation effects expression of ROS detoxifying genes such as superoxide dismutase *(sod)* and catalase *(kat)*. However, transcription studies revealed that there was no difference between the Δ*srrAB* mutant and wild-type in the expression of these genes when exposed to hy-

drogen peroxide (Fig. 4.6A). Thus, the decreased viability of the Δ*srrAB* mutant in stationary phase is not likely to be a function of deficiencies in known responses to oxidative stress. Another possible explanation for the decreased viability of the Δ*srrAB* mutant in stationary phase is that this mutation causes increased ROS production due to increased activity of the electron transport chain. The SrrAB two-component system regulates multiple genes involved in the electron transport chain (83, 84), which can produce ROS as a consequence of the normal activity of these proteins (134, 135). Indeed, there is a slight increase in the concentration of ROS in the Δ*srrAB* mutant relative to the wild-type strain (Fig. 4.3A). Increased respiratory activity could be due to de-repression of the *nar* genes, which are required for the use of nitrate as a terminal electron acceptor (79). To determine if there is increased respiration, assays detecting oxygen or nitrate consumption could be employed. qRT-PCR or promoter fusions reporters could also be used to determine if SrrAB-regulated genes encoding components of the electron transport chain are induced.

What are the roles played by the genes identified in a transposon mutagenesis screen in the induction of cidABC and alsSD expression?

In an effort to reveal the co-inducer molecule of CidR, we performed transposon mutagenesis using a P_{cidABC}*::lacZ* reporter strain to identify genes that affect production of the CidR co-inducer. This screen revealed two mutants that increased *cidABC* expression under non-inducing conditions, and 12 that decreased expression under inducing condi-

tions (Table 4). We then took those recovered mutants and confirmed altered *cidABC* induction by quantitative β-galactosidase assays to verify positive hits.

One of the genes found by the transposon mutagenesis screen to have an effect on the expression of *cidABC* was acetate kinase (*ackA).* The Δ*ackA* mutant has previously been shown to exhibit increased *cidABC* expression (72), which provided confidence that the assay was working as predicted. The other mutation that increased *cidABC* induction was phosphoglucomutase (*pgcA*), which is active in the glycolysis, pentose phosphate and purine synthesis pathways. Many of the mutants recovered appear to have a role in central metabolism, suggesting that the reason that *cidABC* expression was altered was due to redirection of carbon, resulting in depletion of the pool of carbon. HPr (*ptsH)* and PEP phosphotransferase (*ptsI)* are genes involved in the phophotransferase system, and CCR via the interaction of HPr with CcpA. Glucokinase (*glk*) is involved in glycolysis, 6-phosphogluconolactonase (SAUSA300_1902) in the pentose phosphate pathway, and inosine 5' dehydrogenase (*guaB*) in the purine synthesis pathway.

However, there were a number of mutants in genes recovered in which it is difficult to determine how they would alter *cidABC* expression. SAUSA300_1624, as a member of the *mut*/*nudix* family of proteins, is probably a house-keeping enzyme, but what it could be affecting is unknown. SAUSA300_2021 is a metallopeptidase of the SprT family of proteins, which may have a role in transcription elongation. SAUSA300_0495 is a hypothetical protein with no known protein motifs. The glucose-inhibited division protein A gene (*gidA)* is a tRNA uridine 5-carboxymethylaminomethyl modification enzyme. Cytochrome oxidase assembly protein (*ctaA*) is important to the function of the electron

transport chain. The preprotein translocase (*secY)* was found to decrease *cidABC* induction, but what protein it could be translocating that would have an effect on *cidABC* transcription is unknown. Likewise, ribonuclease R (*rnr*) is a component of the bacterial RNA degradation system, but is involved in a regulation of a large number of processes (145), and so it is unclear what it is regulating that alters *cidABC* transcription. It is possible that these genes have an indirect effect on central metabolism. To determine this the concentration of metabolites, such as pyruvate, will need to be measured.

During the course of this study it became obvious that the more we investigated the regulation of *cid*-mediated cell death, the more complex it became. In retrospect, this is not surprising, as this regulatory system controls a process that determines the fate of the cell, not unlike apoptosis in eukaryotes. Thus, much like apoptosis, one would expect the regulation of *cid*-mediated cell death to be complicated. Clearly, much more research is required before a full understanding of this system can be reached.

References

1. **Tong SY, Davis JS, Eichenberger E, Holland TL, Fowler VG, Jr.** 2015. Staphylococcus aureus infections: epidemiology, pathophysiology, clinical manifestations, and management. Clin Microbiol Rev **28:**603-661.

2. **Klevens RM, Morrison MA, Nadle J, Petit S, Gershman K, Ray S, Harrison LH, Lynfield R, Dumyati G, Townes JM, Craig AS, Zell ER, Fosheim GE, McDougal LK, Carey RB, Fridkin SK.** 2007. Invasive methicillin-resistant Staphylococcus aureus infections in the United States. JAMA **298:**1763-1771.

3. **Noble WC, Valkenburg HA, Wolters CH.** 1967. Carriage of Staphylococcus aureus in random samples of a normal population. J Hyg (Lond) **65:**567-573.

4. **Casewell MW, Hill RL.** 1986. The carrier state: methicillin-resistant Staphylococcus aureus. J Antimicrob Chemother **18 Suppl A:**1-12.

5. **Gorwitz RJ, Kruszon-Moran D, McAllister SK, McQuillan G, McDougal LK, Fosheim GE, Jensen BJ, Killgore G, Tenover FC, Kuehnert MJ.** 2008. Changes in the prevalence of nasal colonization with Staphylococcus aureus in the United States, 2001-2004. J Infect Dis **197:**1226-1234.

6. **Kuehnert MJ, Kruszon-Moran D, Hill HA, McQuillan G, McAllister SK, Fosheim G, McDougal LK, Chaitram J, Jensen B, Fridkin SK, Killgore G, Tenover FC.** 2006. Prevalence of Staphylococcus aureus nasal colonization in the United States, 2001-2002. J Infect Dis **193:**172-179.

7. **Lowy FD.** 1998. Staphylococcus aureus infections. N Engl J Med **339:**520-532.

8. **Wertheim HF, Melles DC, Vos MC, van Leeuwen W, van Belkum A, Verbrugh HA, Nouwen JL.** 2005. The role of nasal carriage in Staphylococcus aureus infections. Lancet Infect Dis **5:**751-762.

9. **von Eiff C, Becker K, Machka K, Stammer H, Peters G.** 2001. Nasal carriage as a source of Staphylococcus aureus bacteremia. Study Group. N Engl J Med **344:**11-16.

10. **Landrum ML, Neumann C, Cook C, Chukwuma U, Ellis MW, Hospenthal DR, Murray CK.** 2012. Epidemiology of Staphylococcus aureus blood and skin and soft tissue infections in the US military health system, 2005-2010. JAMA **308:**50-59.

11. **Zinderman CE, Conner B, Malakooti MA, LaMar JE, Armstrong A, Bohnker BK.** 2004. Community-acquired methicillin-resistant Staphylococcus aureus among military recruits. Emerg Infect Dis **10:**941-944.

12. **Pan ES, Diep BA, Carleton HA, Charlebois ED, Sensabaugh GF, Haller BL, Perdreau-Remington F.** 2003. Increasing prevalence of methicillin-resistant Staphylococcus aureus infection in California jails. Clin Infect Dis **37:**1384-1388.

13. **Kazakova SV, Hageman JC, Matava M, Srinivasan A, Phelan L, Garfinkel B, Boo T, McAllister S, Anderson J, Jensen B, Dodson D, Lonsway D, McDougal LK, Arduino M, Fraser VJ, Killgore G, Tenover FC, Cody S,**

Jernigan DB. 2005. A clone of methicillin-resistant Staphylococcus aureus among professional football players. N Engl J Med **352:**468-475.

14. **Gillet Y, Issartel B, Vanhems P, Fournet JC, Lina G, Bes M, Vandenesch F, Piemont Y, Brousse N, Floret D, Etienne J.** 2002. Association between Staphylococcus aureus strains carrying gene for Panton-Valentine leukocidin and highly lethal necrotising pneumonia in young immunocompetent patients. Lancet **359:**753-759.

15. **El Atrouni WI, Knoll BM, Lahr BD, Eckel-Passow JE, Sia IG, Baddour LM.** 2009. Temporal trends in the incidence of Staphylococcus aureus bacteremia in Olmsted County, Minnesota, 1998 to 2005: a population-based study. Clin Infect Dis **49:**e130-138.

16. **Laupland KB, Lyytikainen O, Sogaard M, Kennedy KJ, Knudsen JD, Ostergaard C, Galbraith JC, Valiquette L, Jacobsson G, Collignon P, Schonheyder HC.** 2013. The changing epidemiology of Staphylococcus aureus bloodstream infection: a multinational population-based surveillance study. Clin Microbiol Infect **19:**465-471.

17. **Larsen MV, Harboe ZB, Ladelund S, Skov R, Gerstoft J, Pedersen C, Larsen CS, Obel N, Kronborg G, Benfield T.** 2012. Major but differential decline in the incidence of Staphylococcus aureus bacteraemia in HIV-infected individuals from 1995 to 2007: a nationwide cohort study*. HIV Med **13:**45-53.

18. **Ayliffe GA.** 1997. The progressive intercontinental spread of methicillin-resistant Staphylococcus aureus. Clin Infect Dis **24 Suppl 1:**S74-79.

19. **Lowy FD.** 2003. Antimicrobial resistance: the example of Staphylococcus aureus. J Clin Invest **111:**1265-1273.

20. **Noskin GA, Rubin RJ, Schentag JJ, Kluytmans J, Hedblom EC, Jacobson C, Smulders M, Gemmen E, Bharmal M.** 2007. National trends in Staphylococcus aureus infection rates: impact on economic burden and mortality over a 6-year period (1998-2003). Clin Infect Dis **45:**1132-1140.

21. **Nickerson EK, West TE, Day NP, Peacock SJ.** 2009. Staphylococcus aureus disease and drug resistance in resource-limited countries in south and east Asia. Lancet Infect Dis **9:**130-135.

22. **Laupland KB, Ross T, Gregson DB.** 2008. Staphylococcus aureus bloodstream infections: risk factors, outcomes, and the influence of methicillin resistance in Calgary, Canada, 2000-2006. J Infect Dis **198:**336-343.

23. **Chambers HF, Deleo FR.** 2009. Waves of resistance: Staphylococcus aureus in the antibiotic era. Nat Rev Microbiol **7:**629-641.

24. **Pearson H.** 2002. 'Superbug' hurdles key drug barrier. Nature **418:**469.

25. **Levy SB.** 2005. Antibiotic resistance-the problem intensifies. Adv Drug Deliv Rev **57:**1446-1450.

26. **del Pozo JL, Patel R.** 2007. The challenge of treating biofilm-associated bacterial infections. Clin Pharmacol Ther **82:**204-209.

27. **Stewart PS, Costerton JW.** 2001. Antibiotic resistance of bacteria in biofilms. Lancet **358:**135-138.

28. **Davey ME, O'Toole G A.** 2000. Microbial biofilms: from ecology to molecular genetics. Microbiol Mol Biol Rev **64:**847-867.

29. **Hall-Stoodley L, Costerton JW, Stoodley P.** 2004. Bacterial biofilms: from the natural environment to infectious diseases. Nat Rev Microbiol **2:**95-108.

30. **Leid JG, Shirtliff ME, Costerton JW, Stoodley P.** 2002. Human leukocytes adhere to, penetrate, and respond to Staphylococcus aureus biofilms. Infect Immun **70:**6339-6345.

31. **Moormeier DE, Bose JL, Horswill AR, Bayles KW.** 2014. Temporal and Stochastic Control of Staphylococcus aureus Biofilm Development. MBio **5**.

32. **Otto M.** 2013. Staphylococcal infections: mechanisms of biofilm maturation and detachment as critical determinants of pathogenicity. Annu Rev Med **64:**175-188.

33. **Boles BR, Horswill AR.** 2008. Agr-mediated dispersal of Staphylococcus aureus biofilms. PLoS Pathog **4:**e1000052.

34. **Costerton JW, Lewandowski Z, Caldwell DE, Korber DR, Lappin-Scott HM.** 1995. Microbial biofilms. Annu Rev Microbiol **49:**711-745.

35. **Marti M, Trotonda MP, Tormo-Mas MA, Vergara-Irigaray M, Cheung AL, Lasa I, Penades JR.** 2010. Extracellular proteases inhibit protein-dependent biofilm formation in Staphylococcus aureus. Microbes Infect **12:**55-64.

36. **Mann EE, Rice KC, Boles BR, Endres JL, Ranjit D, Chandramohan L, Tsang LH, Smeltzer MS, Horswill AR, Bayles KW.** 2009. Modulation of eDNA release and degradation affects Staphylococcus aureus biofilm maturation. PLoS One **4:**e5822.

37. **Rice KC, Mann EE, Endres JL, Weiss EC, Cassat JE, Smeltzer MS, Bayles KW.** 2007. The *cidA* murein hydrolase regulator contributes to DNA release and biofilm development in *Staphylococcus aureus*. Proceedings of the National Academy of Sciences of the United States of America **104:**8113-8118.

38. **Heilmann C, Hussain M, Peters G, Gotz F.** 1997. Evidence for autolysin-mediated primary attachment of Staphylococcus epidermidis to a polystyrene surface. Mol Microbiol **24:**1013-1024.

39. **Hirschhausen N, Schlesier T, Schmidt MA, Gotz F, Peters G, Heilmann C.** 2010. A novel staphylococcal internalization mechanism involves the major autolysin Atl and heat shock cognate protein Hsc70 as host cell receptor. Cell Microbiol **12:**1746-1764.

40. **Bose JL, Lehman MK, Fey PD, Bayles KW.** 2012. Contribution of the Staphylococcus aureus Atl AM and GL murein hydrolase activities in cell division, autolysis, and biofilm formation. PLoS One **7:**e42244.

41. **Rice KC, Bayles KW.** 2003. Death's toolbox: examining the molecular components of bacterial programmed cell death. Molecular Microbiology **50:**729-738.

42. **Bayles KW.** 2007. The biological role of death and lysis in biofilm development. Nature Reviews Microbiology **5:**721-726.

43. **Zimorski V, Ku C, Martin WF, Gould SB.** 2014. Endosymbiotic theory for organelle origins. Curr Opin Microbiol **22:**38-48.

44. **McVicker G, Prajsnar TK, Williams A, Wagner NL, Boots M, Renshaw SA, Foster SJ.** 2014. Clonal expansion during Staphylococcus aureus infection dynamics reveals the effect of antibiotic intervention. PLoS Pathog **10:**e1003959.

45. **West SA, Griffin AS, Gardner A.** 2007. Evolutionary explanations for cooperation. Curr Biol **17:**R661-672.

46. **West SA, Griffin AS, Gardner A, Diggle SP.** 2006. Social evolution theory for microorganisms. Nat Rev Microbiol **4:**597-607.

47. **Ross-Gillespie A, Gardner A, West SA, Griffin AS.** 2007. Frequency dependence and cooperation: theory and a test with bacteria. Am Nat **170:**331-342.

48. **Hamilton WD.** 1964. The genetical evolution of social behaviour. I. J Theor Biol **7:**1-16.

49. **Hamilton WD.** 1964. The genetical evolution of social behaviour. II. J Theor Biol **7:**17-52.

50. **Rice KC, Firek BA, Nelson JB, Yang SJ, Patton TG, Bayles KW.** 2003. The Staphylococcus aureus cidAB operon: evaluation of its role in regulation of murein hydrolase activity and penicillin tolerance. J Bacteriol **185:**2635-2643.

51. **Rice KC, Patton T, Yang SJ, Dumoulin A, Bischoff M, Bayles KW.** 2004. Transcription of the *Staphylococcus aureus cid* and *lrg* murein hydrolase regulators is affected by sigma factor B. Journal of Bacteriology **186:**3029-3037.

52. **Groicher KH, Firek BA, Fujimoto DF, Bayles KW.** 2000. The *Staphylococcus aureus lrgAB* operon modulates murein hydrolase activity and penicillin tolerance. Journal of Bacteriology **182:**1794-1801.

53. **Ranjit DK, Endres JL, Bayles KW.** 2011. Staphylococcus aureus CidA and LrgA proteins exhibit holin-like properties. J Bacteriol **193:**2468-2476.

54. **Wang IN, Smith DL, Young R.** 2000. Holins: the protein clocks of bacteriophage infections. Annu Rev Microbiol **54:**799-825.

55. **Young I, Wang I, Roof WD.** 2000. Phages will out: strategies of host cell lysis. Trends Microbiol **8:**120-128.

56. **Rice KC, Bayles KW.** 2008. Molecular control of bacterial cell death and lysis. Microbiology and Molecular Biology Reviews **72:**85-109.

57. **Savva CG, Dewey JS, Deaton J, White RL, Struck DK, Holzenburg A, Young R.** 2008. The holin of bacteriophage lambda forms rings with large diameter. Mol Microbiol **69:**784-793.

58. **Barenboim M, Chang CY, dib Hajj F, Young R.** 1999. Characterization of the dual start motif of a class II holin gene. Mol Microbiol **32:**715-727.

59. **Patton TG, Yang SJ, Bayles KW.** 2006. The role of proton motive force in expression of the *Staphylococcus aureus cid* and *lrg* operons. Molecular Microbiology **59:**1395-1404.

60. **Patton TG, Rice KC, Foster MK, Bayles KW.** 2005. The *Staphylococcus aureus cidC* gene encodes a pyruvate oxidase that affects acetate metabolism and cell death in stationary phase. Molecular Microbiology **56:**1664-1674.

61. **Thomas VC, Sadykov MR, Chaudhari SS, Jones J, Endres JL, Widhelm TJ, Ahn JS, Jawa RS, Zimmerman MC, Bayles KW.** 2014. A central role for carbon-overflow pathways in the modulation of bacterial cell death. PLoS Pathog **10:**e1004205.

62. **Rode TM, Moretro T, Langsrud S, Langsrud O, Vogt G, Holck A.** 2010. Responses of Staphylococcus aureus exposed to HCl and organic acid stress. Can J Microbiol **56:**777-792.

63. **Furlong IJ, Ascaso R, Lopez Rivas A, Collins MK.** 1997. Intracellular acidification induces apoptosis by stimulating ICE-like protease activity. J Cell Sci **110 (Pt 5):**653-661.

64. **Yang SJ, Dunman PM, Projan SJ, Bayles KW.** 2006. Characterization of the *Staphylococcus aureus* CidR regulon: elucidation of a novel role for acetoin metabolism in cell death and lysis. Molecular Microbiology **60:**458-468.

65. **Yang SJ, Rice KC, Brown RJ, Patton TG, Liou LE, Park YH, Bayles KW.** 2005. A LysR-type regulator, CidR, is required for induction of the *Staphylococcus aureus cidABC* operon. Journal of Bacteriology **187:**5893-5900.

66. **Prescott LM, Harley JP, Klein DA.** 2002. Microbiology, 5th ed. McGraw-Hill, Boston.

67. **Somerville GA, Proctor RA.** 2009. At the crossroads of bacterial metabolism and virulence factor synthesis in Staphylococci. Microbiol Mol Biol Rev **73:**233-248.

68. **Richardson AR, Somerville GA, Sonenshein AL.** 2015. Regulating the Intersection of Metabolism and Pathogenesis in Gram-positive Bacteria. Microbiol Spectr **3**.

69. **Somerville GA, Cockayne A, Durr M, Peschel A, Otto M, Musser JM.** 2003. Synthesis and deformylation of Staphylococcus aureus delta-toxin are linked to tricarboxylic acid cycle activity. J Bacteriol **185:**6686-6694.

70. **Collins FM, Lascelles J.** 1962. The effect of growth conditions on oxidative and dehydrogenase activity in Staphylococcus aureus. J Gen Microbiol **29:**531-535.

71. **Strasters KC, Winkler KC.** 1963. Carbohydrate Metabolism of Staphylococcus Aureus. J Gen Microbiol **33:**213-229.

72. **Sadykov MR, Thomas VC, Marshall DD, Wenstrom CJ, Moormeier DE, Widhelm TJ, Nuxoll AS, Powers R, Bayles KW.** 2013. Inactivation of the Pta-AckA pathway causes cell death in Staphylococcus aureus. J Bacteriol **195:**3035-3044.

73. **Seidl K, Muller S, Francois P, Kriebitzsch C, Schrenzel J, Engelmann S, Bischoff M, Berger-Bachi B.** 2009. Effect of a glucose impulse on the CcpA regulon in Staphylococcus aureus. BMC Microbiol **9:**95.

74. **Gorke B, Stulke J.** 2008. Carbon catabolite repression in bacteria: many ways to make the most out of nutrients. Nat Rev Microbiol **6:**613-624.

75. **Fischetti VA.** 2000. Gram-positive pathogens. ASM Press, Washington, D.C.

76. **Chubukov V, Gerosa L, Kochanowski K, Sauer U.** 2014. Coordination of microbial metabolism. Nat Rev Microbiol **12:**327-340.

77. **Jault JM, Fieulaine S, Nessler S, Gonzalo P, Di Pietro A, Deutscher J, Galinier A.** 2000. The HPr kinase from Bacillus subtilis is a homo-oligomeric enzyme which exhibits strong positive cooperativity for nucleotide and fructose 1,6-bisphosphate binding. J Biol Chem **275:**1773-1780.

78. **Galinier A, Kravanja M, Engelmann R, Hengstenberg W, Kilhoffer MC, Deutscher J, Haiech J.** 1998. New protein kinase and protein phosphatase families mediate signal transduction in bacterial catabolite repression. Proc Natl Acad Sci U S A **95:**1823-1828.

79. **Fuchs S, Pane-Farre J, Kohler C, Hecker M, Engelmann S.** 2007. Anaerobic gene expression in Staphylococcus aureus. J Bacteriol **189:**4275-4289.

80. **Green J, Rolfe MD, Smith LJ.** 2014. Transcriptional regulation of bacterial virulence gene expression by molecular oxygen and nitric oxide. Virulence **5:**794-809.

81. **Yarwood JM, McCormick JK, Schlievert PM.** 2001. Identification of a novel two-component regulatory system that acts in global regulation of virulence factors of Staphylococcus aureus. J Bacteriol **183:**1113-1123.

82. **Ulrich M, Bastian M, Cramton SE, Ziegler K, Pragman AA, Bragonzi A, Memmi G, Wolz C, Schlievert PM, Cheung A, Doring G.** 2007. The staphylococcal respiratory response regulator SrrAB induces ica gene transcription and polysaccharide intercellular adhesin expression, protecting Staphylococcus aureus from neutrophil killing under anaerobic growth conditions. Mol Microbiol **65:**1276-1287.

83. **Kinkel TL, Roux CM, Dunman PM, Fang FC.** 2013. The Staphylococcus aureus SrrAB two-component system promotes resistance to nitrosative stress and hypoxia. MBio **4:**e00696-00613.

84. **Wu Y, Zhu T, Han H, Liu H, Xu T, Francois P, Fischer A, Bai L, Gotz F, Qu D.** 2015. Staphylococcus epidermidis SrrAB regulates bacterial growth and biofilm formation differently under oxic and microaerobic conditions. J Bacteriol **197:**459-476.

85. **Henikoff S, Haughn GW, Calvo JM, Wallace JC.** 1988. A large family of bacterial activator proteins. Proc Natl Acad Sci U S A **85:**6602-6606.

86. **Pareja E, Pareja-Tobes P, Manrique M, Pareja-Tobes E, Bonal J, Tobes R.** 2006. ExtraTrain: a database of Extragenic regions and Transcriptional information in prokaryotic organisms. BMC Microbiol **6:**29.

87. **Maddocks SE, Oyston PCF.** 2008. Structure and function of the LysR-type transcriptional regulator (LTTR) family proteins. Microbiology-Sgm **154:**3609-3623.

88. **Momany C, Neidle EL.** 2012. Defying stereotypes: the elusive search for a universal model of LysR-type regulation. Mol Microbiol **83:**453-456.

89. **Schell MA.** 1993. Molecular biology of the LysR family of transcriptional regulators. Annual Review of Microbiology **47:**597-626.

90. **Viale AM, Kobayashi H, Akazawa T, Henikoff S.** 1991. rbcR [correction of rcbR], a gene coding for a member of the LysR family of transcriptional regulators, is located upstream of the expressed set of ribulose 1,5-bisphosphate

carboxylase/oxygenase genes in the photosynthetic bacterium Chromatium vinosum. J Bacteriol **173:**5224-5229.

91. **von Lintig J, Kreusch D, Schroder J.** 1994. Opine-regulated promoters and LysR-type regulators in the nopaline (noc) and octopine (occ) catabolic regions of Ti plasmids of Agrobacterium tumefaciens. J Bacteriol **176:**495-503.

92. **Knapp GS, Hu JC.** 2010. Specificity of the E. coli LysR-type transcriptional regulators. PLoS One **5:**e15189.

93. **Parsek MR, McFall SM, Shinabarger DL, Chakrabarty AM.** 1994. Interaction of two LysR-type regulatory proteins CatR and ClcR with heterologous promoters: functional and evolutionary implications. Proc Natl Acad Sci U S A **91:**12393-12397.

94. **Hagerman PJ.** 1986. Sequence-directed curvature of DNA. Nature **321:**449-450.

95. **Perez-Martin J, Rojo F, de Lorenzo V.** 1994. Promoters responsive to DNA bending: a common theme in prokaryotic gene expression. Microbiol Rev **58:**268-290.

96. **van Keulen G, Girbal L, van den Bergh ER, Dijkhuizen L, Meijer WG.** 1998. The LysR-type transcriptional regulator CbbR controlling autotrophic CO2 fixation by Xanthobacter flavus is an NADPH sensor. J Bacteriol **180:**1411-1417.

97. **Porrua O, Garcia-Jaramillo M, Santero E, Govantes F.** 2007. The LysR-type regulator AtzR binding site: DNA sequences involved in activation, repression and cyanuric acid-dependent repositioning. Mol Microbiol **66:**410-427.

98. **Rice KC, Nelson JB, Patton TG, Yang SJ, Bayles KW.** 2005. Acetic acid induces expression of the *Staphylococcus aureus cidABC* and *lrgAB* murein hydrolase regulator operons. Journal of Bacteriology **187:**813-821.

99. **Moormeier DE, Endres JL, Mann EE, Sadykov MR, Horswill AR, Rice KC, Fey PD, Bayles KW.** 2013. Use of microfluidic technology to analyze gene expression during Staphylococcus aureus biofilm formation reveals distinct physiological niches. Appl Environ Microbiol **79:**3413-3424.

100. **Sadykov MR, Bayles KW.** 2012. The control of death and lysis in staphylococcal biofilms: a coordination of physiological signals. Curr Opin Microbiol **15:**211-215.

101. **Gillaspy AF, Hickmon SG, Skinner RA, Thomas JR, Nelson CL, Smeltzer MS.** 1995. Role of the accessory gene regulator (agr) in pathogenesis of staphylococcal osteomyelitis. Infection and Immunity **63:**3373-3380.

102. **Fey PD, Endres JL, Yajjala VK, Widhelm TJ, Boissy RJ, Bose JL, Bayles KW.** 2013. A genetic resource for rapid and comprehensive phenotype screening of nonessential Staphylococcus aureus genes. MBio **4:**e00537-00512.

2045 103. **Kreiswirth BN, Lofdahl S, Betley MJ, O'Reilly M, Schlievert PM, Bergdoll**
2046 **MS, Novick RP.** 1983. The toxic shock syndrome exotoxin structural gene is not
2047 detectably transmitted by a prophage. Nature **305:**709-712.

2048 104. **Windham IH, Chaudhari SS, Bose JL, Thomas VC, Bayles KW.** 2016. SrrAB
2049 modulates Staphylococcus aureus cell death through regulation of cidABC
2050 transcription. J Bacteriol.

2051 105. **Lehman MK, Bose JL, Sharma-Kuinkel BK, Moormeier DE, Endres JL,**
2052 **Sadykov MR, Biswas I, Bayles KW.** 2014. Identification of the amino acids
2053 essential for LytSR-mediated signal transduction in Staphylococcus aureus and
2054 their roles in biofilm-specific gene expression. Mol Microbiol.

2055 106. **Lewis AM, Matzdorf SS, Endres JL, Windham IH, Bayles KW, Rice KC.**
2056 2015. Examination of the Staphylococcus aureus Nitric Oxide Reductase (saNOR)
2057 Reveals its Contribution to Modulating Intracellular NO Levels and Cellular
2058 Respiration. Mol Microbiol.

2059 107. **Hanahan D.** 1983. Studies on transformation of Escherichia coli with plasmids. J
2060 Mol Biol **166:**557-580.

2061 108. **O'Neill AJ, Miller K, Oliva B, Chopra I.** 2004. Comparison of assays for
2062 detection of agents causing membrane damage in Staphylococcus aureus. J
2063 Antimicrob Chemother **54:**1127-1129.

109. **Bae T, Banger AK, Wallace A, Glass EM, Aslund F, Schneewind O, Missiakas DM.** 2004. *Staphylococcus aureus* virulence genes identified by *bursa aurealis* mutagenesis and nematode killing. Proc Natl Acad Sci U S A **101:**12312-12317.

110. **Sau S, Sun J, Lee CY.** 1997. Molecular characterization and transcriptional analysis of type 8 capsule genes in *Staphylococcus aureus*. Journal of Bacteriology **179:**1614-1621.

111. **Lauderdale KJ, Malone CL, Boles BR, Morcuende J, Horswill AR.** 2010. Biofilm dispersal of community-associated methicillin-resistant Staphylococcus aureus on orthopedic implant material. J Orthop Res **28:**55-61.

112. **Pang YY, Schwartz J, Thoendel M, Ackermann LW, Horswill AR, Nauseef WM.** 2010. agr-Dependent interactions of Staphylococcus aureus USA300 with human polymorphonuclear neutrophils. J Innate Immun **2:**546-559.

113. **Charpentier E, Anton AI, Barry P, Alfonso B, Fang Y, Novick RP.** 2004. Novel cassette-based shuttle vector system for gram-positive bacteria. Applied and Environmental Microbiology **70:**6076-6085.

114. **Fey PD.** Staphylococcus epidermidis : methods and protocols.

115. **Charpentier E, Anton AI, Barry P, Alfonso B, Fang Y, Novick RP.** 2004. Novel cassette-based shuttle vector system for gram-positive bacteria. Appl Environ Microbiol **70:**6076-6085.

116. **Lin WS, Cunneen T, Lee CY.** 1994. Sequence analysis and molecular characterization of genes required for the biosynthesis of type 1 capsular polysaccharide in Staphylococcus aureus. J Bacteriol **176:**7005-7016.

117. **Haskell RE, Hughes SM, Chiorini JA, Alisky JM, Davidson BL.** 2003. Viral-mediated delivery of the late-infantile neuronal ceroid lipofuscinosis gene, TPP-I to the mouse central nervous system. Gene Ther **10:**34-42.

118. **Sadykov MR, Olson ME, Halouska S, Zhu Y, Fey PD, Powers R, Somerville GA.** 2008. Tricarboxylic acid cycle-dependent regulation of Staphylococcus epidermidis polysaccharide intercellular adhesin synthesis. J Bacteriol **190:**7621-7632.

119. **Schmittgen TD, Livak KJ.** 2008. Analyzing real-time PCR data by the comparative C(T) method. Nat Protoc **3:**1101-1108.

120. **Nicholson WL.** 2008. The Bacillus subtilis ydjL (bdhA) gene encodes acetoin reductase/2,3-butanediol dehydrogenase. Appl Environ Microbiol **74:**6832-6838.

121. **Flemming HC, Wingender J.** 2010. The biofilm matrix. Nat Rev Microbiol **8:**623-633.

122. **Seidl K, Goerke C, Wolz C, Mack D, Berger-Bachi B, Bischoff M.** 2008. Staphylococcus aureus CcpA affects biofilm formation. Infect Immun **76:**2044-2050.

123. **Bayles KW.** 2014. Bacterial programmed cell death: making sense of a paradox. Nat Rev Microbiol **12:**63-69.

124. **Setsukinai K, Urano Y, Kakinuma K, Majima HJ, Nagano T.** 2003. Development of novel fluorescence probes that can reliably detect reactive oxygen species and distinguish specific species. J Biol Chem **278:**3170-3175.

125. **Smith J, McFeters G.** 1997. Mechanisms of INT (2-(4-iodophenyl)-3-(4-nitrophenyl)-5-phenyl tetrazolium chloride), and CTC (5-cyano-2,3-ditolyl tetrazolium chloride) reduction in Escherichia coli K-12. Journal of Microbiological Methods **29:**161-175.

126. **Brunskill EW, Bayles KW.** 1996. Identification of LytSR-regulated genes from *Staphylococcus aureus*. Journal of Bacteriology **178:**5810-5812.

127. **Masalha M, Borovok I, Schreiber R, Aharonowitz Y, Cohen G.** 2001. Analysis of transcription of the Staphylococcus aureus aerobic class Ib and anaerobic class III ribonucleotide reductase genes in response to oxygen. J Bacteriol **183:**7260-7272.

128. **Ding Y, Liu X, Chen F, Di H, Xu B, Zhou L, Deng X, Wu M, Yang CG, Lan L.** 2014. Metabolic sensor governing bacterial virulence in Staphylococcus aureus. Proc Natl Acad Sci U S A **111:**E4981-4990.

129. **Xiao G, Deziel E, He J, Lepine F, Lesic B, Castonguay MH, Milot S, Tampakaki AP, Stachel SE, Rahme LG.** 2006. MvfR, a key Pseudomonas

aeruginosa pathogenicity LTTR-class regulatory protein, has dual ligands. Mol Microbiol **62:**1689-1699.

130. **Ibarra JA, Perez-Rueda E, Carroll RK, Shaw LN.** 2013. Global analysis of transcriptional regulators in Staphylococcus aureus. BMC Genomics **14:**126.

131. **Sadykov MR, Hartmann T, Mattes TA, Hiatt M, Jann NJ, Zhu Y, Ledala N, Landmann R, Herrmann M, Rohde H, Bischoff M, Somerville GA.** 2011. CcpA coordinates central metabolism and biofilm formation in Staphylococcus epidermidis. Microbiology **157:**3458-3468.

132. **Kohler C, von Eiff C, Liebeke M, McNamara PJ, Lalk M, Proctor RA, Hecker M, Engelmann S.** 2008. A defect in menadione biosynthesis induces global changes in gene expression in Staphylococcus aureus. J Bacteriol **190:**6351-6364.

133. **Cadenas E, Davies KJ.** 2000. Mitochondrial free radical generation, oxidative stress, and aging. Free Radic Biol Med **29:**222-230.

134. **Imlay JA.** 2013. The molecular mechanisms and physiological consequences of oxidative stress: lessons from a model bacterium. Nat Rev Microbiol **11:**443-454.

135. **Messner KR, Imlay JA.** 1999. The identification of primary sites of superoxide and hydrogen peroxide formation in the aerobic respiratory chain and sulfite reductase complex of Escherichia coli. J Biol Chem **274:**10119-10128.

136. **Stewart PS.** 2003. Diffusion in biofilms. J Bacteriol **185:**1485-1491.

137. **Ledala N, Zhang B, Seravalli J, Powers R, Somerville GA.** 2014. Influence of iron and aeration on Staphylococcus aureus growth, metabolism, and transcription. J Bacteriol **196:**2178-2189.

138. **Monferrer D, Tralau T, Kertesz MA, Dix I, Sola M, Uson I.** 2010. Structural studies on the full-length LysR-type regulator TsaR from Comamonas testosteroni T-2 reveal a novel open conformation of the tetrameric LTTR fold. Mol Microbiol **75:**1199-1214.

139. **Clark T, Haddad S, Neidle E, Momany C.** 2004. Crystallization of the effector-binding domains of BenM and CatM, LysR-type transcriptional regulators from Acinetobacter sp. ADP1. Acta Crystallogr D Biol Crystallogr **60:**105-108.

140. **Ezezika OC, Haddad S, Neidle EL, Momany C.** 2007. Oligomerization of BenM, a LysR-type transcriptional regulator: structural basis for the aggregation of proteins in this family. Acta Crystallogr Sect F Struct Biol Cryst Commun **63:**361-368.

141. **Patton TG.** 2005. The regulation of the *cid* and *lrg* operons and their effect on viability and lysis in *Staphylococcus aureus* (*doctoral dissertation*). PhD. University of Idaho.

142. **Axler-Diperte GL, Miller VL, Darwin AJ.** 2006. YtxR, a conserved LysR-like regulator that induces expression of genes encoding a putative ADP-ribosyltransferase toxin homologue in Yersinia enterocolitica. J Bacteriol **188:**8033-8043.

143. **Seidl K, Bischoff M, Berger-Bachi B.** 2008. CcpA mediates the catabolite repression of tst in Staphylococcus aureus. Infect Immun **76:**5093-5099.

144. **Heil G, Stauffer LT, Stauffer GV.** 2002. Glycine binds the transcriptional accessory protein GcvR to disrupt a GcvA/GcvR interaction and allow GcvA-mediated activation of the Escherichia coli gcvTHP operon. Microbiology **148:**2203-2214.

145. **Domingues S, Moreira RN, Andrade JM, Dos Santos RF, Barria C, Viegas SC, Arraiano CM.** 2015. The role of RNase R in trans-translation and ribosomal quality control. Biochimie **114:**113-118.